STRUCTURAL BEHAVIOR OF GROUTED-BAR BAMBOO COLUMN BASES

by

Derek Randal Mitch

Bachelor of Science in Engineering, University of Pittsburgh, 2009

Submitted to the Graduate Faculty of

The Swanson School of Engineering in partial fulfillment

of the requirements for the degree of

Master of Science in Civil Engineering

University of Pittsburgh

2010

UNIVERSITY OF PITTSBURGH

SWANSON SCHOOL OF ENGINEERING

This thesis was presented

by

Derek Mitch

It was defended on

July 23, 2010

and approved by

Dr. John K. Aidoo, Assistant Professor, Civil Engineering, Rose Hulman IT

Dr. John Brigham, Assistant Professor, Civil and Environmental Engineering

Thesis Advisor:

Dr. Kent A. Harries, Associate Professor, Civil and Environmental Engineering

STRUCTURAL BEHAVIOR OF GROUTED-BAR BAMBOO COLUMN BASES

Derek Mitch, M.S.

University of Pittsburgh, 2010

Engineering knowledge of bamboo is surprisingly limited and often focuses on issues associated with ‘signature structures’ while the behavior of vernacular structures commonly used in the developing world have gone largely unstudied.

This document concentrates on understanding the behavior of one of the simplest and most common types of multi- and single-culm foundation connections, termed ‘grouted-bar column bases’. These connections consist of a reinforcing bar embedded in a concrete foundation and then grouted into the bamboo column. The objective of this work is to develop an understanding of the complex behavior of these column bases systems in the context of the behavior of a prototype bamboo framing system.

Full scale tests of single and four-culm grouted bar column bases were conducted. Additional direct tension pull-out tests of grouted bar connections were also performed. All tests were carried out using Tre Gai (*Bambusa Stenostachya*) bamboo. Test parameters included the bar size and embedment length of the grouted bar.

A basic failure mechanism associating longitudinal splitting of the bamboo culm and slip of the grout plug was identified. Effective properties of the column base suitable for modeling were identified and the relationship between effective flexural properties and fundamental material properties was verified.

TABLE OF CONTENTS

LIST OF TABLES

LIST OF FIGURES

ACRONYMS

ACI	American Concrete Institute
ASTM	American Society for Testing and Materials
DWT	Draw-Wire Transducer
INBAR	International Network for Bamboo and Rattan
ISO	International Organization for Standardization
LVDT	Linear Variable Differential Transformer
MCSI	Mascaro Center for Sustainable Innovation
NBCI	National Building Code of India
NGO	Non-Governmental Organization
PITT	University of Pittsburgh
SHED	Sustainable Hills Environment and Design
UH	University of Hawaii
UW	University of Washington

NOMENCLATURE

A	area
c_b	smaller of distance from center of bar to nearest concrete surface
d_b	bar diameter
d	distance from the centroid
D_o	outside diameter
E_s	steel reinforcement elastic modulus
f'_c	grout compressive strength
f_y	steel reinforcement yield strength
h	height of bending test
H_i	height of specimen at shear plane
I_{culm}	moment of inertia of a single culm
I_{column}	moment of inertia of a four culm column
I^*_{column}	moment of inertia of a fully effective four column cross section
I_{eff}	effective moment of inertia
K_{tr}	transverse reinforcement index
K_Θ	rotational spring constant
l_d	development length
M	applied moment

NA	neutral axis
P	applied compressive load
t_i	average culm wall thickness at shear plane
t	wall thickness
V	applied horizontal load
Δ_1	displacement of LVDT 1
Δ_2	displacement of LVDT 2
σ	stress
δ	total displacement
δ_θ	displacement due to rigid body rotation
Θ	rotation
λ	modification factor for lightweight concrete
ψ_t	modification factor based on reinforcement location
ψ_e	modification factor based on reinforcement coating
ψ_s	modification factor based on reinforcement size
φ	equivalent material resistance factor

This work was completed using US units throughout except where noted. Work conducted by others is reported in 'native' units to avoid contradiction with the cited documents. The following "hard" conversion factors were used:

1 inch = 25.4 mm

1 kip = 4.448 kN

1 ksi = 6.895 MPa

Reinforcing bar sizes are given using the designation cited in the appropriate reference. In the thesis, a bar designated with a “#” followed by a number refers to the standard inch-pound designation used in the United States (e.g.: #7). The number refers to the diameter of the bar in eights of an inch. A bar designated with an “M” after the number refers to the standard metric designation. The number refers to the nominal bar diameter in millimeters (e.g.: 20M).

ACKNOWLEDGEMENTS

This work would certainly not have been possible without a tremendous amount of support from a variety of sources. The following organizations and individuals have my profound thanks:

The Mascaro Center for Sustainable Innovation (MCSI) and the Civil and Environmental Engineering Department - for support that varied from the practical to the theoretical.

The Watkins Haggart Structural Engineering Laboratory - for providing a place for the advancement of the field of civil engineering.

Dr. Kent Harries – not only for essential advice and assistance but for always expecting more from his students; you made us better.

Charles “Scooter” Hager – for lending a hand with everything and anything that occurred in the structures lab.

Bhavna Sharma – for providing much needed advice and assistance whenever possible.

Michael Richard and Jarret Kasan – because life would have been boring without you guys.

My friends and family - for standing by me and being there when I needed them.

And finally, I would like to thank the late Dr. Alec Stewart; your vision of a university and the quality of students it should produce inspired many, including myself. You will be sorely missed.

1.0 INTRODUCTION AND LITERATURE REVIEW

1.1 INTRODUCTION

The work presented in this thesis is part of a larger body of work focusing on the use of sustainable construction practices and materials and their relation to issues associated with hazard mitigation. The focus of this work is the use of full-culm bamboo (as opposed to processed bamboo products) as a structural material. The following introduction, drafted by all research team members, is offered to provide context to the reported work.

1.1.1 Motivation, History and Context

A recent Rand Corporation report (Silberglitt et al. 2006 and "Civil" 2006) anticipates an increasing socio-technical-economic gap developing between scientifically 'advanced' countries (e.g.: United States, Western Europe) and those that are 'proficient' (e.g.: India, China), 'developing' (e.g.: Mexico, Turkey) and 'lagging' (e.g.: Egypt, Nepal). Additionally, particularly within countries expected to experience great growth, a similar widening gap between urban and rural populations is anticipated. Sixteen so-called 'new technologies' are predicted to proliferate by 2020; most involve aspects of the civil infrastructure. Indeed the Rand report cites the lack of stable infrastructure (including electricity, potable water, roads, schools and transportation systems) as the primary barrier to the adoption of technology. The report further cites the increased emphasis by advanced countries on 'sustainable practices' as being largely

unattainable (by 2020) for proficient, developing or lagging regions. Two key new technologies cited in the Rand report are the focus of the present work: inexpensive, autonomous housing as well as 'green' manufacturing [and construction].

A critical aspect of sustainable infrastructure is its ability to perform under both service conditions and extreme events. Safety in the built environment is a fundamental right.[1] Recent 'great' natural catastrophes have resulted in unacceptably high casualty tolls. The 2001 earthquake in Bhuj, India left over 19,700 dead; the 2003 Bam (Iran) earthquake: over 26,000 dead; the 2004 Aceh earthquake and subsequent tsunami: over 275,000 dead; the 2005 Kashmir earthquake: over 80,000 dead; the 2008 Sichuan earthquake: 70,000 dead, the 2010 Haitian earthquake: at least 230,000 dead. The injured are many times these numbers and the displaced are often an order of magnitude or two greater. In reviewing this litany of statistics, one must acknowledge the clear disparity between developed and less developed regions: the 2010 Chilean earthquake, for instance, was the fifth largest event ever recorded yet the death toll was less than 300.

As demonstrated by the October 8, 2005 Kashmir earthquake, the Himalayan region is at particular risk. It is exposed to a high seismic hazard, relatively densely populated by relatively poor people, and is geographically remote. The Himalayan range has experienced approximately 20 devastating earthquakes since 1900. Indian seismological maps indicate high hazard regions as far south as Delhi. Of particular concern is the 'Himalayan gap' – a 600 km long region of the central Himalayas extending across Nepal – which has not experienced a recent major event.

[1] Article 25 of the United Nations Universal Declaration of Human Rights states that "Everyone has the right to a standard of living adequate for the health and well-being of himself and of his family, including food, clothing, housing and medical care and necessary social services..." Principle #10 of the 1994 Special Rapporteur's Report to the United Nations Commission on Human Rights states: "All persons have the right to adequate housing, land tenure and living conditions in a secure, healthy and ecologically sound environment."

Seismologists suggest that this region is capable of generating multiple events with moment magnitudes greater than 8.0 (Bilham et al. 2001).

1.1.2 Bamboo as a Sustainable Construction Material

In 2004, the International Organization for Standardization (ISO), in partnership with the International Network for Bamboo and Rattan (INBAR), a Beijing-based agency whose aim is to promote bamboo and rattan for poverty alleviation in developing countries, published a standard on structural design using bamboo (ISO 2004a) and a series of methods for determining the mechanical properties of bamboo (ISO 2004b and ISO 2004c). If the use of bamboo is limited to rural areas, the standard recognizes established "experience from previous generations" as being an adequate basis for design. However, if bamboo is to realize its full potential as a sustainably obtained and utilized building material on an international scale, issues of the basis for design, prefabrication, industrialization, finance and insurance of building projects, and export and import all require some degree of standardization (Janssen 2005).

The ISO standard aims at prescribing a modern limit states design approach to traditional designs and practice. Precisely because of this dichotomy, however, the standard approach is simultaneously inadequate on both counts in the context of developing regions. A limit states approach requires specialized knowledge and engineering which may not be readily available. The traditional approach, while often adequate for service conditions, is unable to address ultimate limit states, particularly those associated with extreme events such as earthquakes.

1.1.3 Physical Properties and Terminology Associated with Bamboo

Bamboo is not a material well known to civil engineers, thus it is the intent of this work to help characterize its *in situ* mechanical properties. For an overview of the properties of bamboo as they relate to structural applications, the reader is directed to Janssen (1981) or Arce-Villalobos (1993). Both Janssen and Arce-Villalobos also provide a review of the extensive nomenclature associated with bamboo and are cited later in this work.

1.1.4 Darjeeling Region of Northeast India

For the sake of appropriate contextualization, this project considers the hill region of the Darjeeling area in northern West Bengal. This area is an economically depressed region of a rapidly emerging country, India. This region epitomizes what Silberglitt et al. (2006) refer to as the "widening gap between urban and rural populations". The selection of this region for context is largely independent of the technical goals of this work. Nonetheless, it is important to provide context, if only to better define the scope of the work. The selection of this region is supported by contact with Ms. Gayatri Kharel and a number of other contacts made during a three week visit to Darjeeling, Kalimpong, Mungpoo and Gangtok (Sikkim) in May 2008 (Sharma et al. 2008). A return visit was made in May 2010.

The Mascaro Center for Sustainable Innovation (MCSI) team, of which the author was a member, visited the Darjeeling region of Northeastern India in May 2008 in order to assess the challenges faced in bamboo construction and related sustainable engineering practices in the region. The team discovered that the concept of sustainability was generally accepted by those who had advanced education, while the general populace had little appreciation of the concepts

involved. An amusing example of the misunderstanding regarding the ‘green movement’ was the market district in Gangtok, Sikkim. In addition to turning the main market street into a pedestrian mall, the local government also painted the mall buildings green in order to ‘go green’. While the ‘green mall’ is a new local amenity, its development has resulted in increased congestion in the adjacent streets and has done little to promote sustainability in the city (although it has been successful from a social perspective). Despite the marginal outcome, the interest of the local government leads one to believe that sustainability has a future in this region.

The particular site which serves as a prototype for this work is the construction of St. Joseph’s School in Mungpoo (Figure 1.1). St. Joseph’s was being developed under the auspices of St. Joseph’s College at North Point, Darjeeling and the local NGO Sustainable Hills Environment and Design (SHED). A feature of this school was to have been that the structures would all be constructed of locally harvested bamboo. A nearby cinchona plantation has been partially converted to grow bamboo in an effort to support St. Joseph’s and similar construction in addition to providing a source of bamboo from which a home-grown crafts industry may be developed. This had the additional benefit of keeping the cinchona plantation viable: cinchona is the source of the natural anti-malarial quinine. Quinine production has declined significantly as it has been replaced by compounded pharmaceuticals. Thus finding a viable alternative crop for the plantation (that continues to specialize in plants raised for the pharmaceutical industry) will support the plantation and the local economy.

A challenge faced in the hill region is the threat of earthquake and earthquake- and rain-induced landslide. SHED and other NGOs are championing the consideration of these hazards in sustainable hill architecture/engineering. The use of bamboo at St Joseph’s addressed SHED’s primary goals in that it is both a more sustainable product than reinforced concrete, and due to its

lighter weight, it is far less prone to cause/experience a fatal collapse in an earthquake. Regrettably, due to 'political' issues associated with the development of St. Joseph's, the school is not proceeding as originally planned as a showcase for sustainable practices. Ironically, a few of these issues stem from concerns over the performance of the bamboo structures which this research is engaged in overcoming. Nonetheless, the prototype structures shown in this work exist although the remainder of the project will be completed using more conventional means. The research team continues, however, to work with SHED on related projects.

(a) Administrative building and (uncompleted) canopy over assembly hall.

(b) Classroom building.

(c) Classroom building end elevation.

Figure 1.1 St. Joseph's school in Mungpoo, West Bengal (Photos: Mitch).

The design and construction of the original bamboo structures of St Joseph's School are described as follows. Main column members consist of four bamboo culms seated together on a

concrete plinth or footing. The plinths are tied together with grade beams to form a raft-like foundation. Additional stability is provided by infilling the foundation raft with stone (Figure 1.2a) Steel reinforcing bars project from the plinths and are embedded and subsequently grouted into the bamboo culms. The roof system is composed of bamboo trusses connected to the four-culm columns using a series of single bolt connections. The resulting three-dimensional connection (Figure 1.2b) is able to resist moments associated with lateral forces. The behavior of these connections is a focus of Sharma (2010) and will be described briefly in Section 1.2.3 in as far as they relate to the present work. The walls are made out of a woven bamboo mat that will eventually be covered with a local mud-plaster. The roof is constructed from corrugated sheets of galvanized steel, which, along with large gutters, form a rainwater collection system.

(a) Foundation with plinths and four-culm columns

(b) details of roof truss to column connection

Figure 1.2 Details of St. Joseph's School bamboo structures (Photos: Harries).

As can be seen in Figure 1.3, a set of four bamboo culms are used to make up each column. The behavior of the joint at the base of this column is not well understood and is the focus of the present work.

Figure 1.3 Four-culm columns (Photo: Mitch).

1.2 LITERATURE REVIEW

1.2.1 Bamboo and its Physical Properties

Bamboo is being given an increasing amount of attention in developed and developing countries alike, and for good reason. Bamboo grows at a much more rapid rate than the hard- and soft wood species that are commonly utilized for construction. This rapid growth rate translates into

an equally rapid harvesting rate – usually a two or three year cycle for structural species of bamboo - thus reducing the amount of land and resources necessary for timber production. Bamboo may also be cultivated on marginal land and generally requires little pesticide application or management. This reduced development cost means that it is easier to manage bamboo production at a sustainable rate. Additionally, bamboo species may be grown throughout the temperate, subtropical and tropical world; and as long as the bamboo is grown locally, it will reduce the cost and harmful byproducts of transportation.

Bamboo has been put to extensive use in both the developed and the developing world. In the developed world it tends to be used in value-added applications such as cutting boards, utensils, and flooring. In the developing world it is used in a more utilitarian manner, as either structural members or as strips used for weaving mats (used for walls and flooring). The focus of the present work is with the structural application of bamboo. Before beginning a discussion of the structural uses of bamboo, a brief explanation of bamboo and relevant terms is required.

Bamboo is a member of the grass family, but is unusual in the fact that it is mostly comprised of a rapidly growing woody stem and grows to a very tall height (see Figure 1.4). The stem is the hollow cylinder that most people associate with bamboo, and is commonly referred to as a “culm”. Bamboo culms also possess a unique physical characteristic known as a “node” (see Figure 1.5). Nodes serve the purpose of allowing a location for leaves to grow, and as a result, the longitudinal fibers of the bamboo are forced to change directions in those areas. This leads to reduced structural properties, such as tensile strength, at the nodes (Arce-Villalobos 1993). Nonetheless, the nodes provide a degree of stability to the very long – thin-walled culms. In addition to node spacing, culms vary widely in their length, diameter, wall thickness, and material properties depending on the species and height along the culm (Janssen 1981). Bamboo

has a higher concentration of fibers towards the outer edge of the culm (Amada 2001). For this reason bamboo may be considered a functionally graded material as shown in Figure 1.6.

Figure 1.4 Bamboo stand in Kalimpong, West Bengal (Photo: Mitch).

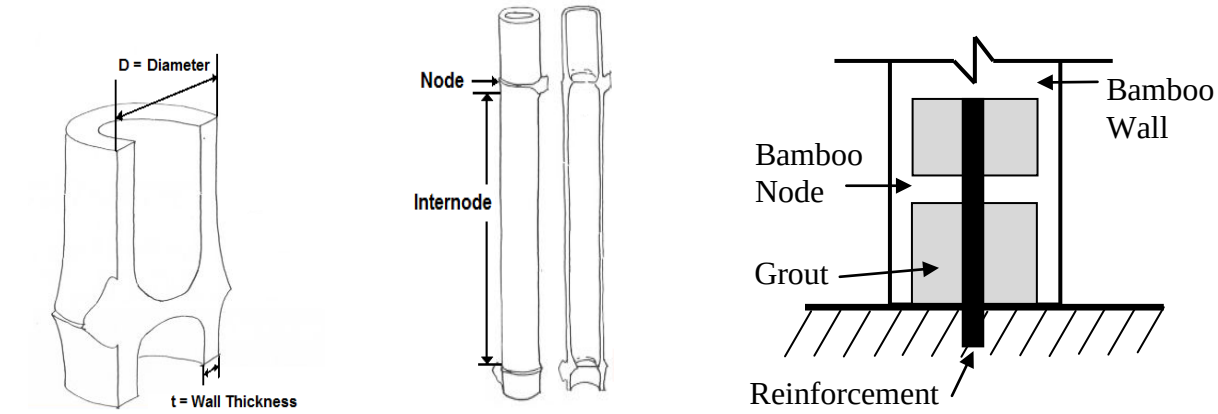

(a) longitudinal section of culm (b) node and internode regions (c) Connection terminology

Figure 1.5 Sections of bamboo culm and associated terminology (Janssen 1981).

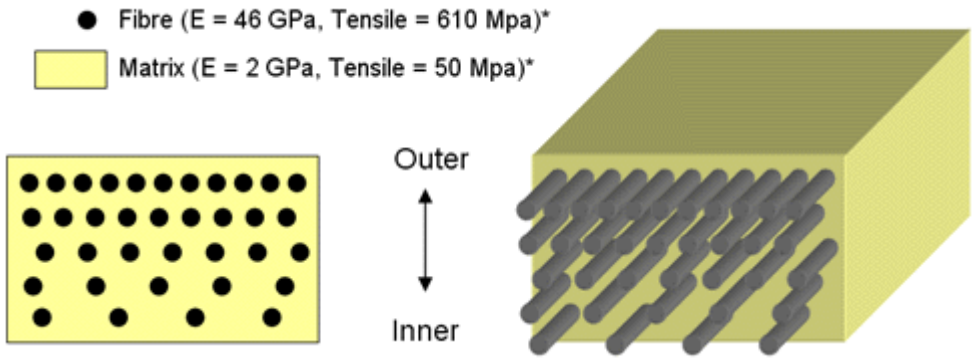

Figure 1.6 Through-thickness grading of bamboo culm wall. Fiber/matrix analogy suggests modeling strategy similar to that used for fiber reinforced polymer (FRP) materials.

Despite its many theoretical advantages, the widespread ‘engineered’ use of bamboo is still hindered by many problems. The three most important ones being: a) the way societies view bamboo; b) its perceived inadequate durability; and c) the lack of sufficient engineering knowledge. Throughout most of the world, bamboo is regarded as “the poor man’s timber”; where available, various types of wood are generally preferred. For bamboo to be broadly adopted, this negative mentality must change. It is proposed that by establishing a firmer engineering basis for bamboo construction, the stigma associated with its use may be improved. As this work focuses on the mechanical properties of bamboo rather than socio-political issues, the public perception of bamboo will not be explored further.

The second serious problem facing the widespread adoption of bamboo in construction is the fact that even with treatment, bamboo, in some cases, does not last as long as other woods. Untreated bamboo that is in direct contact with the ground tends to last about 2 years, and about 4-7 years when not in direct contact with the ground. Treated bamboos, however, may last for more than 30 years (Kumar 1994). While testing has been done on a broad range of bamboo preservatives and preservation methods, no single method has been exhaustively studied or standardized. Treatment choice tends to be regional and based on convenience. This has led to confusion regarding the effectiveness of individual treatments as well as uncertainty about the effects that the treatment methods have on mechanical properties. For bamboo to realize its full potential, an effective method that will enable bamboo to last as long as common woods will have to be developed and broadly accepted.

The third major obstacle to the wider use of bamboo is the lack of sufficient engineering knowledge for design purposes. Most modern buildings are constructed out of three primary materials: wood, steel, or concrete. Each of these materials has [inter]nationally recognized

design standards that list commonly encountered material properties as well as design aids to simplify and formalize the task of designing a structure. The first significant standard concerning bamboo is the ISO Model Code for Bamboo Construction (ISO 2004a) which was first published in 2004. This code, and other regional research, forms the basis for the most extensive standardization of bamboo construction: Chapter 6, Section 3 of the National Building Code of India (NBCI 2005). This section of the Indian Code is cursory at best; it provides fundamental material properties for about 20 species of bamboo and guidance for design for fundamental actions of compression and flexure. The Indian Code is effectively a performance-based standard as far as bamboo is concerned: if an engineer can demonstrate that a system can adequately resist prescribed loads, then the system is compliant. No other criteria, such as deformation or ductility are considered. The Indian Code is silent on how to qualify or determine material properties of bamboo species other than those listed. A second ISO Model Standard (ISO 2004b and 2004c) reports standard test methods for bamboo, but again, these are cursory and critical guidance is absent. For engineers to fully embrace bamboo as a building material it will need more thorough documentation and research as well as a history of successful use.

The history of engineering knowledge with regards to bamboo is surprisingly recent. The first major work was completed by Janssen (1981) of the University of Eindhoven, The Netherlands. In his 1981 dissertation, Janssen first explored the composition of a bamboo culm. He developed a mathematical model of the culm by considering it to be a structure composed of a number of substructure ‘cells’. Janssen then explored different mechanical properties of bamboo including bending, shear, tension and compression. Finally, he explored different truss systems and various ways to connect bamboo elements.

From his work on the composition of bamboo, Janssen (1981) drew several conclusions:

1. Although bamboo has more than double the number of layers of cell walls as softwood, this does not have an influence on the stresses and displacements of bamboo.
2. The angle that the microfibrils of bamboo make with the cell axis has a large impact on the stresses and displacements.
3. A numerical model of a single substructure cell may be used to predict the Poisson ratio and tensile strength, but cannot be used to predict the compressive strength as pectin prevents the buckling of individual fibers; a more expansive model is required to accurately predict compressive strength.

In addition to simple mechanical tests of bamboo, Janssen applied statistics and linear models in an attempt to discover which parameters are related to bamboo's material properties. Some of his conclusions are as follows:

4. An increase in moisture content decreases compressive strength, and the compressive strength increases with the height along the culm from which the sample was taken (i.e.: compressive strength increases from the bottom to the top of a culm).
5. Shear stress is the cause of failure for smaller spans, and the limiting *in situ* shear stress is much lower than a typical shear test would indicate.
6. In bending, dry bamboo behaves better; strength decreases with the height from which the sample is taken from the culm (i.e.: flexural strength decreases from the bottom to the top of a culm); and there is a possible relationship between ultimate bending stress and density.
7. A new shear test was needed to determine the correct shear strength of bamboo. Janssen designed such a test method which was adopted by ISO (2004b).

8. Shear strength and density are related.
9. A new test method is needed to determine bamboo's tensile strength.

The work of Arce-Villalobos (1993) work is essentially an extension of Janssen's. He begins with a more in-depth examination of the tensile properties of bamboo. This examination included tensile strength both parallel (along culm) and perpendicular (transverse) to the primary orientation of the fibers. Arce-Villalobos also attempted to relate different mechanical properties. His most important conclusions are as follows:

1. Transverse tension capacity and density are not correlated whereas longitudinal tension capacity and density are.
2. Tension modulus, E, in the transverse direction is about 1/8 that measured in the longitudinal direction.
3. There may be a universal maximum transverse strain that bamboo may experience before failure. Three different species exhibited similar values during testing, approximately 0.0012.
4. Variation in cross-section dimensions generally produces a reduction of no more than 15% in the bending and axial stiffness compared to the values a theoretical uniform member would yield; the presence of nodes can reduce bending stiffness an additional 40%, and axial stiffness an additional 12%.
5. The slenderness ratios of compression elements should be kept below 50 to avoid global buckling or splitting resulting from second-order flexural behavior.

The present understanding of the material properties of bamboo expressed in the ISO Standards (2004a) and the Indian Code (2005) stem largely from the work done in the Netherlands by Janssen and Arce-Villalobos. While these standards are a start, there are many

areas that still require further exploration. One of the most critical is the area of connection design.

Further investigation of bamboo material properties – particularly those associated with splitting behavior – has been conducted by the author and is reported in Mitch (2009) and Mitch et al. (2010).

1.2.2 Bamboo Columns Bases

While there are numerous methods available to connect bamboo columns to concrete foundations, the three that are most prevalent are: the steel-pin connection, embedment of the bamboo into the concrete, and the grouted-bar connection. The latter is the focus of the present work. The steel-pin connection involves grouting a piece of reinforcing bar into the end of a culm and then placing the free end into a joint made of concrete. By leaving a small space between the end of the bamboo and the start of the concrete joint, a pinned connection - affected by only the reinforcing bar - is created due to the flexibility of the reinforcement (see Figure 1.7). Such connections are well suited to space-truss structures (Figure 1.7) although they have not been observed in ‘post-and-beam’ construction.

(a) Steel-pin connection prior to concreteing; soda bottles are used as ‘formwork’ for the grouted connection into the culm.

(b) Steel-pin connection (after concrete)

(c) Model of bamboo structure with steel-pin connections

Figure 1.7 Steel-pin connection (Photos: Kharel).

The second type of connection is the embedment of the bamboo culms directly into a concrete plinth, foundation or grade beam (Figure 1.8). This type of connection has the advantage of producing a fixed end condition, which can be more desirable depending on the design. The disadvantages of this system are that a larger plinth is required and the bamboo has a tendency to rot at the connection interface (Figure 1.8b). This system was employed in the Community Center at Camburi, Brazil (Figure 1.8a).

(a) embedded multi-culm foundation
(Photo: www.bamboostic.be)

(b) approximately 20-year old embedded culm showing damage to concrete foundation and rotten bamboo resulting from pooling water
(Photo: Harries).

Figure 1.8 Bamboo culms embedded in concrete.

The grouted-bar connection involves steel reinforcing bars extending from the concrete foundation directly into the culms where they are grouted. The interface has the entire culm bearing upon the concrete. This connection is the type used in St. Joseph's school in Mungpoo (Figure 1.3 and 1.5) and is the subject of this work.

1.2.3 Bamboo Connection and Frame Behavior

While significant work has been done on proprietary connections (see Sharma 2010), simple connections that are most likely to be employed in rural construction have not been thoroughly investigated. The ISO Standard (2004a) concerning the structural applications of

bamboo makes no mention of column base connections and states that joints may be designed based on full-scale tests. The National Building Code of India (NBCI 2005) also makes no mention of these types of column base connections.

As previously mentioned, the structure at St. Joseph's (Figure 1.1) consists of a reinforced concrete grade-beam foundation with stone infill (see Figure 1.2a) which supports concrete plinths with multiple bamboo culms forming a single column (Figure 1.3). Each culm is joined to the plinth using a grouted reinforcing bar. The roof framing and panels are connected to the bamboo columns using bolted connections.

The objective of using bolted connections with bamboo is to enforce a truss-like behavior for the individual culms. Such a behavior is desirable due to the fact that typically the governing limit state for bamboo is splitting. The shear strength of bamboo is small compared to its very high tensile and compressive strength. Thus, a truss-like behavior avoids flexure and the associated shear flow (VQ/I), which can result in longitudinal splitting failure. With the four-culm column arrangement, however, moment resisting connections are still possible (Figure 1.2b and 1.3) permitting relatively rigid frame structures to be erected. In an effort to better understand the structural behavior of these bamboo frame systems, Sharma (2010; also Sharma et al. 2010) conducted a series of pullout tests and a half-scale portal frame pushover test. A summary of these tests is presented in the following sections.

1.2.3.1 Pull-Out Tests (Sharma 2010)

In related frame tests (see following section), considerable slip, associated with prying action that is present at the base of a bamboo column connection was observed. The pull-out test was intended to assess the tension capacity of a grouted reinforcing bar connection. The pull-out tests consisted of 12 mm diameter threaded rod which was grouted into a bamboo culm and then

affixed to the laboratory strong floor. The embedment length of the rod into the four specimens varied from 528 mm – 824 mm, and the grout sockets were approximately 41 mm in diameter, or 3.4 times the bar diameter. The culms were of the species *Phyllostachys aurea* with a nominal outside diameter of 50 mm and an average wall thickness of 4.4 mm. The culms were loaded vertically using a 2 ton engine hoist until failure (see Figure 1.9a). Two of the four culms experienced a grout plug pull-out failure (failure type (c) discussed in section 2.4.2). The other two culms experienced a loading apparatus failure as the loading bolts tore through the bamboo wall . The pull-out failures represent true ultimate strengths, whereas the loading apparatus failures are a lower bound for a pull-out failure.

The results are summarized in Table 1.1 and in Figure 1.9b. Sharma (2010) found that the mortar molded to the interior of the culm, forming a mechanical 'shear key' at the culm diaphragm and that considerable friction could be developed once slip of the mortar plug was engaged. Sharma states that specimen P-PA-4, which had a softer response, demonstrated this behavior by allowing slip (small amount of friction) before the shear key was engaged. It should be noted that the culms used in Sharma's work were not as straight as those used in the current test program (see Figure 1.9c) which may result in a larger friction component. Voids and poorly consolidated grout are also believed to have affected the test results (Figure 1.9c).

Table 1.1 Pull-out test results (Sharma 2010).

Specimen	Embedment Length L_e	Culm Diameter D_o	Failure Type	Maximum Load P_{max}	Slip at Maximum Load Δ	Nodes Engaged
	mm	mm		N	mm	
P-PA-1	528	45	Loading Apparatus	9410	1.04	2
P-PA-2	824	50	Loading Apparatus	13570	4.34	5
P-PA-3	541	50	Plug Pull-out	8849	3.98	2
P-PA-4	706	49	Plug Pull-out	6590	20.97	4

(a) Pull-out test set up at PUC-Rio

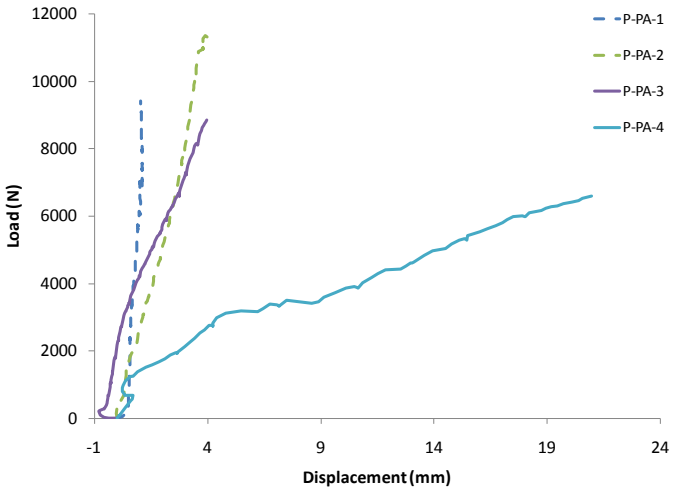

(b) Load vs. displacement behavior for pull-out tests

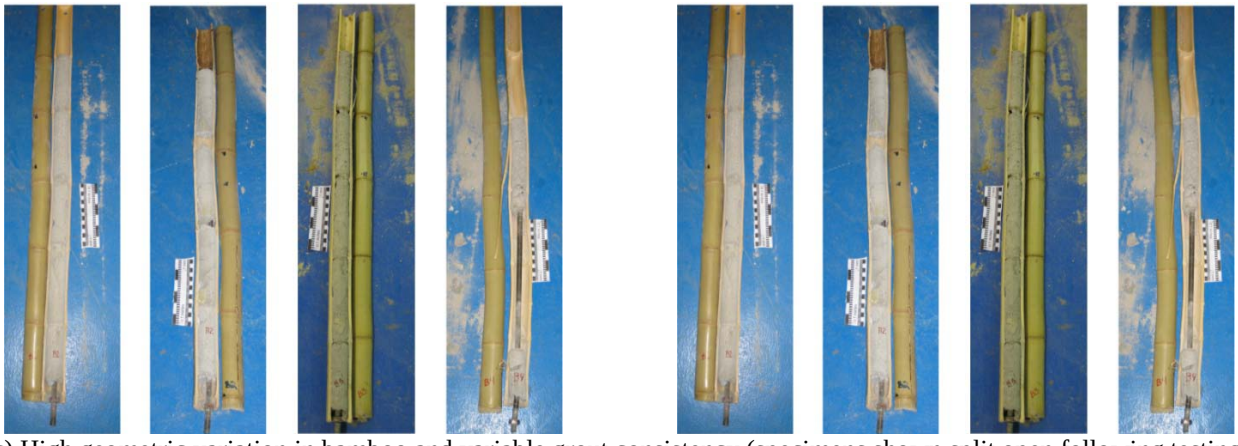

(c) High geometric variation in bamboo and variable grout consistency (specimens shown split open following testing)

Figure 1.9 Pull-out tests by Sharma (2010).

1.2.3.2 Portal Frame Pushover Behavior (Sharma 2010)

The primary objective of Sharma's (2010) work was the pushover test of a half-scale bamboo portal frame based on the design of St. Joseph's school in Mungpoo (Figure 1.10). *Phyllostachys aurea* bamboo was used, with 50 mm diameter culms for the columns and 40 mm diameter culms for the lateral, roof, and tension tie members. The column culms had grouted-bar base connections consisting of a 12 mm diameter threaded rod with an embedment length of 500 mm. These rods were then bolted to a steel channel which acted as the foundation and provided a 'fixed connection' at the base of each culm. The top-of-column bolted frame connections (see Figure 1.2b) were made using 8 mm diameter threaded rod. Out-of-plane framing was included in the connections and out-of-plane stability of the two-dimensional frame was provided by an external reaction frame (partially seen in Figure 1.11b).

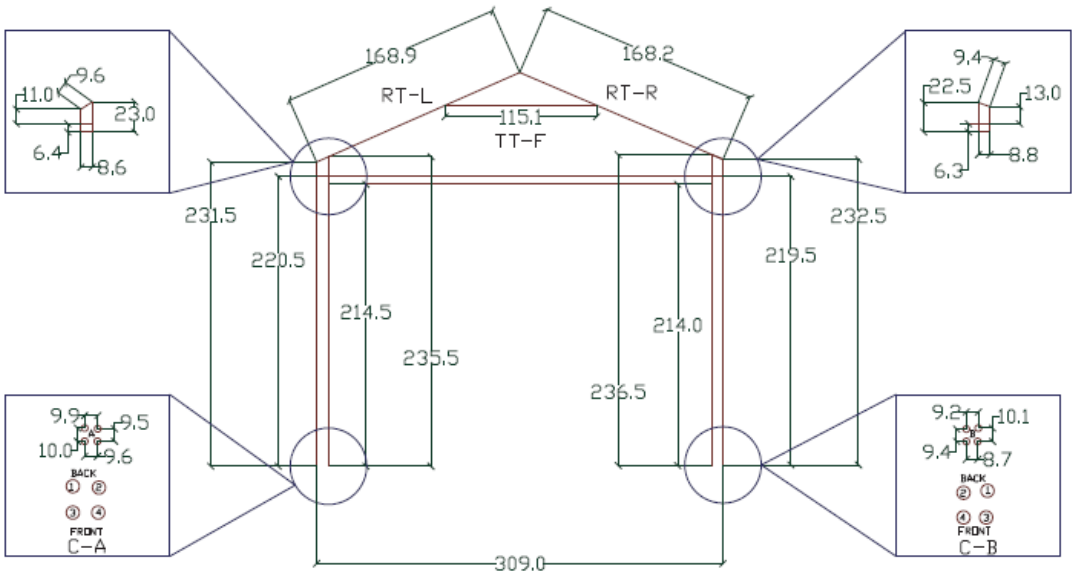

Figure 1.10 Dimensions (in cm) of prototype frame used by Sharma (2010).

Lateral load was applied to the frame at the level of the horizontal roof truss member and a pushover-type test was conducted (see Figures 1.11a and b). The column displacement was measured at four points along the column; at the base, mid-height, the location of the lower

horizontal member, and at the roof truss bolt connections. The results indicated that the lateral displacements at the tops of both columns were nearly identical and the deflections are dominated by rigid body rotations at the column base. While not behaving as a perfect pin, the column base was felt to be much more flexible than anticipated (Figure 1.11d). Understanding this unanticipated column base behavior is the motivation and objective of the present work.

Due to the relative flexibility of the column bases, the upper frame connections were subject to greater demand than anticipated and were found to dominate the response of the portal frame system (Figure 1.11c).

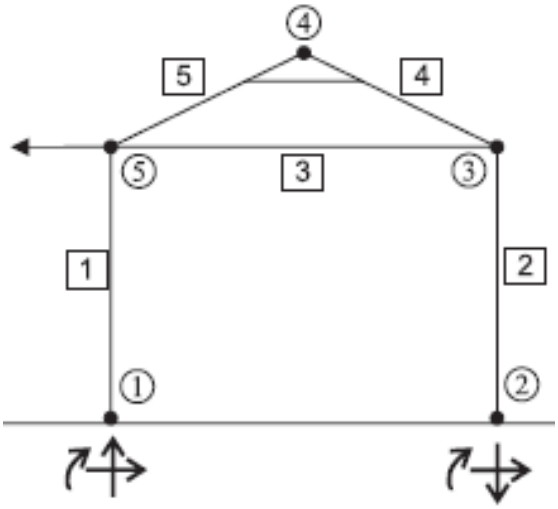

(a) Conceptualized portal frame setup

(b) Portal frame specimen

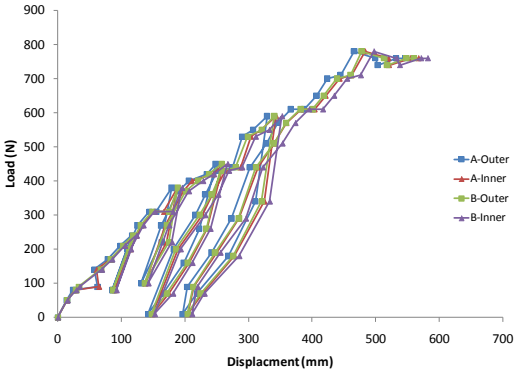

(c) Lateral load vs. displacement (pushover) of portal frame.

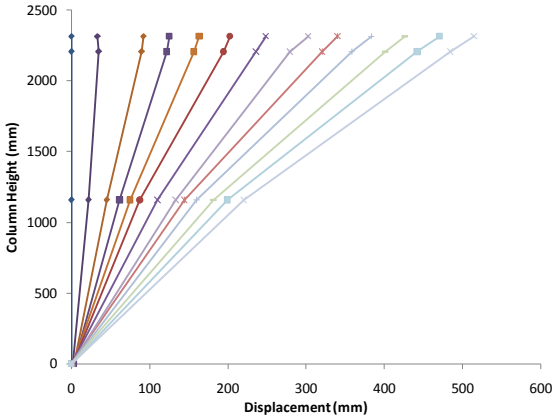

(d) Lateral displacement along column height at various load levels.

Figure 1.11 Portal frame test (Sharma 2010).

1.3 OBJECTIVE OF PRESENT WORK

As part of the overall goal of developing an engineering basis for the design of bamboo structures, this work concentrates on understanding the behavior of the grouted connection between the reinforcing bar, bamboo, and concrete foundation at the base of multi- and single-culm bamboo columns. These connections will be termed ‘grouted-bar column bases’. The primary objectives are to determine the degree of fixity that this connection provides when utilized in a frame system well as the governing factors for the pull-out (tension) strength of the connection.

2.0 EXPERIMENTAL PROGRAMME

This chapter reports the material properties of the bamboo, reinforcing steel and grout used in this study. The method of specimen fabrication is also reported followed by detailed descriptions of the pull-out and column base tests conducted.

2.1 MATERIAL PROPERTIES OF BAMBOO

As a transversely isotropic graded material, bamboo has significantly different material properties in different directions. Further complicating the accurate determination of material properties is the fact that, as bamboo is an organic material, the individual culms have a high variation of geometric properties, such as outside diameter and wall thickness, both between different culms and in different locations along the same culm.

For the column base connection investigated here, the most important physical parameters are the compression strength parallel to the fibers and the shear strength parallel to the fibers as there will be high compressive forces on the leading edge of the bamboo as well as the accompanying shear forces. The most important geometric values are the outside diameter of the culms and the wall thickness, as these also play a role in determining the amount of force the connection can resist before failure. The following results for compression strength, shear strength, and geometric variation are taken from previously reported work conducted by the

author (Mitch 2009 and Mitch et al 2010) and supplemented as required for the present work. The bamboo used in the present work is from the same 'batch' of borate treated Tre Gai (*Bambusa Stenostachya*) sourced from the same supplier and is therefore assumed to be representative of the material properties for the bamboo used in the present study of column base behavior.

2.1.1 Compression Test

The compression tests conducted followed the method prescribed in ISO 22157-1, *Bamboo – Determination of physical and mechanical properties* (ISO 2004b). In this direct compression test (Figure 2.1), the compressive strength of the bamboo is determined by dividing the load at failure by the net cross-sectional area of the culm, which is determined by averaging the outside diameter (measured at two orthogonal locations across the section) and wall thickness (measured at four locations spaced 90^o around the section) at both the top and bottom of the specimen. These measurements yield the inner and outer diameters of the culm, which are used to calculate the area of the cross-section and, subsequently, the failure stress.

According to the ISO standard, the specimens are to be cut to a length equal to the culm diameter and loaded in the longitudinal direction in displacement control with the crosshead traveling at a rate of 0.01 mm/s (0.0004 in/s). Additionally, the culms require an intermediate layer to reduce friction between the steel loading plates and the bamboo specimen. The ISO standard recommends the use of steel finger shims although it also suggests in the associated *Laboratory Manual* (ISO 2004c) that sulfur-based capping compound (as is used for concrete cylinder compression tests) is also acceptable. The latter was used in the present study. Anecdotal evidence suggests that the use of finger shims, while accomplishing the desired

behavior, is very difficult to implement accurately in practice. In order to have a specimen having a clear height of one culm diameter following capping, specimens were cut at overall lengths of between 1.25 and 1.5 culm diameters. While this is longer than the capping compound requires, the additional height did not have an adverse effect on the compressive strength (Mitch 2009).

Testing was carried out in a Universal Testing Machine with a fixed lower platen and an upper platen equipped with a ball-joint to account for non-symmetric specimen geometry. A total of twelve tests were performed. All specimens experienced the same type of failure, namely longitudinal splitting followed by buckling of the resulting longitudinal 'strips' (Figure 2.1c). The average bamboo compressive strength was found to be 8220 psi having a coefficient of variation of 12%. Despite the relatively high level of variability inherent in the material properties of bamboo, the compressive strength of the culms exhibited relatively low variation, having a standard deviation of only 12%. This observation is consistent with that of Arce-Villalobos (1993) discussed previously.

Three compression tests were instrumented with two vertically-oriented electrical resistance strain gages on opposing sides at mid height. From these tests, the compressive modulus of the culm section was determined to be approximately 1700 ksi with a standard deviation of 8.1% through loads equal to half the ultimate compressive capacity. It must be noted that the compressive modulus determined in this manner is that for the entire culm section. It must be acknowledged that the actual modulus at any point in the culm section is affected by the graded nature of the culm wall (Figure 1.6). Nonetheless, the modulus based on the entire culm section is most appropriate for full-culm column design.

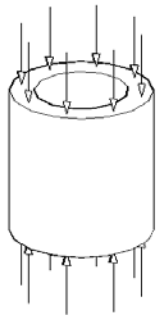

(a) schematic of test specimen

(b) test specimen in test machine

(c) typical compressive failure

Figure 2.1 Compression test.

2.1.2 Shear Test

The shear test conducted followed the method prescribed in ISO 22157-1, *Bamboo – Determination of physical and mechanical properties* (ISO 2004b). In this test, developed by (Janssen 1981) the cross-section of the specimen is divided into four quadrants. Two opposing quadrants are loaded on the top and two are loaded on the bottom of the culm, which produces four vertical shear failure planes in the culm. The test set-up is shown in Figure 2.2 and consists of four 'teeth' making up the quadrants. The teeth were aligned such that there was a 3 mm (0.125 in.) gap between them creating the 'shear planes' in the specimen. The test set-up for this study was fabricated of aluminum and was designed to be loaded into a universal test frame having self-centering hydraulic grips. This facilitated reliable and repeatable test alignment. Janssen's original design included a self-centering core, however this precludes testing bamboo specimens that include a node. The test was carried out in displacement control with the crosshead traveling at a rate of 0.01 mm/s (0.0004 in/s). The shear stress is equal to the failure load divided by the sum of the area of the four failure planes located at the intersections of the teeth:

$$\sigma = \frac{P}{\sum_{i=1}^{4} H_i t_i} \qquad \text{(Eq. 2.1)}$$

Where H_i = height of the specimen at shear plane i

t_i = culm wall thickness at shear plane i, taken as the average of the thicknesses at the top and bottom of the specimen.

The shear test series consisted of 17 specimens including 9 nodal and 8 internode specimens. The average shear capacity of the nodal and internodal specimens was 9.6MPa and 8.8MPa, respectively. According to Janssen (1981), the shear strength should be greater at the nodal regions. The reason being that in the internodal regions the fibers run in one direction only, which allows shear forces to propagate in the weaker matrix material. Thus, at a nodal region, where the fibers run in multiple directions, the shear stress must propagate beyond the matrix and overcome a number of stronger fibers, thereby increasing the shear strength. The expectation of higher shear strength at the node was confirmed by the results of the tests. The standard deviation of the test series was 25%, which is more than twice that of the compression test (12%). The internodal shear tests exhibit a higher variation (30%) than the nodal specimens (22%).

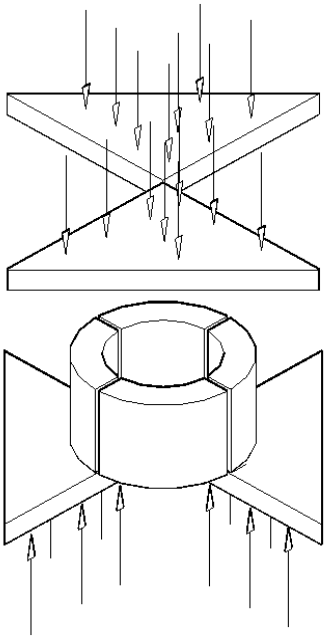

(a) schematic of test specimen and setup

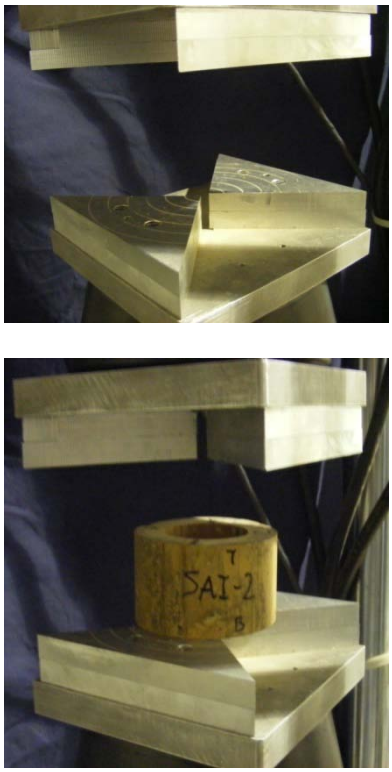

(b) test set up (top) and specimen in test machine

(c) typical shear failures with four failure planes

Figure 2.2 Shear test.

2.1.3 Experimentally Derived Bamboo Material Properties

Listed in Table 2.1 are the values that were determined from the University of Pittsburgh (PITT) test program (Mitch 2009) reported in the previous two sections as well as values that were reported in literature from the University of Washington (UW) (Washington 2002), the University of Hawaii (UH) (unpublished data), and two versions of the ICC Evaluation Services ESR-1636 report on properties of Tre Gai bamboo (ICC 2004 and 2006). Also shown are the average values for bamboo in the Group A classification, into which Tre Gai would fall, of the National Building Code of India (NBCI 2005). The values that are presented in the table are either the mean (m), or the mean minus two standard deviations (m-2s) which represents useable

design values. The values given in Group A for the NBCI did not specify the amount of the reduction from the mean used to obtain the design values. While not important for the current work, the tension parallel to the fibers, tension perpendicular to the fibers, and the flexural strength of Tre Gai are also listed in Table 2.1 where they are available. Finally, a comparison to reported material properties of common timber species (American Forest 1997) is also presented.

The variation in reported properties of purportedly the same bamboo species is striking. Reasons for this variation cannot be established with certainty but may include: a) the age at which the bamboo is harvested; b) the location along the culm at which the material properties are determined; c) the moisture content at testing; d) the storage conditions (long term moisture conditions); e) the treatment (if any) of the culm; and f) the age of the culm. For instance, the Tre Gai tested in the present study was harvested in Vietnam and borate-treated prior to being exported to a US supplier. Once at PITT, the bamboo has been stored in a dry laboratory condition and tested similarly. As previously noted, older, drier bamboo will have a markedly increased compressive strength as is noted in Table 2.1. Unfortunately, due to the need to order bamboo from suppliers, harvesting, age and storage data is uncertain. Such information is similarly not specified in the other studies cited in Table 2.1.

Table 2.1 Comparison of design values for Tre Gai bamboo (adapted from Mitch 2009).

Study	**value reported** m = mean s = std. dev.	**Compression**	**Shear**	**Tension Parallel to Fibers**	**Tension Perpendicular to Fibers**	**Flexure**
		ksi (MPa)	psi (MPa)	ksi (MPa)	psi (MPa)	ksi (MPa)
Present study	m	8.22 (56.7)	1330 (9.2)	-	153 (1.06)	-
	m-2s	6.19 (42.7)	670 (4.6)	-	86 (0.59)	-
University of Washington	m-Ks	2.31 (15.9)	413 (2.85)	4.35 (30.0)	-	5.87 (40.5)
ESR-1636-2004	m-2s	2.58 (17.8)	460 (3.17)	4.89 (33.7)	-	6.63 (45.7)
ESR-1636-2006		1.33 (9.2)	420 (2.88)	2.51 (17.3)	-	3.36 (23.2)
NBCI Group A avg	m-Ks	1.89 (13.0)	-	-	-	2.9 (20.0)
University of Hawaii	m	2.38 (16.4)	440 (3.03)	4.74 (32.7)	-	3.7 (25.5)
	m-2s	1.68 (11.6)	-	-	-	-
Douglas Fir	m-Ks	1.70 (11.7)	95 (0.66)	1.00 (6.9)	-	1.5 (10.3)
Southern Pine		2.1 (14.5)	100 (0.69)	1.6 (11.0)	-	2.85 (19.7)

2.1.4 Geometric Variation

As previously mentioned, the fact that bamboo is an organic material means that there is a significant amount of geometric variability between culms and between different locations on the same culm. Table 2.2 is a summary of the geometric properties of the Tre Gai specimens described in the preceding sections. These specimens were cut from six different eight foot long culms. As can be seen, compared to an engineered material such as sawn lumber, the geometric variation is quite high.

While the outside diameter does vary, the variation is small (average standard deviation is 4.4%) compared to the variation in the wall thickness (17.7%). The variation in wall thickness is also more important than the variation in diameter, as the failure of bamboo is often associated with a splitting or shear failure, and a single thinner section of bamboo wall could cause an early failure. Finally, recall that these variations in geometry are in addition to the variations in

physical properties such as compressive and shear strength, which when combined, can result in a high degree of uncertainty when trying to design a structure using bamboo. For example, based on the test method and 'allowable stresses' reported by ICC (2006) shown in Table 2.1, the equivalent material resistance factor, conventionally denoted φ, is only 0.44 (Mitch 2009).

Table 2.2 Measured specimen dimensions.

	Outside Diameter, in. (mm)			**Culm Wall Thickness, in. (mm)**		
Culm	**mean**	**Standard deviation (ratio)**	**n**	**mean**	**Standard deviation (ratio)**	**n**
1	3.57 (90.7)	0.023	27	0.82 (20.7)	0.099	64
2	3.59 (91.1)	0.022	11	0.84 (21.2)	0.107	28
3	3.31 (84.0)	0.016	17	0.64 (16.3)	0.144	36
4	3.50 (89.0)	0.016	9	0.60 (15.3)	0.094	24
5	3.86 (98.0)	0.013	4	0.58 (14.7)	0.047	4
6	3.56 (90.5)	0.010	4	0.53 (13.5)	0.053	8
Entire Sample	3.52 (89.35)	0.019	72	0.732 (18.6)	0.106	168

2.2 REINFORCING STEEL AND GROUT PROPERTIES

The following sections describe the material properties of the reinforcing steel and grout used to fabricate the grouted-bar column base specimens.

2.2.1 Material Properties of #4 and # 5 Reinforcing Steel

Three #4 and three #5 bar samples from the batch used to fabricate the grouted-bar specimens were tested in tension until failure in a universal tension machine. The full bar section tests were

generally compliant with the requirements of ASTM E8 (2009). Strain was measured using an external clip gage which was removed following yield (to avoid damage to the gage). Ultimate strain was recorded by measuring the final deformation of a predetermined gauge length (punch mark method). The load was measured using the internal load cell in the universal testing machine. The results of the six tests are summarized in Table 2.3 and Figure 2.3. All bars are conventional ASTM A615 Grade 60 bars.

Table 2.3 Reinforcing Bar Material Properties.

Bar Size	Yield Stress	Ultimate Stress	Elongation at Rupture	Average Yield Stress	Average Ultimate Stress
	ksi	ksi	%	ksi	ksi
4	68.3	107.0	17.9	65.3	103.8
4	64.4	101.9	19.3		
4	63.1	102.4	17.6		
5	59.5	106.6	9.4	61.4	106.2
5	62.0	105.8	16.4		
5	62.6	106.0	18.0		

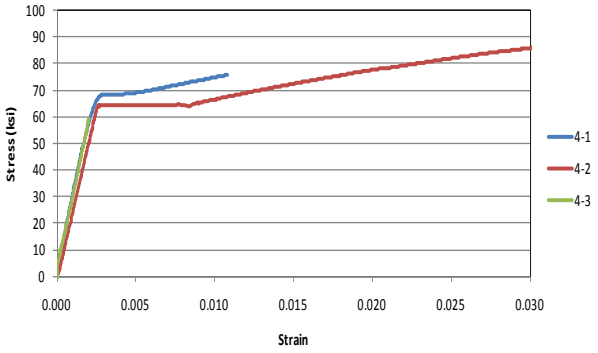

(a) Stress vs. strain for #4 bars

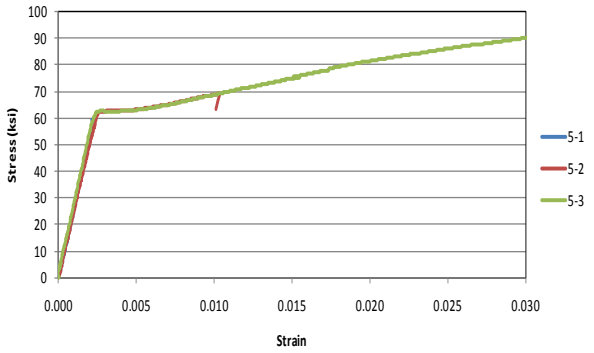

(b) Stress vs. strain for #5 bars

Figure 2.3 Measured stress vs. strain response of reinforcing bars used in grouted-bar column base connections.

2.2.2 Material Properties of Grout

The grout used in all of the connections was SikaGrout 212 (Sika 2003). This is a non-shrink grout (although not an expansive grout) and therefore should permit friction between the grout and the bamboo wall to develop. To facilitate flow into the culms, the grout was necessarily mixed with more water than would be normally required. Thus, it is not anticipated that the manufacturer specified material properties would be attained. A series of 2 in. grout cubes were cast during column base specimen construction and were allowed to cure for 28 days in a 100% humidity cure room, which represented better curing conditions than those that would be encountered in the field. Compression testing was done according to ASTM C942 (2004) and resulted in an average compressive strength of 3400 psi. This is significantly lower than the 5800 psi value given by the manufacturer for the "fluid flow condition" grout and is most likely due to the excessive amount of water added to the grout to ensure flowability. Also, as the author has had first-hand experience with the construction practices in the Darjeeling region of India, the author can confidently state that the laboratory mix is still likely to have better material properties and consistency than that encountered in the field.

2.3 GROUTED-BAR CONNECTION CONSTRUCTION TECHNIQUE

For both the column base tests and the pull-out tests described below, the same construction technique was used to create the grouted reinforcing bar/bamboo connections. Due to the treatment technique, the bamboo used in this program came with a hole (approximately 1 in. diameter) drilled down the center of the culm through the nodal regions. The nodal regions were

not broken out further since this hole was deemed large enough to allow the fluid grout to flow as desired. The method of fabrication was as follows (Figure 2.4):

1. The bottom of the culm was sealed with duct tape.
2. Weep/fill holes were drilled horizontally through the culm wall at the top of each internodal region up to the top of the desired embedment length.
3. The grout was poured into the uppermost hole, and as the level of the grout rose in the culm, each subsequent hole was closed off with a layer of duct tape. Using the weep holes ensured that each internodal region was entirely full of grout and allowed the air to escape.
4. The grout-filled culm was placed over top of the embedded reinforcing bar (already in position), and pushed down until the bar was forced through the tape and the culm was resting on the concrete base.

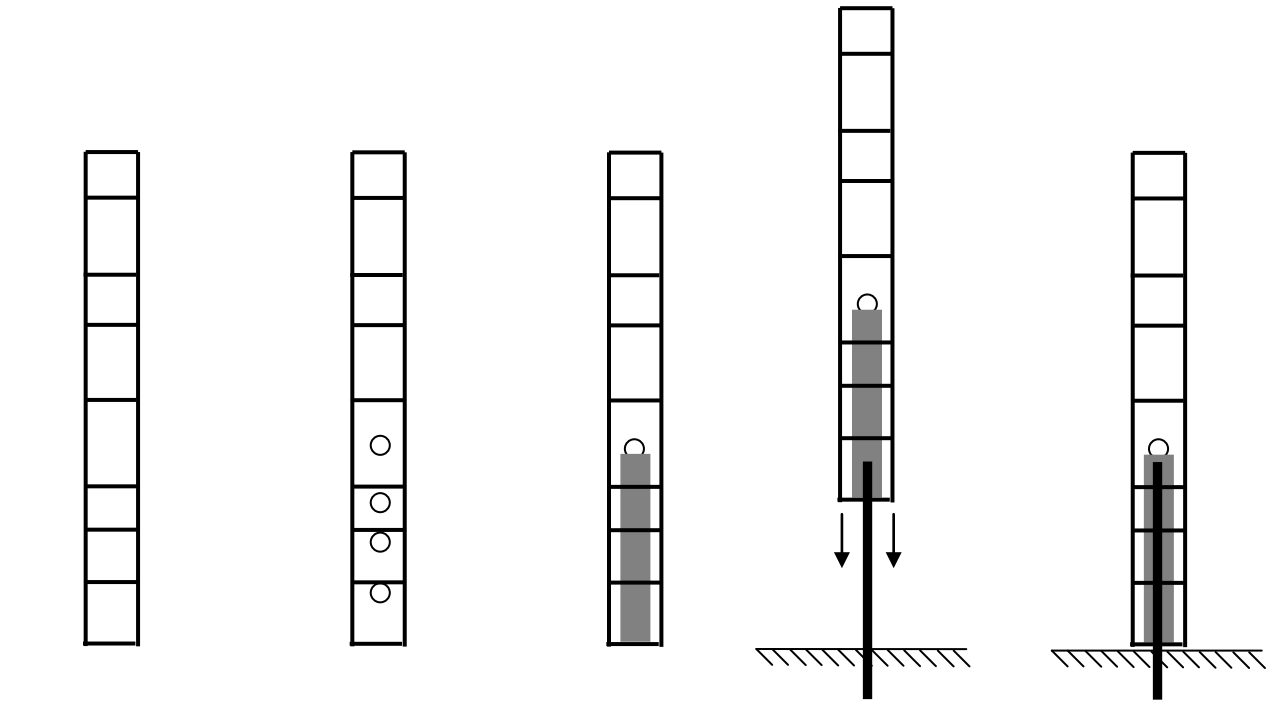

Figure 2.4 Construction stages.

2.4 GROUTED-BAR PULL-OUT TESTS

2.4.1 Setup and Basic Instrumentation

An analysis of the pull-out strength of the grouted-bar connection depends on two behaviors: the behavior of the reinforcing bar within the grout and the behavior of the grout within the culm. The behavior of reinforcing bars within concrete has been studied extensively and thus will not be investigated in this work. Rather, this test series focused on the behavior of the bar and grout within the bamboo culm. The test specimen is shown in Figure 2.5. Each specimen contains two grouted connections, one at the top and one at the bottom. This setup was chosen as it allows one piece of bamboo to be used for two tests and allows the specimen to be tested in direct tension using a universal testing machine. It is noted that two reinforcing bars are used, the bar is not continuous through the specimen.

To monitor the failure of the specimen, two Linear Variable Differential Transformers (LVDT's) were used for each connection. The LVDTs were clamped to the portion of the reinforcing bar extending from the culm, with the first LVDT touching the grout and the second touching the bamboo wall (see Figure 2.5b). Thus, the first LVDT measures the displacement of the bar relative to the grout (reinforcing bar pull-out) and the second LVDT measures the displacement of the bar relative to the bamboo (grout plug pull-out).

As these specimens contained two grouted connections, a method was required that would allow one connection to fail, and then have its capacity increased enough to allow the second connection to fail. To achieve this additional strength after failure, hose clamps were applied to the side that failed in order to increase the amount of friction and to close any cracks

(see Figure 2.5c). This approached worked very well, effectively mitigating further slip of the initial failure.

(a) Pull-out test specimen

(b) Pull-out test instrumentation

(c) Hose clamps used as reinforcement

Figure 2.5 Pull-out test.

A construction technique similar to that used for the single and four culm column base tests was used for the pull-out tests. The specimens were capped on the end with duct tape and were filled node by node until the desired embedment length was reached. The culms were then placed on top of the desired bars and downward force was applied until the bars pierced the duct tape and went into the culm; the excess displaced grout was allowed to bleed out of the uppermost hole. After 48 hours, the specimens were inverted and the same procedure was followed for the second set of bars. This technique allowed the bars to be grouted with the high degree of precision necessary for the direct tension test to result in concentric loading of both connections while still ensuring that there was no interaction between the top and bottom grout regions. The grout was allowed to cure for at least one week before testing. The specimens were

tested in a universal tension testing machine with self-centering grips at a loading rate of approximately 50 lb/sec. Four tests were conducted: two having #4 bars and two with #5 bars. Embedment lengths of 12 and 24 inches were provided as described in Section 3.1.

2.4.2 Possible Failure Modes

There are three possible failure mechanisms for the pull-out test: a) yield of the reinforcing bar (likely outside the culm embedment); b) failure at grout-reinforcing bar interface resulting in bar pull-out (reinforcing bar development length-related failure); and, c) failure at the grout-bamboo interface resulting in grout plug pull-out. The latter failure results in shear failure of all engaged nodes. These failures are shown schematically in Figure 2.6.

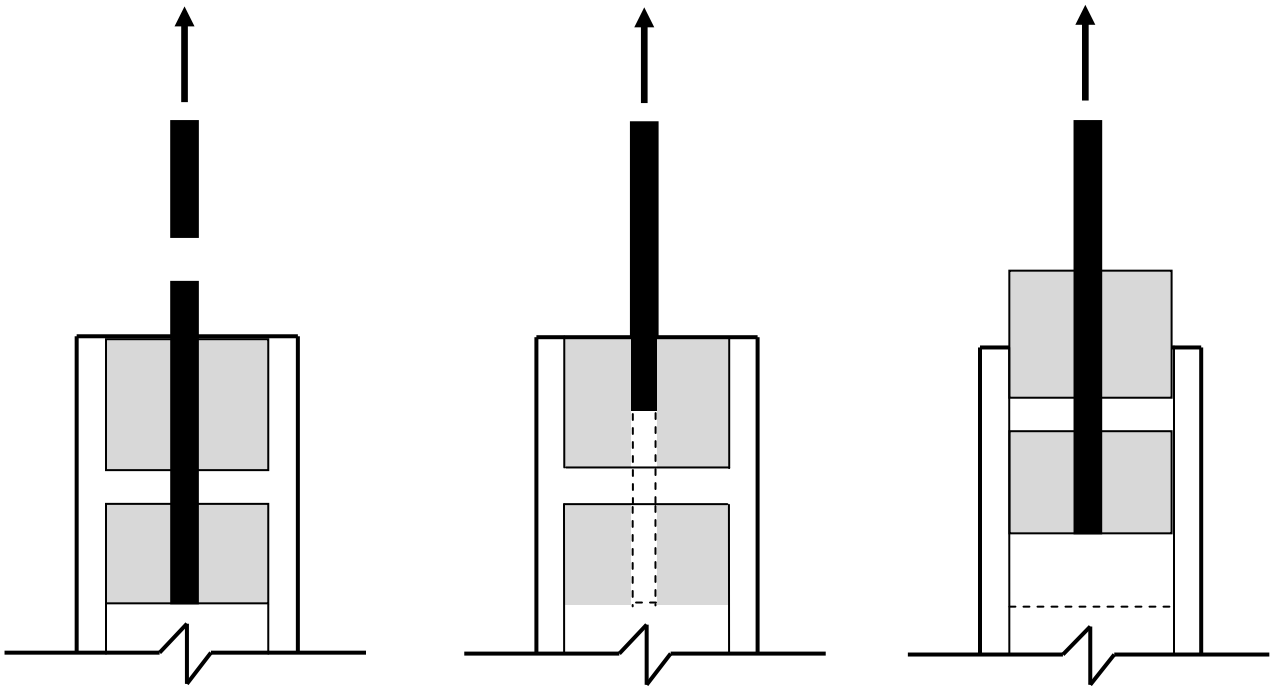

(a) Bar Failure (b) Bar Pull-Out (c) Plug Pull-Out

Figure 2.6 Potential failure modes for pull-out test.

The specimens were expected to fail in the third mode: extracting the entire grouted region from the bamboo, as was seen in Sharma's (2010) tests. If the resistance to such plug pull-out failure was especially high, the bar might be expected to yield. The development lengths of #4 and #5 bars are calculated to be 12.3 and 15.4 inches, respectively, based on ACI 318 (2008) equation 12-1 for development length. This calculation assumes that the confinement provided by the culm is adequate to result in bar pull-out (i.e.: $(c_b + K_{tr})/d_b = 2.5$):

$$l_d = \frac{3}{40}\frac{f_y}{\lambda\sqrt{f_c'}}\frac{\psi_t\psi_e\psi_s}{\left(\frac{c_b+K_{tr}}{d_b}\right)} = \frac{3}{40}\frac{60000}{1\sqrt{3400}}\frac{1*1*0.8}{(2.5)} = 24.7\,d_b = 15.4 \text{ for \#5 and } 12.3 for\ \#4 \qquad \text{(Eq. 2.2)}$$

The use of the limiting value of $(c_b + K_{tr})/d_b = 2.5$ is felt to be justified provided the bamboo culm remains intact. If the culm splits, certainly the confinement will be lost ($K_{tr} = 0$, resulting in ratio of $c_b/d_b \approx 1$ in this case), however if the culm does split, the resistance to grout-plug pull-out is lost and this failure mode will dominate. Based on previous observations, including those of Sharma (2010), it is not anticipated that the bar capacity or bar pull-out will be achieved, but rather failure will be dominated by grout-plug pull-out.

2.5 GROUTED-BAR COLUMN BASE TESTS

The objective of the single culm and four-culm column base tests is to determine the behavior of the grouted-bar column base connections subject to lateral load. The portal frame test conducted by Sharma (2010) demonstrated that the column base behavior is critical to the frame behavior and was not as stiff as anticipated. The column base tests are full-scale tests of single and four-culm columns. Lateral load is applied at the midheight of the column, representing the conceptual point of inflection for a fixed column. The connections are representative of those

encountered in service in India (Figure 1.3) consisting of a reinforcing bar embedded in a concrete base (plinth in Figure 1.3). The extended portion of reinforcing bar is then grouted into the bamboo culm as described in Section 2.3. Parameters tested include bar size (#4 and #5) and embedment length (12 and 24 inches).

In all tests, the reinforcing bar is embedded into existing concrete beams which are intended to serve as the foundations. The two beams used were previously tested fatigue specimens (Soltani 2010). The beams were 16 in. deep, 12 in. wide and 18.5 ft long, weighing approximately 3700 lbs – thus they were 'rigid' bases and provided stability for the self-reacting test set-up used. The concrete strength was 9800 psi. The reinforcing bars for this test were grouted into drilled holes. The holes were located inside the existing beam reinforcing bar cage and were thus confined in the foundation. In no test was any distress to the embedded connection or the beams noted. Thus the concrete foundation may be considered rigid and will not be addressed further in this study.

Specimens were tested in pairs, resulting in self-reacting test set-ups. Once the first of a specimen pair failed, it was reinforced and the testing of the second specimen continued. The load set-ups are described in the following sections.

2.5.1 Single Culm Grouted-Bar Column Base Tests

The single-culm column base test setup is shown in the Figure 2.7. The culms are four feet tall, which corresponds to the half height (i.e.: point of inflection) of culms that are found in the field. In order to investigate the effect of reinforcing bar size and embedment length, #4 and #5 bars, each having 12 inch and 24 inch embedment lengths into the bamboo culm were tested.

The specimens were tested in pairs. The load was applied using a tension tie arranged between the culms and the culms were pulled toward each other. The tension tie consisted of two 9 in. stroke turnbuckles and a load cell arranged between and the tops of the bamboo culms. The connection between the turnbuckles and the load cell were simple threaded connections. The connections from the turnbuckles to the bamboo culms were complicated since the geometry of the bamboo is difficult to load without causing a localized failure. To achieve distributed loading unlikely to damage the culm, the top internode of the bamboo was filled with non-shrink grout, a steel plate was placed on top of the culm, and a 5 in. long bolt was placed through the plate and into the grout-filled top of the bamboo. The setup was then left to cure for 48hrs to ensure sufficient grout strength. A hose clamp was placed at the top of the culm to provide additional splitting resistance.

To avoid introducing unwanted torsional effects, two separate joints were used in each connection. Each turnbuckle ends in a vertically oriented clevis, which avoids any unwanted rotation about the y-axis (shown in Figure 2.8b) that may be introduced by the load arrangement through the large deflections anticipated. A second vertically oriented bolt loosely connected the clevis to the plate previously attached to the culm; thus eliminating out-of-plane rotation (about the z axis). The entire loading arrangement is shown in Figures 2.8a and b.

Since two culms were tested at the same time, one side failed before the other. This meant that a braced had to be employed on the side that failed in order to continue loading the second side to failure. A simple knee brace (Figure 2.8c), consisting of 2 x 4 in. lumber at a 45 degree angle was used. The brace was placed to support the failed side, clamped into place, and the test resumed.

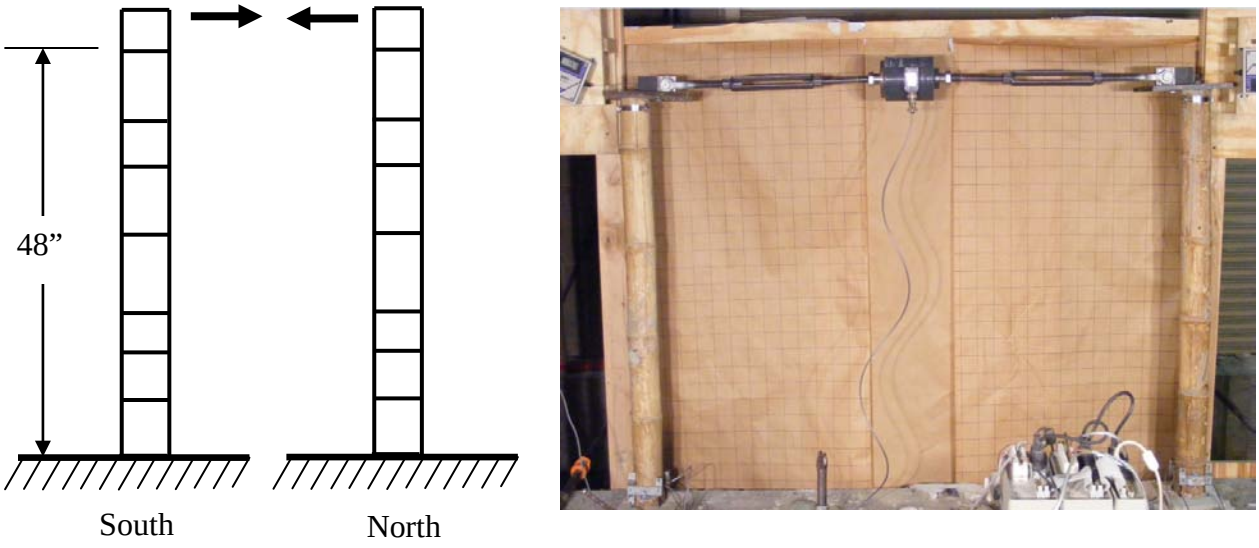

(a) Conceptualized column base test setup (b) Actual column base test setup

Figure 2.7 Single culm column base test.

Loading is applied using alternating turns on the turnbuckles (thus keeping the length of each turnbuckle similar and the load cell centered. The loading of the single culm specimens was done in increasing increments of 50 pounds. The load was applied, released and re-applied to the next increment. This load history permitted both the capacity and hysteretic behavior of the column bases to be assessed. The hysteretic behavior is important since the over-riding motivation of this research program is hazard mitigation in a seismic environment.

The deflection at the location of the applied load of each culm was measured using a draw-wire transducer (DWT) as shown in Figure 2.8d. The total applied load was determined from a load cell placed between the two culms (see Figure 2.8).

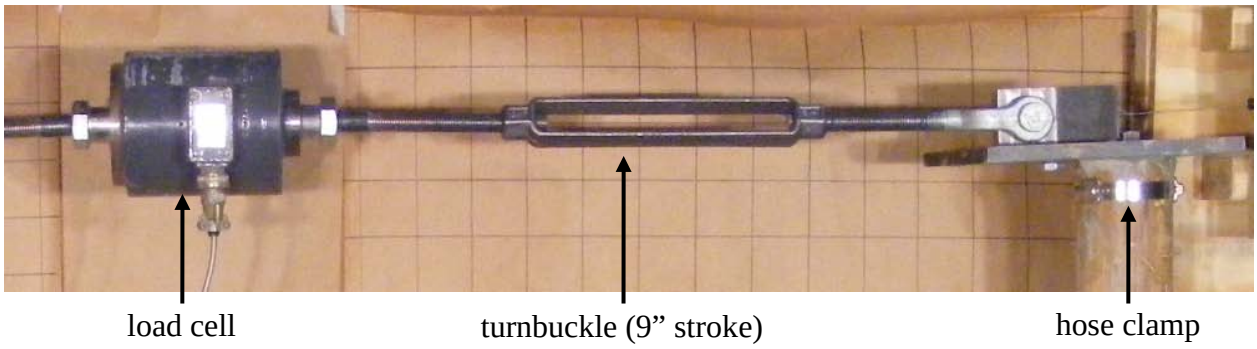

(a) Tension tie components

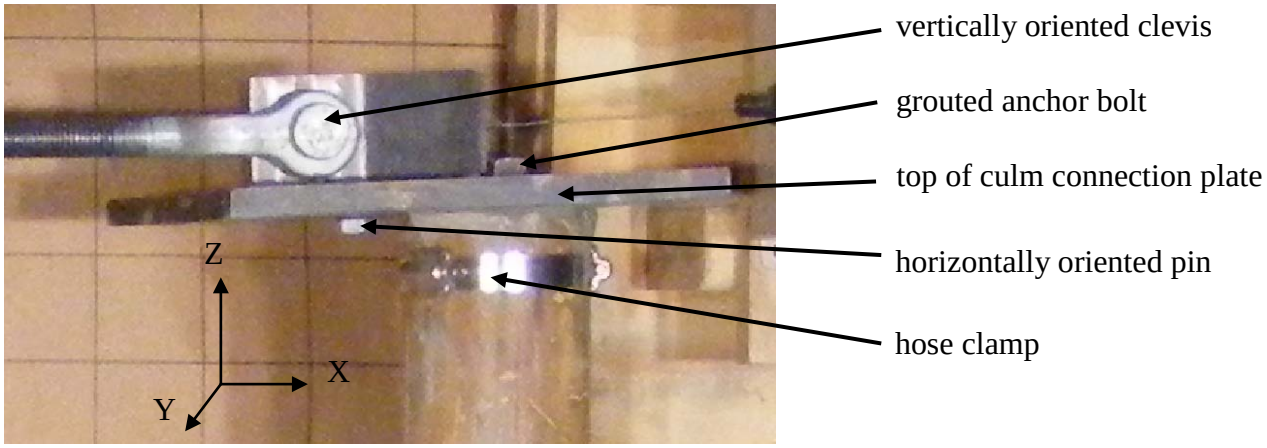

(b) Connection to culm (see right-hand side of Figure a)

(c) Brace used to support first failed column

(d) Draw-wire transducer – measures total displacement at location of applied load

Figure 2.8 Single culm column base test components.

2.5.1.1 Rigid body rotation of culm

The total lateral deflection of each culm (δ) was assumed to be due to a combination of rigid body rotation at the base ($\delta_\theta = \theta h$) or flexural along the cantilever length ($\delta - \delta_\theta = Vh^3/3EI_{culm}$) as shown in Figure 2.9. This type of combined behavior is difficult to capture and thus required additional instrumentation for each specimen.

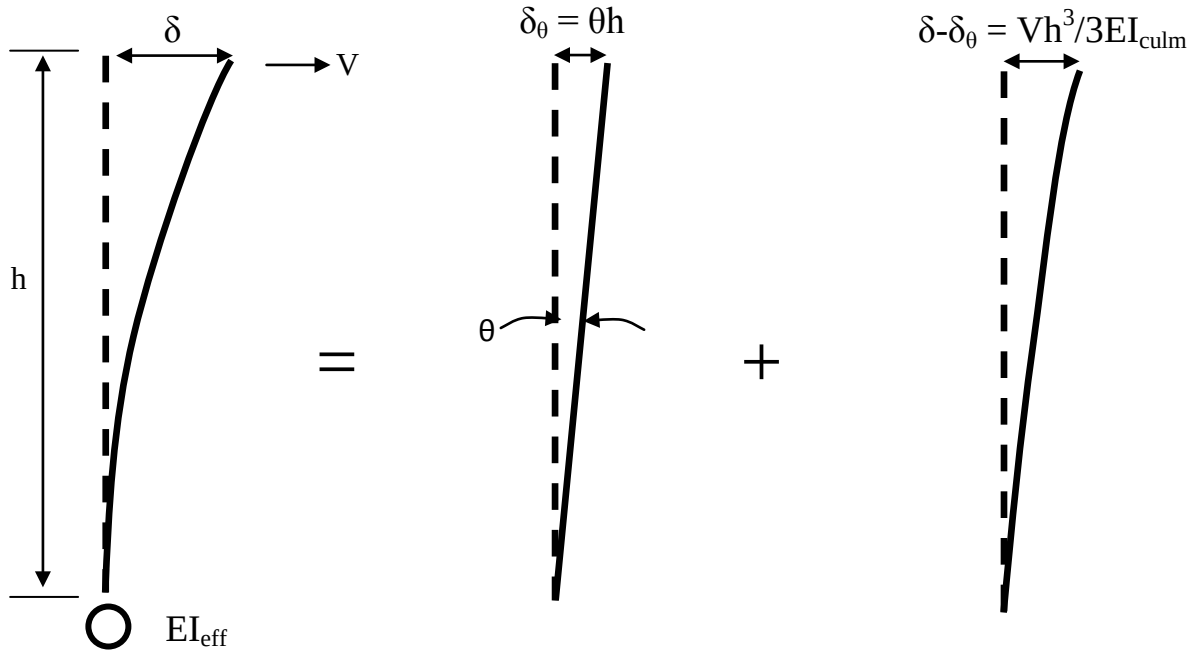

(a) Total displacement (b) Rigid body rotation about base (c) Flexural behavior of cantilever

Figure 2.9 Components of cantilever column specimen deflection.

Determining the rotation of the culm at the base is complicated by the fact that the centroid of the bamboo culm is not necessarily the neutral axis of the grouted culm connection. If the reinforcing bar provided the only flexural resistance – as a notional hinge – the lateral load capacity of the column base tested is only 15 lbs and 30 lbs for #4 and #5 bars, respectively. The moment resistance of the connection results from the couple developed between the compression at the leading face of the bamboo and tension in the reinforcing bar (see Figure 2.10). This presents a difficulty in determining the size of the compression block at the leading edge of the

bamboo. Complicating this determination is the fact that the bamboo or grout at the leading (compression) face may yield or crush, which means that the size of the compression block can change throughout the test. To account for and capture this complicated behavior, a “rotation gauge” was developed and two were placed at the base of each culm (Figure 2.11). These gauges were affixed to the bamboo culm using epoxy in order to avoid any stress concentrations a screw or bolt hole would induce in the bamboo. A flat plaster pad was placed beneath each LVDT in order to minimize effects of the uneven concrete surface (Figure 2.11b).

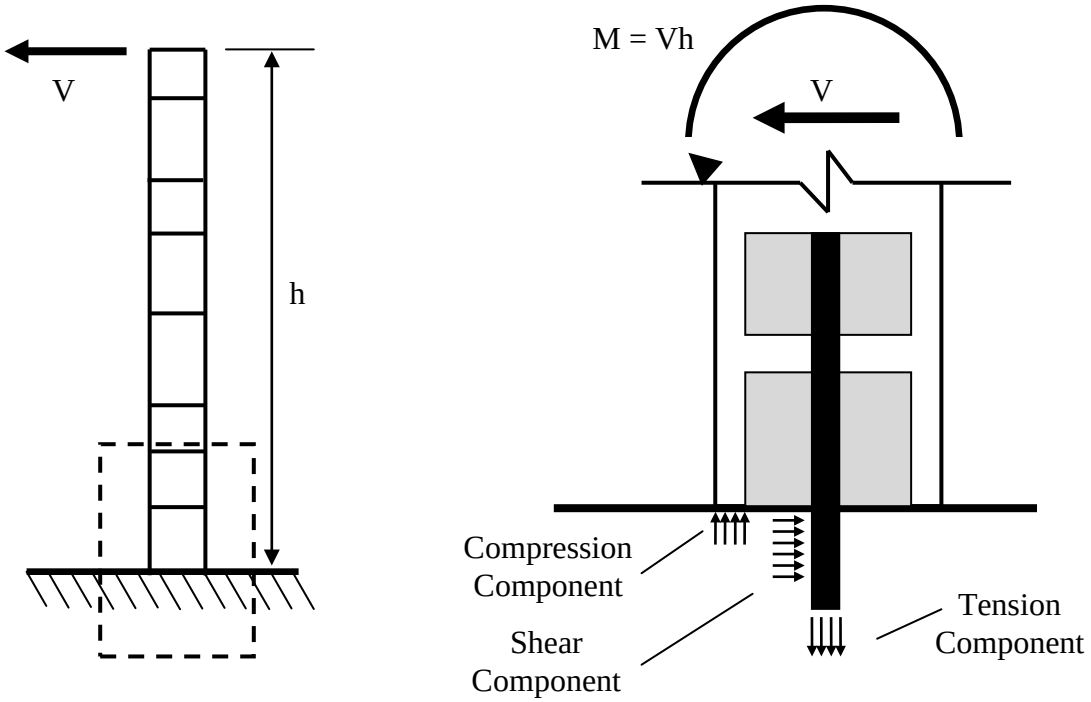

(a) Single culm in bending

(b) Moment couple between compression in bamboo wall and tension in reinforcing bar

Figure 2.10 Expected joint behavior.

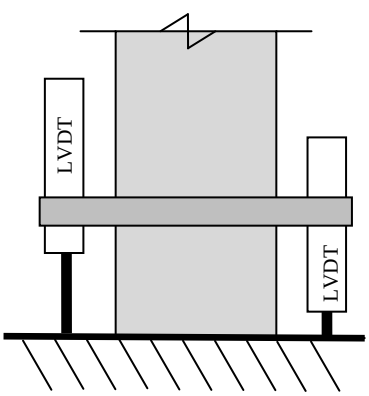

(a) Schematic of rotation gauge (column loaded toward left)

(b) Actual gauge

(c) Gauges in use

Figure 2.11 Rotation Gauge.

The rotation gauges gives the displacement at each end of the gauge length. Based on this, and the gauge and culm dimensions, the location of the neutral axis and column base rotation (θ) may be determined (assuming that plane sections remain plane) as follows and is shown in Figure 2.12.

The first step in determining the rotation (θ) is determining the location of the neutral axis. Using a plane sections assumption, the ratio of the absolute displacement of one LVDT (Δ_1) to the absolute sum of the measured displacements ($\Delta_1 + \Delta_2$) multiplied by the gauge length (3.125 in.) will give the location of the neutral axis relative to the location where Δ_1 is measured (Figure 2.12d):

$$NA = \left(\frac{\Delta_1}{\Delta_1+\Delta_2}\right) * 3.125 \qquad \text{(Eq. 2.3)}$$

Now that the location of the neutral axis has been determined, the rotation (θ) can be determined from trigonometry. Assuming small angles:

$$\theta = \sin^{-1}\left(\frac{\Delta_1}{NA}\right) \qquad \text{(Eq. 2.4)}$$

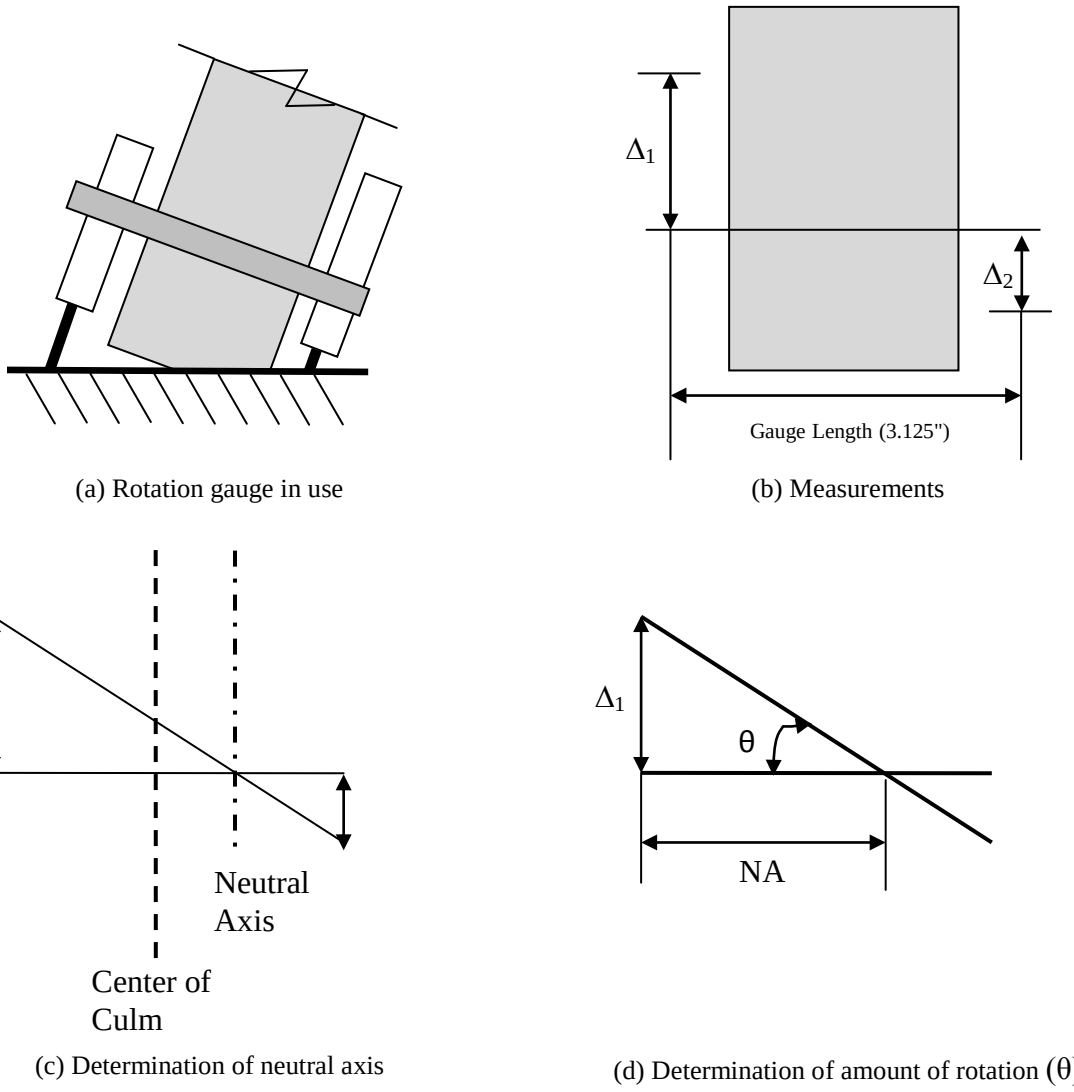

(a) Rotation gauge in use

(b) Measurements

(c) Determination of neutral axis

(d) Determination of amount of rotation (θ)

Figure 2.12 Geometry of culm rotation measurements.

Once the rotation at the base of the culm (θ) has been determined, one can obtain the component of displacement at the location of the applied load associated with rigid body rotation as simply $\delta_\theta = \theta h$. Thus, two of the three displacement components are known; the total displacement and the displacement due to rigid body motion. By subtracting the displacement due to rigid body rotation from the total displacement, one obtains the displacement associated with flexure of the cantilever column. Based on the flexural behavior of the cantilever column,

an apparent flexural stiffness, EI_{culm}, of the culm may be calculated based on the cantilever height, h, and the deflection associated with flexure, δ-δ_θ:

$$EI_{culm} = \frac{Vh^3}{3(\delta - \delta_\theta)} \quad \text{(Eq. 2.5)}$$

Similarly, an effective flexural stiffness, EI_{eff}, accounting for rigid body rotation may be calculated based on total lateral deflection, δ:

$$EI_{eff} = \frac{Vh^3}{3\delta} \quad \text{(Eq. 2.6)}$$

2.5.2 Four Culm Grouted-Bar Column Base Tests

For a variety of reasons, columns comprised of four-culms are often used (Figures 1.1-1.3). Four culm arrangements have a) greater axial and lateral load carrying capacity; b) lend themselves well to concentric connections (Figure 1.2b); c) allow the use of more easily handled and/or readily available smaller culm sizes; and d) can, through judicious culm matching, mitigate effects of culm out-of straightness. For the four-culm columns considered in this work and those found at St. Joseph's School (Figures 1.1 – 1.3), no shear transfer between the culms along their length is provided. The culm geometry is, however, constrained at both the base (concrete plinth) and top (roof truss connection). Since no shear transfer is provided, the behavior of the individual culms in the four culm column base is anticipated to be similar to the behavior of the culms in the single culm column base tests. A series of four-culm column base tests (Figure 2.13) was conducted; the results will be contrasted with those of the single culm column tests in order to develop a model for such column base behavior. It should be noted that the culms used in the four culm column tests were smaller than those used in the single culm column tests.

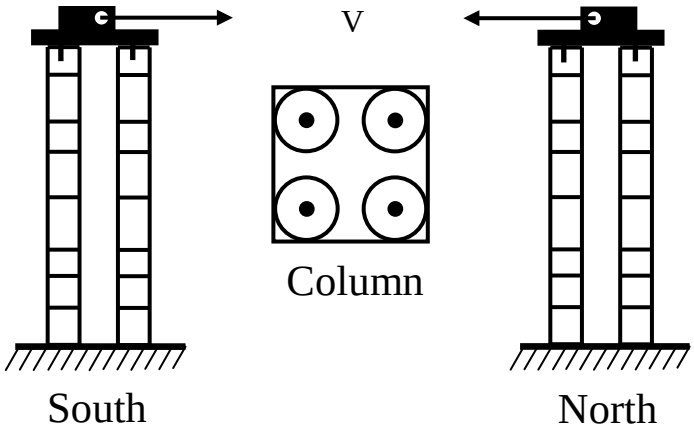

(a) Conceptual setup of four culm bending test

(b) Actual four culm bending test

c) Test components for four culm test setup

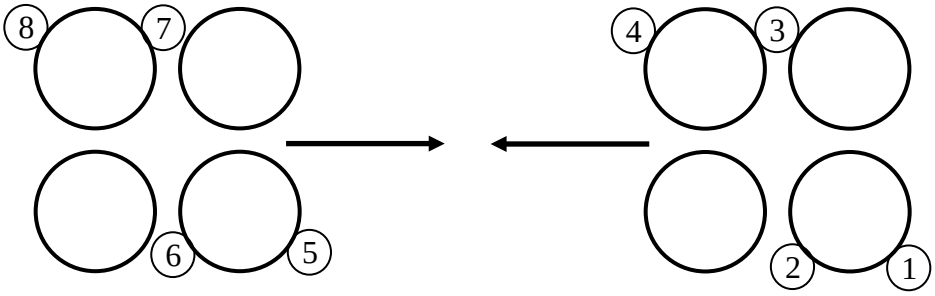

d) Location of rotation gauges

Figure 2.13 Four culm bending test setup.

The construction, instrumentation, and testing of the four-culm column base specimens was essentially the same as that for the single culm tests reported in the previous section. Each culm was mounted to the loading plate as for the single culm tests. The plate effectively

constrained the four culm geometry at this location (Figure 2.13c). All other details of the plate (clevises, etc.) remain the same; indeed, the same plates were used for both one and four culm tests.

2.5.2.1 Rigid body rotation of culms

Since there are a total of eight culms per test, each culm cannot have a rotation gauge as was the case in the single culm tests. Instead, two culms from each four culm column received a gauge, as shown in Figure 2.13d. This instrumentation scheme permits comparison of the behavior of one culm on the trailing or "tension" face of the column to one culm on the leading or "compression" face. The total lateral deflection of the specimen (δ) was assumed to be due to a combination of rigid body rotation of each culm ($\delta_\theta = \theta h$) which is analogous to shear distortion (racking) of the four-culm column as shown in Figure 2.14 and flexural along the cantilever length ($\delta - \delta_\theta = Vh^3/3EI_{column}$), as shown schematically in Figure 2.9.

The basis of calculation is the same as given for the single culm column. Based on the flexural behavior of the cantilever column, an apparent flexural stiffness, EI_{column} of the four culm column may be calculated based on the cantilever height, h, and the deflection associated with flexure $\delta - \delta_\theta$:

$$EI_{\text{column}} = \frac{Vh^3}{3(\delta - \delta_\theta)} \qquad \text{(Eq. 2.7)}$$

Similarly, an effective flexural stiffness for the entire column, EI_{eff}, accounting for rigid body rotation may be calculated based on total lateral deflection, δ, as given by Equation 2.7.

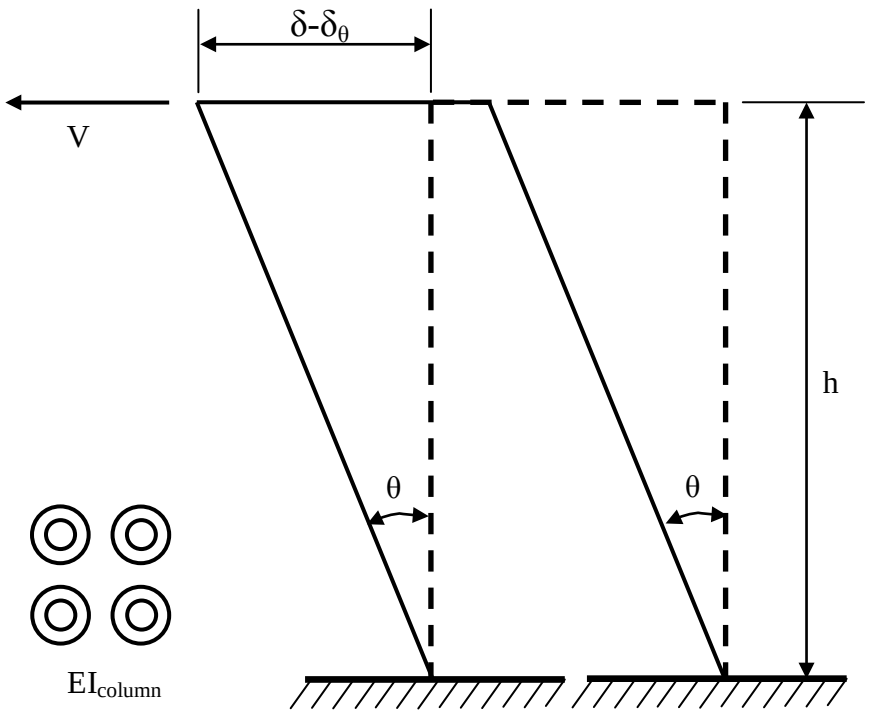

Figure 2.14 Racking behavior of four culm test.

2.6 BAMBOO SELECTION

The bamboo used in this work was taken from a total of 15 individual culms of Tre Gai (*bambusa Stenostachya)* bamboo. The culms were roughly sorted based on outside diameter, with the smaller culms being used in the four culm column base tests and the larger culms being used in the single culm column base tests and pull-out tests. The culms were provided in lengths of twelve feet, which were cut into three four foot pieces. The pieces used in the four culm tests were taken from different culms, in order to prevent any single culm from dominating a test. As three four foot pieces were obtained from each culm, it was possible to use the same piece of bamboo for both a single culm test and a pull out test. Specimen details, including culm selection are presented in the following chapter.

3.0 RESULTS FROM EXPERIMENTAL PROGRAM

3.1 NAMING CONVENTIONS

All pull-out tests, single culm bending tests, and four culm bending tests follow a similar naming convention. Four "tests" were conducted consisting of two duplicate specimens each, for a total of eight specimens for each test. In all test series, the test identification corresponds to both a bar size and embedment length as indicated in Table 3.1.

Table 3.1 General Naming Convention.

Test Name	Bar Size	Embedment Length
Test A	#4	12 in.
Test B	#4	24 in.
Test C	#5	12 in.
Test D	#5	24 in.

3.1.1 Pullout Tests

Four separate pull-out tests were conducted. As each test consisted of two specimens within one culm, the tests were named PA through PD and were assigned a "T" or "B" for the top and bottom of the specimen, respectively. Thus PAT refers to the top half of the pull out test specimen having a #4 bar with 12 in. embedment length.

3.1.2 Single Culm Column Base Tests

Four single culm tests were named according to the procedure listed in Table 3.1: Tests 1A through 1D. As each test was made up of two culms, the side that failed first was named "1A" through "1D". This was then braced and the second culm was tested to failure. The second (or retest) was named "$1A_R$" through "$1D_R$".

3.1.3 Four Culm Column Base Tests

Four four-culm tests were named according to the procedure listed in Table 3.1: Tests 4A through 4D. As each test was made up of eight culms but only four were instrumented, each test has four culms of interest. The side that failed first was named "4A1" and "4A2" through "4D1" and "4D2", where the "1" and "2" designate the instrumented culm as shown in Figure 3.8. The failed column was braced and the second column was tested to failure; this was designated "4AR1" and "4AR2" through "4DR1" and "4DR2".

3.2 PULL-OUT TESTS

Four pull-out tests, each containing two specimens (top and bottom), were conducted. The bar size used was either #4 (cross sectional area = 0.2 in^2) or #5 (0.31 in^2) and the embedment length into the bamboo was either 12 or 24 in. Following failure of one end of the specimen, hose clamps were applied to that end and the specimen was reloaded until the second end failed. All failures were of the "grout plug pull-put" (Figure 2.6c) type and occurred following significant

longitudinal splitting at the ends of the specimen. The results are summarized in Table 3.2 and examples of the failures are shown in Figure 3.1.

Table 3.2 Pull-out test results.

Specimen	Culm	Bar Size	Embedment Length	Culm Outside Diameter	Culm Wall Thickness	Applied Load at failure	Number of Nodes Engaged
			in	in	in (avg)	lb	
PAB	O2	#4	12	3.53	0.50	130	0
PAT	O2	#4	12	3.69	0.44	2822	1
PBB	N3	#4	24	3.52	0.74	6400	3
PBT	N3	#4	24	3.65	0.98	7800	3.5
PCB	L3	#5	12	3.12	0.62	3603	1
PCT	L3	#5	12	2.97	0.53	1640	1
PDB	M1	#5	24	3.09	0.64	5908	3
PDT	M1	#5	24	3.45	0.80	9169	4

(a) Specimen PCB (b) Specimen PDB

Figure 3.1 Splitting and grout plug pull-out at ends of pull-out tests.

Pull-out test results are shown in Figure 3.2. Each plot shows both the grout plug movement relative to the culm and the reinforcing bar slip relative to the grout plug. The latter

data is only available for the bottom (P*x*B) data since the top of each culm was located at a node. Because the tests were effectively conducted in displacement control, the load is seen to drop instantaneously at the each instance of culm longitudinal cracking.

As can be seen in Figure 3.2, there was essentially no motion of the bar relative to the grout. This should be expected since the greatest stress developed in the reinforcing steel was only approximately $0.65f_y$ = 39 ksi (specimen PBT). Little bar slip is expected at these elastic stresses. Conversely, there is a large displacement of the grout plug out of the bamboo culm. Most of the specimens experience a slight stiffening behavior after a portion of the load has been applied. This can be explained as the grout plug having to travel a small distance before it fully engages the nodal regions. Following the initial softer behavior, the stiffness is relatively constant for the majority of the loading history. As the specimens approach their failure load, progressive softening is observed. Failure is associated with the development of a dominate longitudinal splitting crack in the culm. At this point confinement is lost and the remaining friction resistance is degraded as this crack propagates. Following the peak load (failure), the grout plug is simply pulled from the split culm. The splitting is believed to result from prying action in the form a radially oriented stress component resulting from the grout plug bearing against the nodal region. This behavior is described in greater detail in Chapter 4.

Tests PA and PC had 12 in. embedment lengths and both developed their maximum capacity around 0.05 in. of displacement. Tests PB and PD, having 24 in. embedment, both developed their maximum capacity around 0.13 in of displacement. This result suggests that when longer embedment lengths are used (i.e. more nodes engaged), the grout plug may travel farther before it engages all nodes along its length.

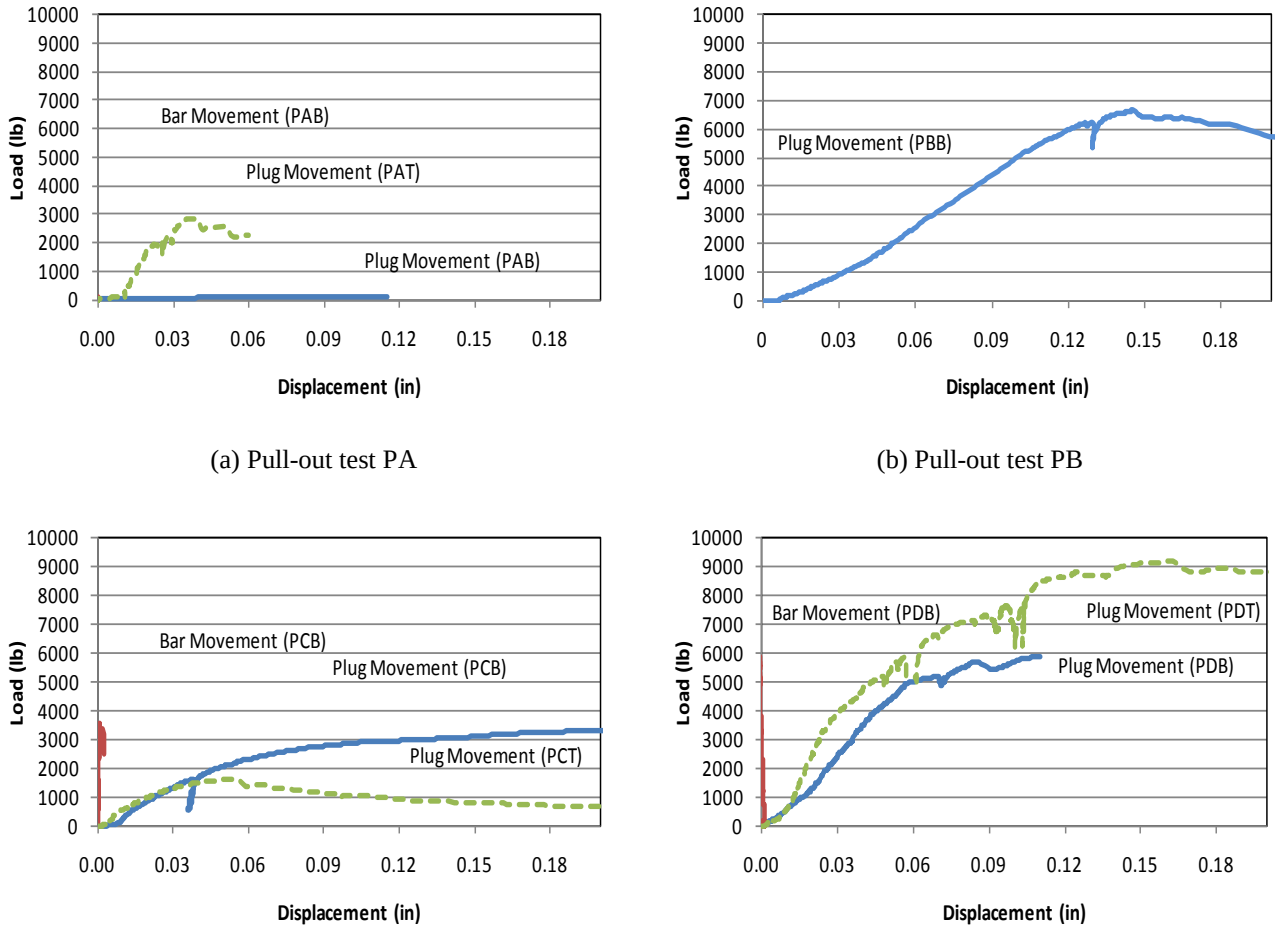

(a) Pull-out test PA

(b) Pull-out test PB

(c) Pull-out test PC

(d) Pull-out test PD

Figure 3.2 Pull-out tests – load vs. displacement behavior.

3.3 SINGLE CULM GROUTED-BAR COLUMN BASE TESTS

Four single culm column base tests were conducted resulting in eight specimens. The bar size used was either #4 or #5 and the embedment length into the bamboo was either 12 in or 24 in. Following failure of one culm, a brace was applied to that culm and the specimen was reloaded until the second culm failed. Table 3.3 provides a summary of test results. All failures were dominated by longitudinal splitting of the culms. Most splitting emanated from the compression

interface and was therefore associated with ‘crushing’ behavior of the bamboo. Such vertical splitting is commonly observed in direct compression tests (see Figure 2.1c). Some splitting was also observed on the sides and the tension face of the culm. This behavior is associated with the poor transverse tensile capacity of the bamboo being unable to accommodate the rotation demand of the culm. Such splitting is likely initiated by slip of the grout plug and the resulting prying action against the nodal regions as was observed in the pull-out tests. This behavior is described in greater depth in Chapter 4. Figure 3.3 shows schematically the location of dominate splitting cracks and Figure 3.4 shows examples each of these cracks.

Table 3.3 Single culm column base test results.

Specimen	Culm	Bar Size	Embedment Length	Ultimate Load	Moment at Culm Base	Number of Nodes Engaged	Culm Wall Thickness	Culm Outside Diameter	Culm Moment of Inertia
			in	lb	lb-ft		in	in	in^4
1A	O3	#4	12	193	772	1	0.54	3.65	6.54
$1A_R$	O1	#4	12	241	964	1.5	0.49	3.72	6.66
1B	N2	#4	24	155	620	3	0.54	3.36	4.91
$1B_R$	N1	#4	24	292	1168	3	0.55	3.37	5.06
1C	L2	#5	12	143	572	2	0.69	3.13	4.26
$1C_R$	L1	#5	12	133	532	1	0.75	3.15	4.49
1D	M2	#5	24	311	1244	3	0.66	3.23	4.67
$1D_R$	M3	#5	25	365	1460	2	0.53	3.43	5.22

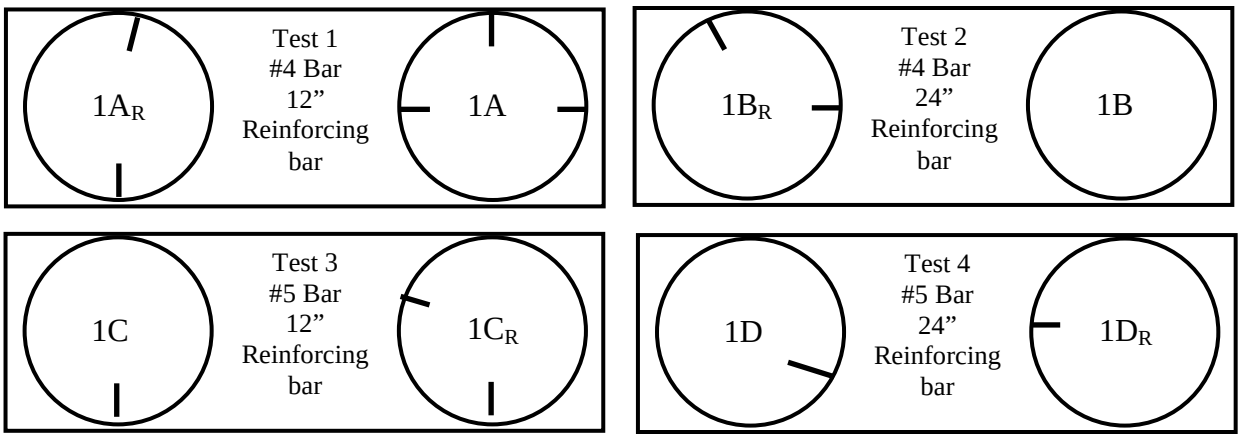

Figure 3.3 Single culm column bases – summary of tests and locations of splitting failures.

(a) Splitting on compression face
Specimen 1D

(b) Splitting on sides
Specimen 1C

(c) Splitting on tension face
Specimen 1A

Figure 3.4 Single culm column base splitting failures.

3.3.1 Load - Displacement Behavior

As part of the motivation for this work is to provide an engineering basis for the design of hazard resistant structure, the hysteric behavior of the column basis is a primary concern. By increasing the load in 50lb cycles during the test, the load versus displacement plots shown in Figure 3.5 were obtained for the column base connections.

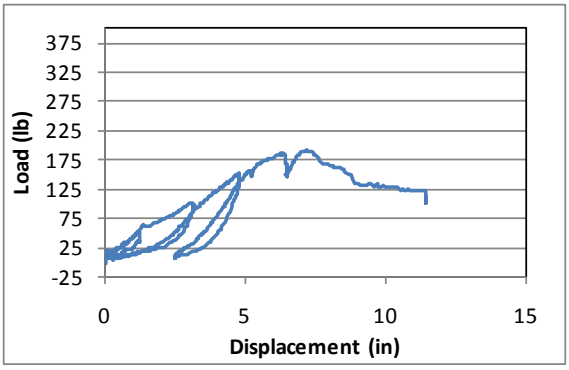

(a) Load – Displacement 1A

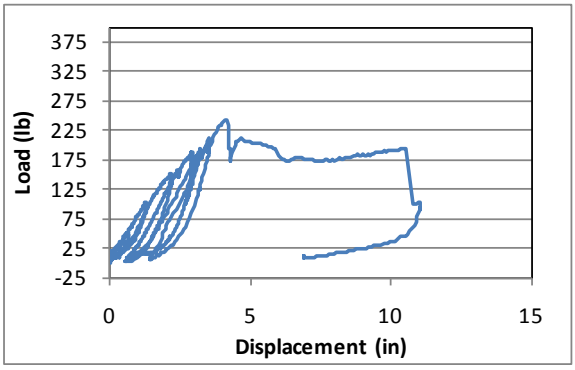

(b) Load – Displacement $1A_R$

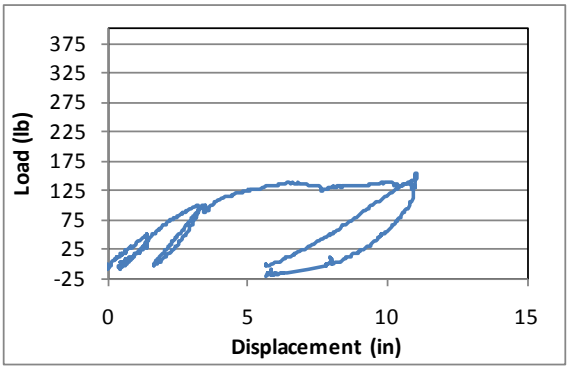

(c) Load – Displacement 1B

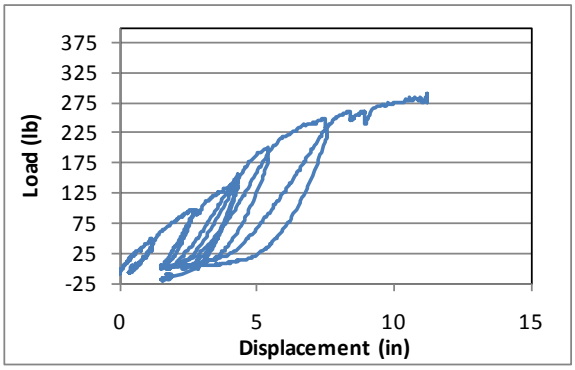

d) Load – Displacement 1BR

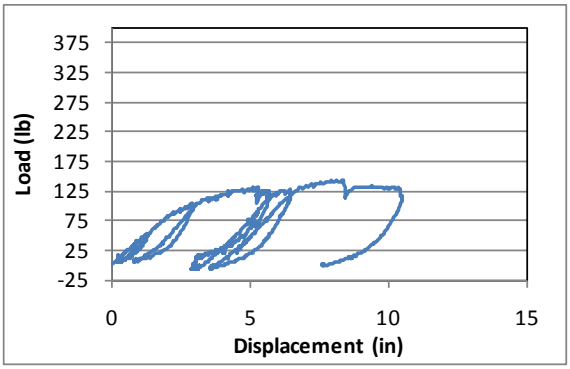

(e) Load – Displacement 1C

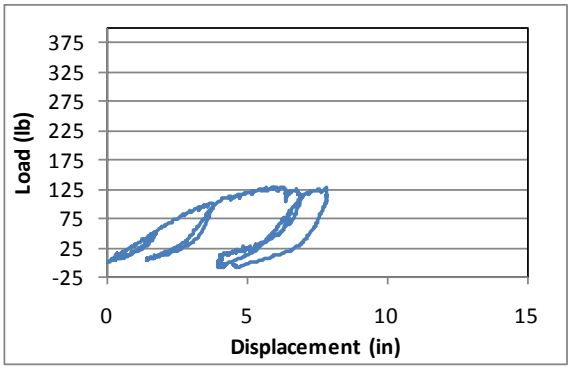

(f) Load – Displacement 1CR

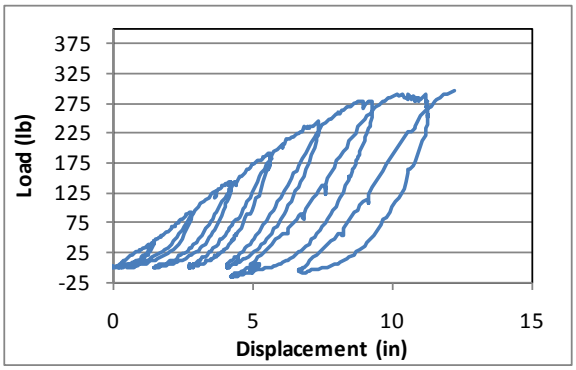

(g) Load – Displacement 1D

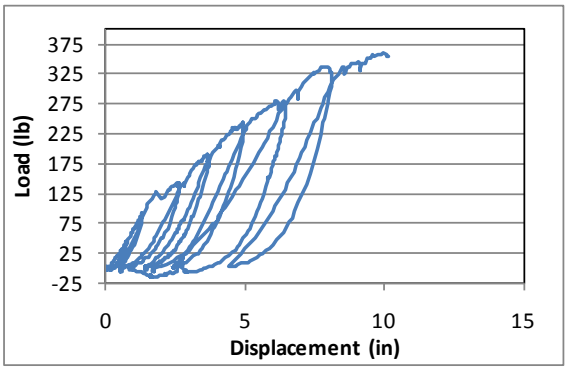

(h) Load – Displacement $1D_R$

Figure 3.5 Single culm column base tests – load – displacement behavior.

The hysteric behavior of the bamboo connections was similar. Specimens with a longer embedment length (B and D) resisted higher loads than those with smaller embedment lengths (A and C), and thus had greater energy dissipation behavior. All specimens showed an elastic range at the beginning followed by and plastic range which resulted in permanent displacements. Some hysteresis was noted with cycling and all curves exhibit considerable pinching. Following unloading, all specimens showed a reloading curve which was softer than the initial loading curve but recovered the initial stiffness upon exceeding the peak load of the previous cycle. Both of these behaviors reflects the dominance of the culm rigid body rotations in the specimen response. Overall displacements could be quite large, on the order of 6 to 8 inches.

The pinching behavior is especially important for earthquake loading, during which the columns would experience rapid load-reversals through large displacements. The reduction in stiffness during unloading (pinching) indicates that there would be regions of very large displacements with essentially no stiffness provided by the columns.

3.3.2 Moment – Rotation Behavior

Calculated base moment versus rotation behavior is shown in Figure 3.6. As can be seen from this figure, the grouted-bar connection demonstrates a mostly bilinear moment-rotation behavior with the post-peak branch having negligible stiffness. The failure is generally “soft”, with a sudden appearance or elongation of a dominant longitudinal crack occurring when the capacity is reached. Following the ultimate load, cracks continue to appear and elongate in a controlled manner as the connection is able to sustain a slowly degrading load.

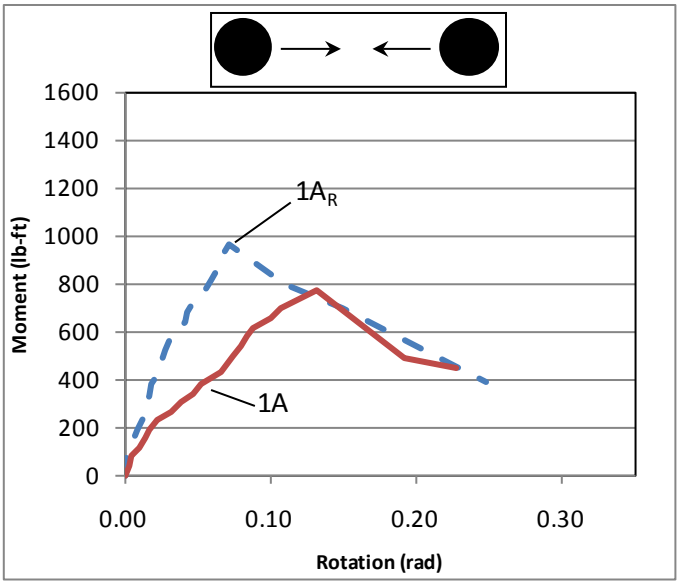

(a) Moment-rotation of Test A- #4 at 12”

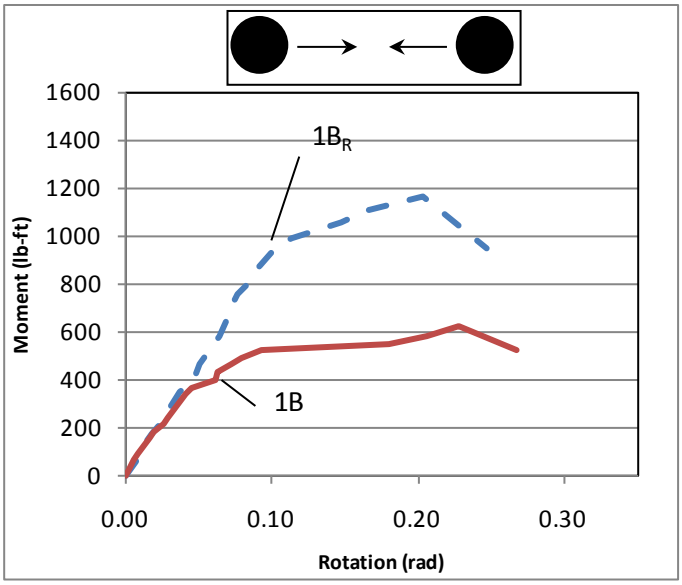

(b) Moment-rotation of Test B - #4 at 24”

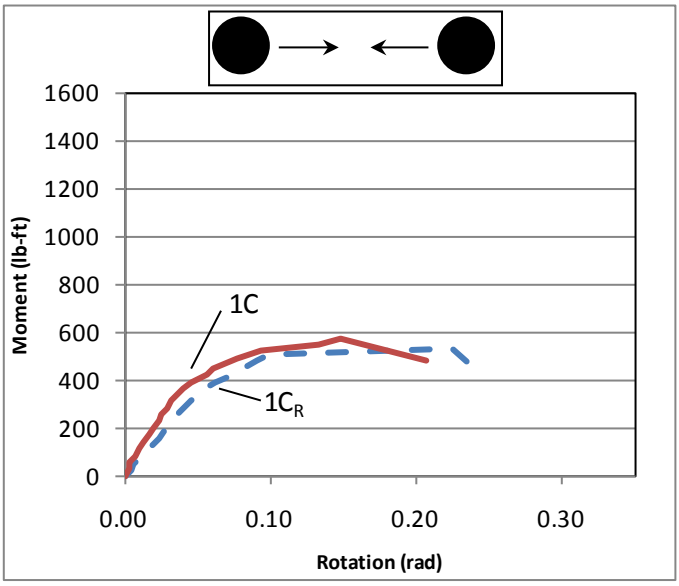

(c) Moment-rotation of Test C - #5 at 12”

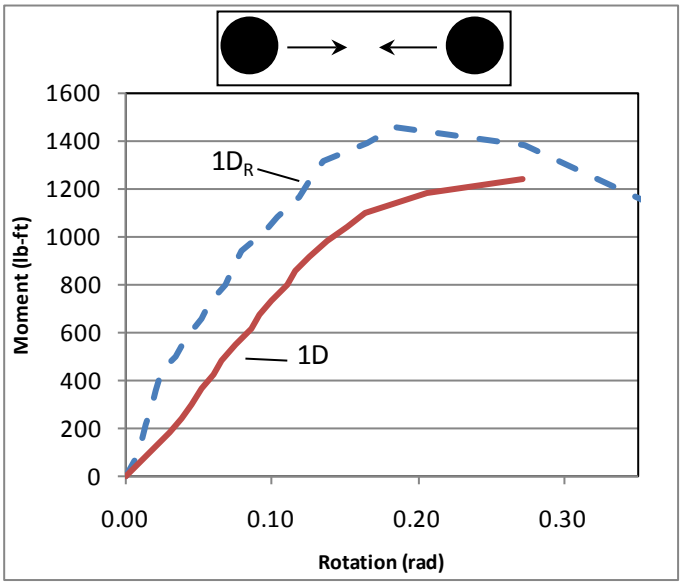

(d) Moment-rotation of Test D - #5 at 24”

Figure 3.6 Single culm column base tests – moment-rotation behavior.

3.4 FOUR CULM GROUTED-BAR COLUMN BASE TESTS

Four, four-culm column base tests, having two specimens each were tested. The bar size used was either #4 or #5 and the embedment length into the bamboo was either 12 in or 24 in. Following failure of one four-culm column, a brace was applied to that column and the specimen was reloaded until the second column failed. Each specimen was comprised of four culms selected from eleven used for this series of tests. Figure 3.7 shows the culm designation used for each specimen (recall that three specimens were cut from each culm). Table 3.4 provides the average culm dimensions for these culms. Figure 3.8 shows the location and naming convention of the two instrumented culms for each specimen (four per test). A summary of test results is presented in Table 3.5.

Table 3.4 Four culm column specimen culm dimensions.

Culm	Outside Diameter	Wall Thickness
	in	in
A	2.59	0.41
B	2.53	0.49
C	2.54	0.67
D	2.88	0.53
E	2.91	0.58
F	2.92	0.57
G	2.67	0.68
H	2.92	0.63
I	2.76	0.61
J	2.96	0.48
K	2.98	0.46

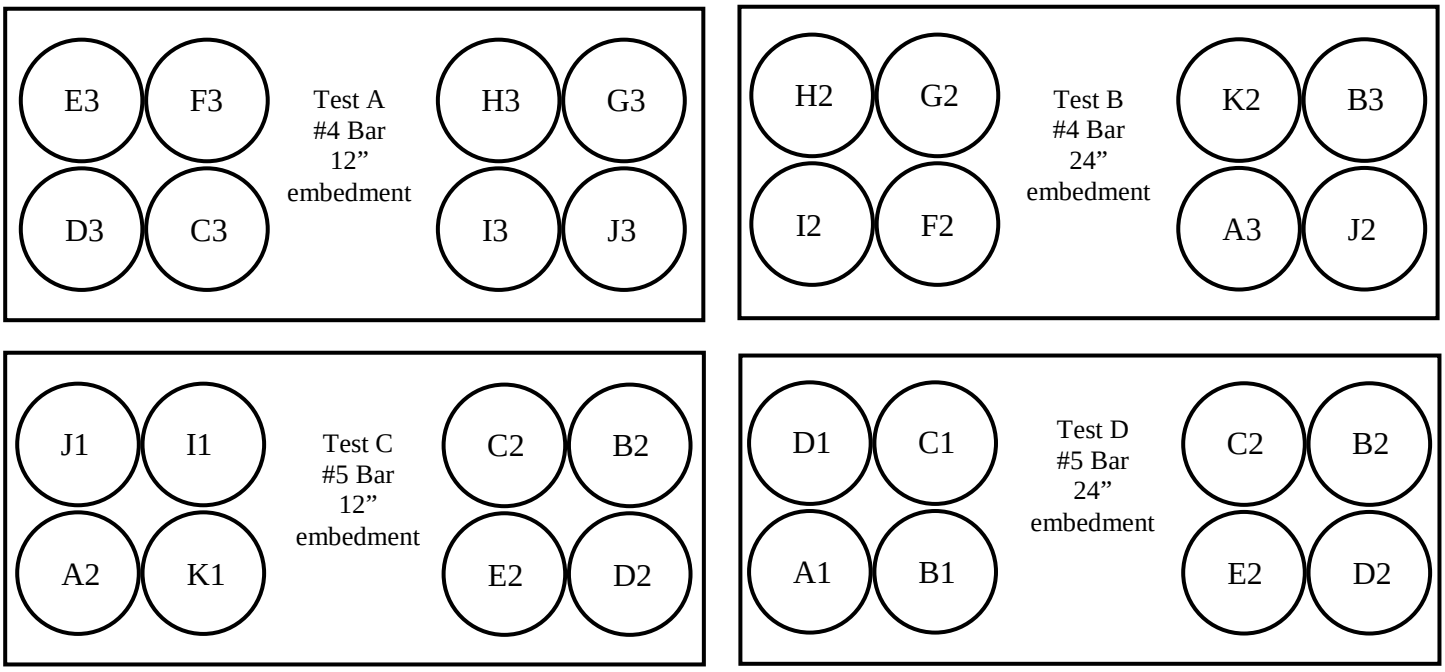

Figure 3.7 Four culm specimen culm selection and location.

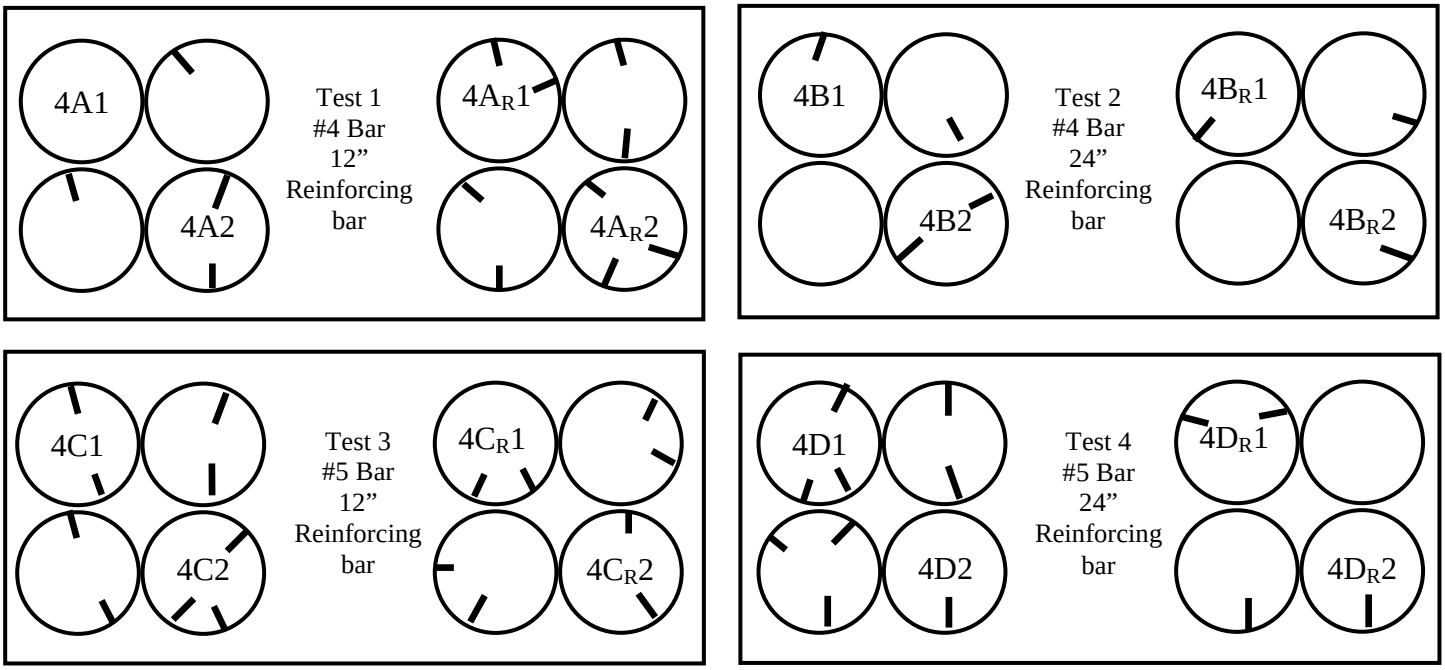

Figure 3.8 Four culm specimen instrumented culm designation and location of dominate splitting cracks.

Table 3.5 Four culm column base test results.

Specimen	Culm	Bar Size	Embedment Length	Ultimate Load	Moment at Column base	Number of Nodes Engaged Per Culm	Average Culm Wall Thickness	Average Culm Outside Diameter	Column Moment of Inertia
			in	lb	lb-ft	avg	in	in	in^4
4A1	E	#4	12	342	1368	2	0.59	2.81	10.9
4A2	C	#4	12	342	1368				
$4A_R1$	H	#4	12	559	2236	1.75	0.60	2.91	12.4
$4A_R2$	J	#4	12	559	2236				
4B1	H	#4	24	870	3480	3	0.62	2.82	11.2
4B2	F	#4	24	870	3480				
$4B_R1$	K	#4	24	980	3920	3.5	0.46	2.77	9.3
$4B_R2$	J	#4	24	980	3920				
4C1	J	#5	12	682	2728	1.5	0.50	2.82	10.3
4C2	K	#5	12	682	2728				
$4C_R1$	C	#5	12	946	3784	1.5	0.57	2.72	9.5
$4C_R2$	D	#5	12	946	3784				
4D1	D	#5	24	992	3968	2	0.57	2.72	9.5
4D2	B	#5	24	992	3968				
$4D_R1$	C	#5	24	1130	4520	2.5	0.61	2.86	11.7
$4D_R2$	D	#5	24	1130	4520				

Failure behavior was very similar to the single culm tests with all failures being associated with dominate longitudinal splitting cracks in the individual culms. Figure 3.9 shows examples of these failures and Figure 3.8 identifies the locations of these dominate splitting cracks.

(a) Specimen 4C2

(b) Specimen $4D_R2$

Figure 3.9 Four culm column base splitting failures.

3.4.1 Load - Displacement Behavior

The hysteric behavior shown in Figure 3.10 of the bamboo joint was obtained by increasing the load in 50 lb increments during the test.

Gauge failure

(a) Gauge failure 4A

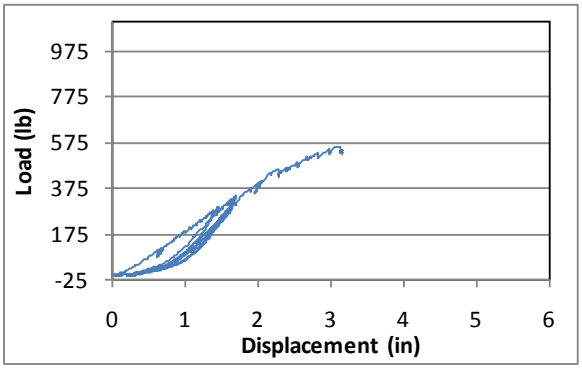

(b) Load – Displacement $4A_R$

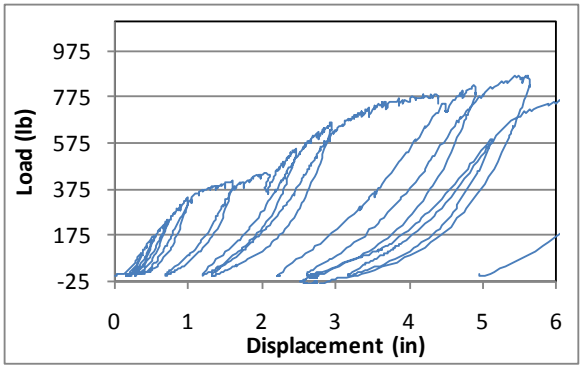

(c) Load – Displacement 4B

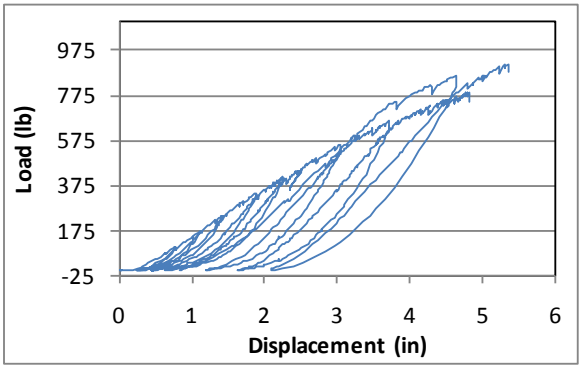

d) Load – Displacement 4BR

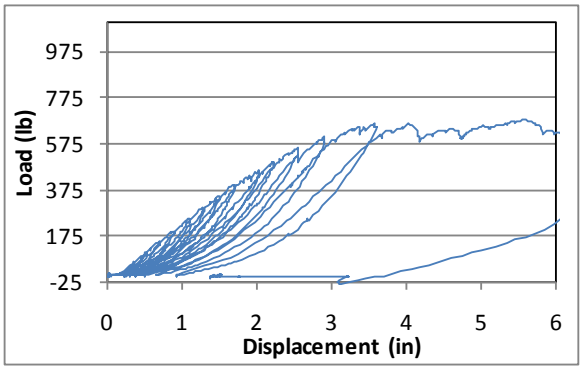

(e) Load – Displacement 4C

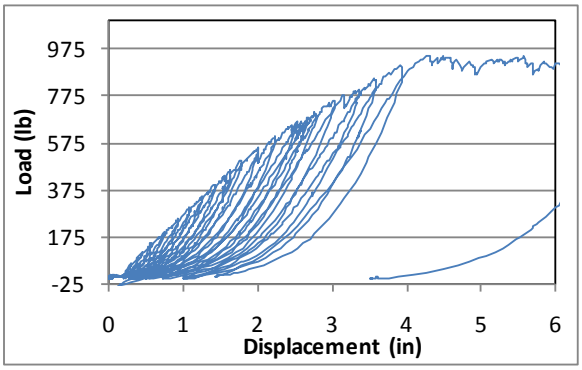

(f) Load – Displacement 4CR

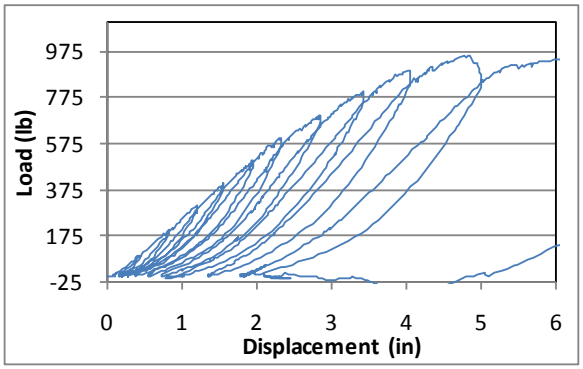

(g) Load – Displacement 4D

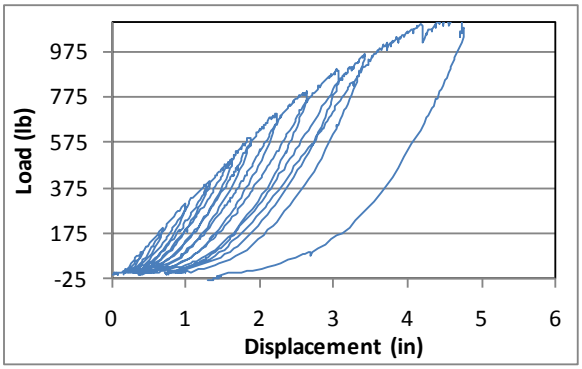

(h) Load – Displacement $4D_R$

Figure 3.10 Four culm column base tests – load – displacement relationship**.**

The hysteric behavior of the four-culm bamboo column bases was similar to that of the single culm bases. It is noted that the capacities of these column bases cannot be directly compared since the culm sizes were different. Once again, specimens with a longer embedment length (B and D) resisted higher loads than those with smaller embedment lengths (A and C), and thus had greater energy dissipation behavior. Pinching and reloading behavior was similar to that of the single culm tests although the deterioration of reloading stiffness was not as pronounced. Overall displacements were smaller than in the single culm tests but were still quite large, on the order of three to four inches.

3.4.2 Individual Culm Moment-Rotation Behavior

The moment-rotation responses from the eight specimens are shown in Figure 3.11. Two culms, one from Test A (4A2) and one from Test D ($4D_R1$), are not reported due to instrumentation failure. Comparing the individual culm moment-rotation response of the four-culm arrangement to the single culm arrangement, the overall behavior of the grouted-bar joint remains relatively ductile, but the failures do appear to be more abrupt in the four culm arrangement. The available rotation capacity at failure is also lower with the four culm arrangement achieving a maximum capacity at a rotation of approximately 0.12, whereas the single culm tests generally reached a maximum capacity at approximately 0.17.

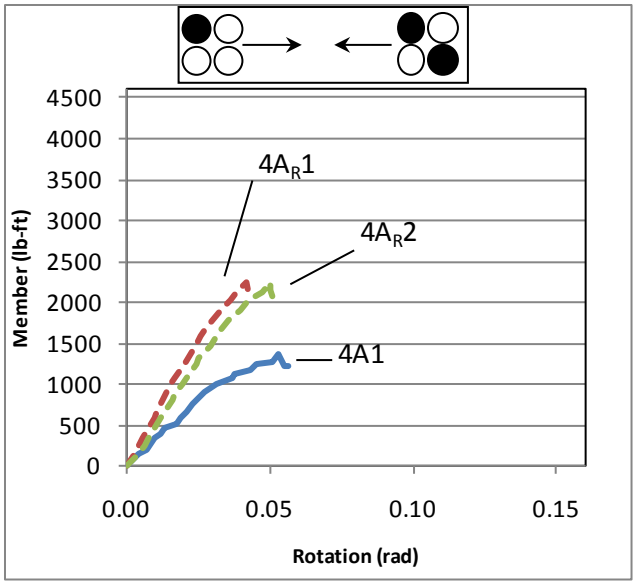

(a) Moment-rotation of Test A- #4 at 12”

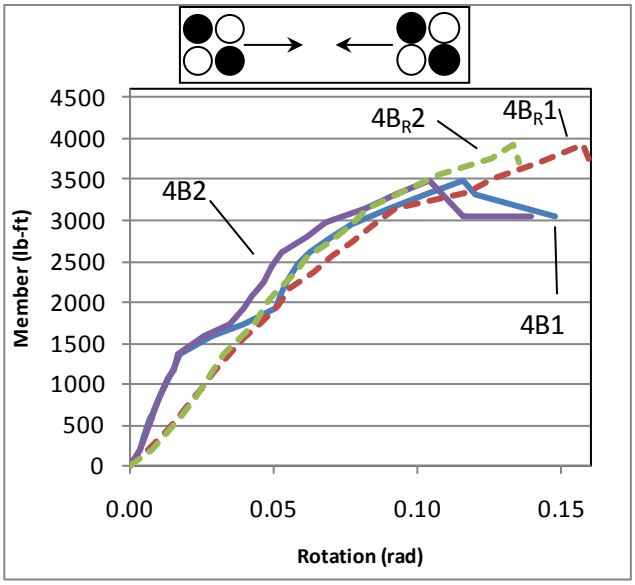

(b) Moment-rotation of Test B - #4 at 24”

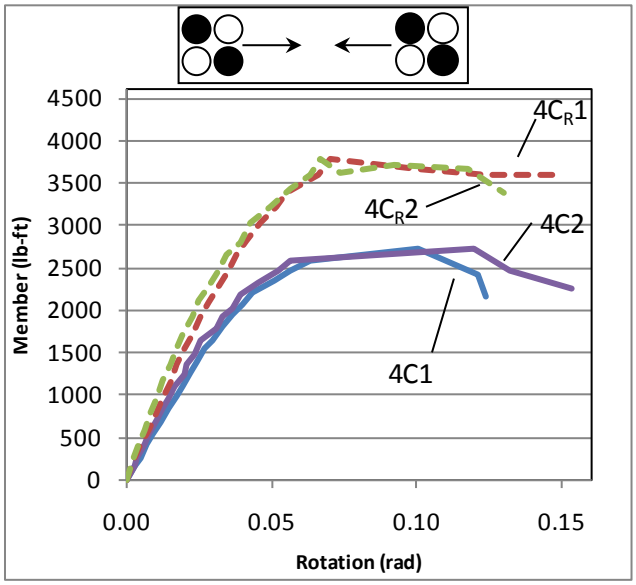

(c) Moment-rotation of Test C - #5 at 12”

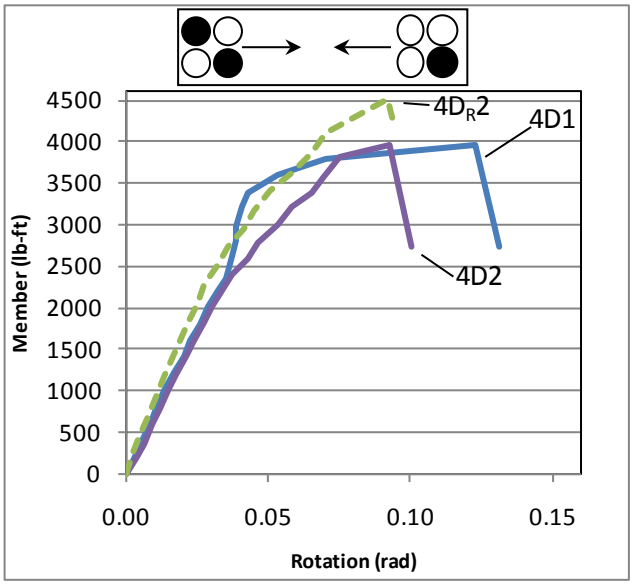

(d) Moment-rotation of Test D - #5 at 24”

Figure 3.11 Four culm column base tests – moment-rotation behavior.

4.0 DISCUSSION OF TEST RESULTS

4.1 GROUTED-BAR PULL-OUT TESTS

Pull-out tests were dominated by pull-out of the grout plug from the bamboo culm. Therefore, as expected the bar size (#4 or #5) had little effect on the ultimate load of the pullout specimens (Figure 4.1) since reinforcing bar stresses remained elastic in all cases. Since grout plug slip and pull out was dominate, friction between the grout plug and culm must contribute to the resistance. Thus, again as expected, a longer embedment length results in a greater pull-out capacity (Figure 4.2). Although results have a large degree of scatter, the pull-out capacity increased more than 250% when the embedment length increased from 12 to 24 inches. As the resistance due to friction was believed to be based on the contact area, capacity increase associated only with friction should be essentially proportional to embedment length. It was not; therefore a further resisting action is present.

Upon examining the data, specimen PAB, which was initially believed to have been an outlier, actually provided strong evidence for an alternate explanation. Considering only embedment length, PAB, having a 12 in. embedment, should have developed loads similar to PAT, PCT and PCB. PAB exhibited a pull-out capacity of only 130 lbs, compared to between 1600 and 3600 lbs for the other specimen having the same 12 in. embedment length. The difference in the specimens was the number of nodes engaged by the grout plug (see Table 3.2). Indeed, a very clear relationship, shown in Figure 4.3, is established between the pull-out

capacity and the number of nodes engaged. Furthermore, this relationship, and the results of PAB suggest that friction between the grout plug and culm is in fact negligible.

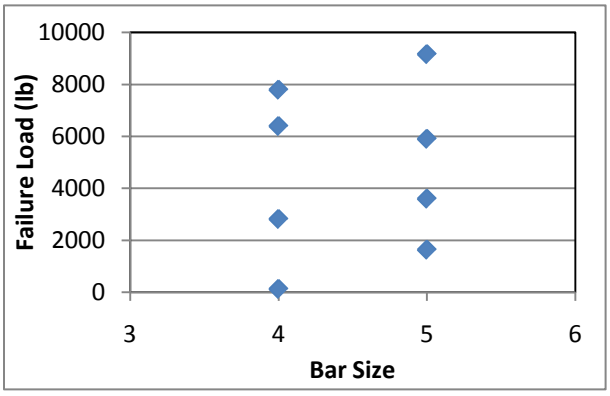

Figure 4.1 Bar size vs. pull-out failure load
Yield of #4 and #5 bars would be approximately 12,000 and 18,600 lbs, respectively.

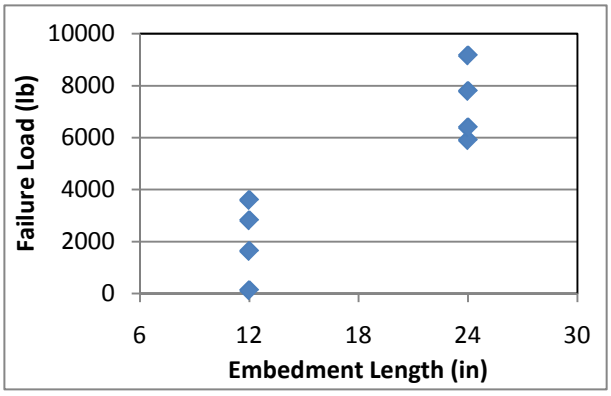

Figure 4.2 Embedment length vs. pull-out failure load.

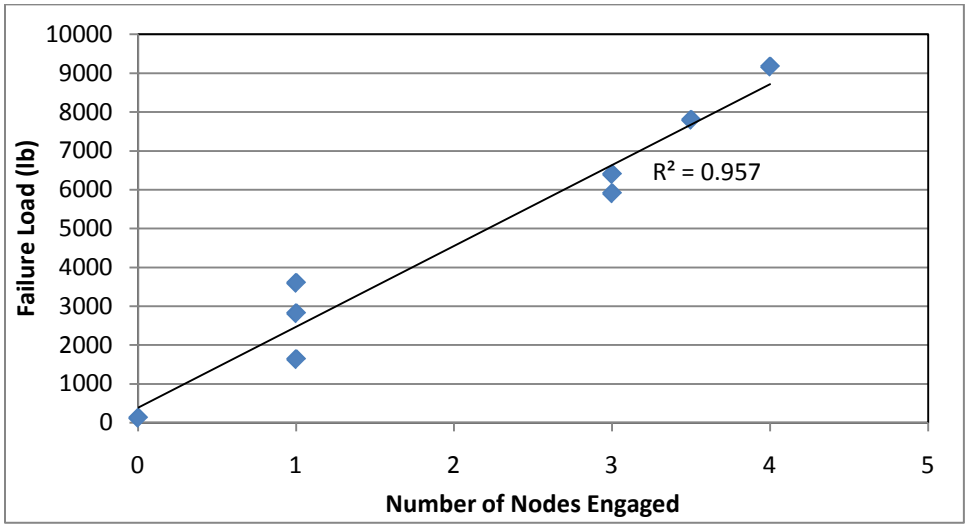

Figure 4.3 Number of nodes engaged vs. pull-out failure load.

4.1.1 Friction between grout plug and culm wall

The reason that the friction between the grout plug and culm is negligible may result partially from the fabrication process. In the process followed in this study, a very wet grout was placed in a dry culm. The water in the grout may have been absorbed out of the grout, into the culm,

resulting in a layer of poor quality grout at the interior culm wall surface. Some evidence of this was seen in the very ‘dusty’ appearance of the pulled-out grout plugs. It should be noted that in the field, bamboo is not soaked prior to grout application. Had the culm been saturated prior to grouting, the grout water would not be lost and the quality of the grout-bamboo interface may have been better. A potential drawback of saturating the bamboo prior to grouting is that it will swell. This may result in a ‘gap’ surrounding the grout plug forming once the culm dries again.

Another possible solution to the poor interface friction is to use an expansive grout. In this study, a dimensionally stable, ‘non-shrink’ grout was used. The relatively small transverse tensile capacity of the bamboo, however, makes it very important that any grout expansion be carefully controlled if the grout is not to split the bamboo as it cures. Such control is usually affected through water content of the grout mix and may be difficult to control in the present application.

One cannot discount friction entirely. Sharma (2010) (see Section 1.2.3.1) reports modest frictional capacity for specimens having very little node material engaged - the nodes were very thin and were mostly removed to accommodate grouting. Similarly, active clamping pressure - in the form of hose clamps used in this test program - engaged sufficient friction to arrest slip entirely. This final observation supports the hypothesis that a small gap develops between the cured grout and culm wall due to shrinkage of the grout and/or swelling and subsequent shrinkage of the bamboo itself.

Further investigation of these effects is required. The preliminary results of this study indicate that little grout-to-culm wall friction may be developed. Using the single data point of specimen PAB, the friction developed was on the order of only 1.4 psi!

4.1.2 Engagement of Nodes

The nodes within the grout plug act as mechanical shear keys. As the grout plug slips, the nodal regions of the culm are engaged, resisting further slip. As loading is increased, the nodes will shear off and post failure slip will progress with only residual frictional resistance; enhanced, perhaps by the 'captured' nodes that are now slipping as well.

This mechanism also explains the prevalence of the longitudinal splitting observed. The nodal region of the culm is somewhat rounded (see Figure 1.5a). As a result, there is a radially oriented component of the longitudinal pull-out force acting at the nodal region. This force may be envisioned as a 'bursting' force concentrated at the node location. The poor transverse tensile capacity of the bamboo is unable to resist this force and splitting ensues. The splitting likely weakens the shear key behavior of the node and certainly reduces any available friction force. This behavior is shown schematically in Figure 4.4.

Post test forensic investigation of the pull-out specimens supports this interpretation of pull-out behavior. All tested specimens experienced significant longitudinal splitting prior to failure. Following splitting, the nodal regions sheared off inside of the culm and allowed the entire grout plug to be pulled through the specimen as is evident in Figure 4.5. As can be seen in Figure 4.5, the nodes of the Tre Gai bamboo species are relatively large (thick) and therefore offer relatively good shear resistance. Based on Figure 4.3, each node provides approximately 2200 lbs pull-out resistance, this is approximately 340 pounds per circumferential inch.

Based on the need to engage the nodes to develop pull-out resistance, the practice of knocking out the nodes to facilitate grouting (as was done by Sharma 2010), is not advised. Nodes that have been drilled but have their edges remaining are clearly superior. The drawback,

of course, is that there is less clear space to ensure complete grouting around the bars. This was overcome in the present study by grouting each internode individually (see Section 2.3).

(a) Pre-failure image

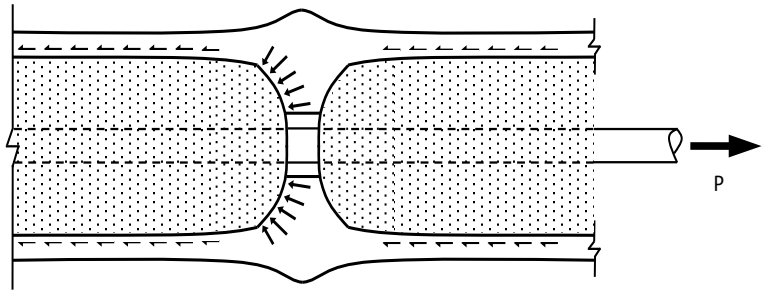

(b) Mechanical shear key behavior prior to failure. Radially oriented forces may lead to longitudinal splitting of the culm.

(c) Post-failure image

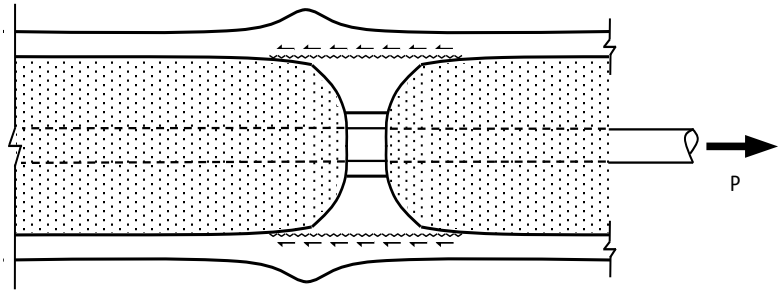

(d) Residual friction resistance post failure

Figure 4.4 Mechanism of node region engagement.

(a) Longitudinal splitting and failure of node near end of Specimen PAT

(b) Failure of nodal region of Specimen PCB having a 12 in. embedment engaging only a single node

(c) Failure of nodal regions of Specimen PDT having a 24 in. embedment engaging four nodes (three shown).

Figure 4.5 Evidence of shear key action of nodal regions in pull-out tests.

4.2 SINGLE CULM COLUMN BASE TESTS

In Figure 4.6, the applied lateral load at failure of each of the single culm bending tests is plotted against six test parameters: bar size, embedment length, culm outside diameter, number of nodes engaged, wall thickness, and moment of inertia. As can be seen, only the embedment length (Figure 4.6b) illustrates a clear trend with longer embedment resulting in greater flexural capacity.

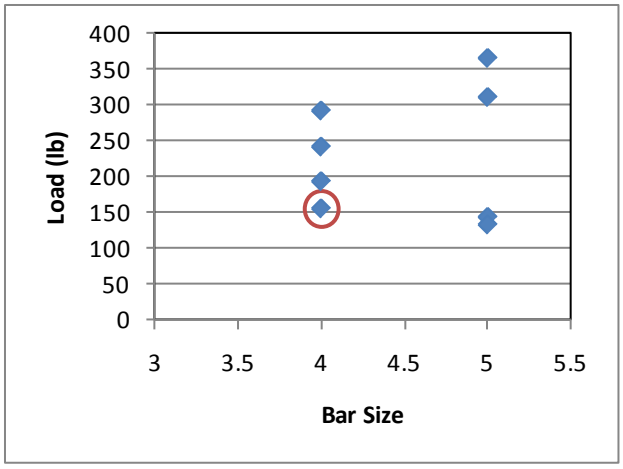

(a) Bar size vs. load (lb)

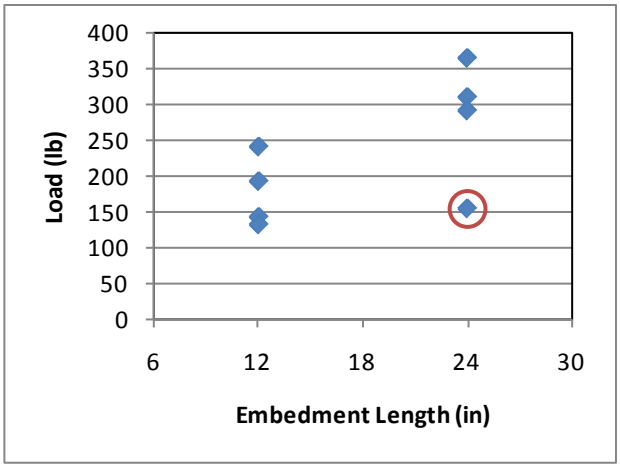

(b) Embedment Length vs. load (lb)

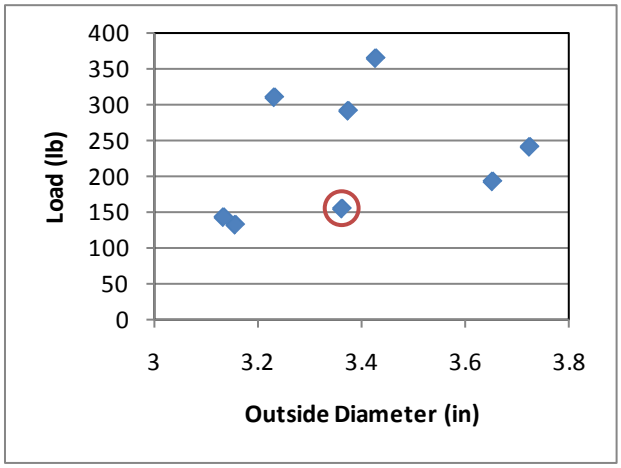

(c) Outside diameter vs. load (lb)

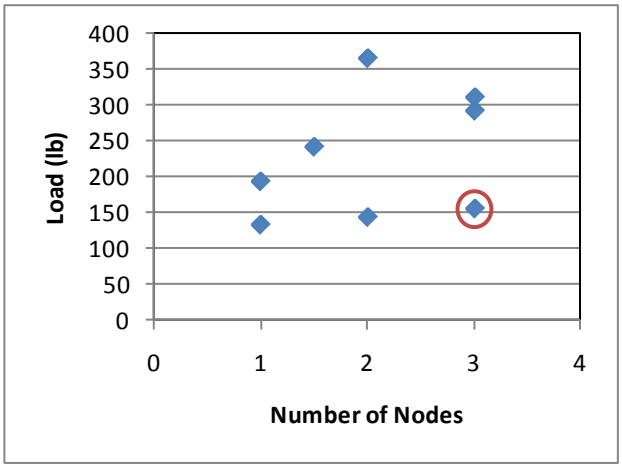

(d) Number of nodes engaged vs. load (lb)

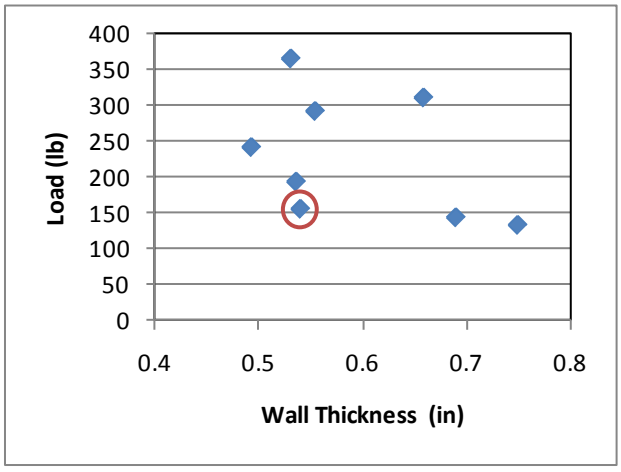

(e) Wall thickness vs. load (lb)

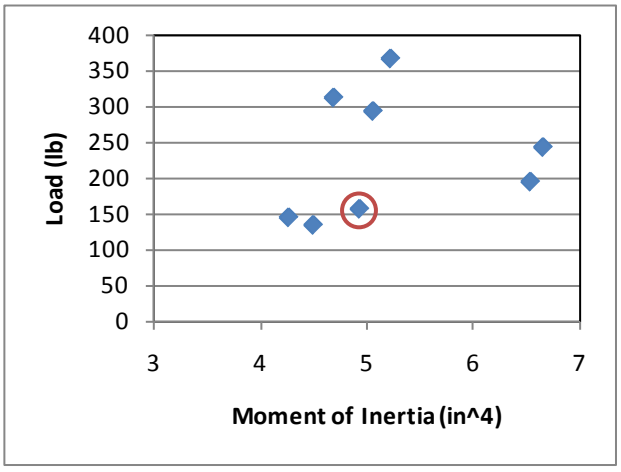

(f) Moment of inertia vs. load (lb)

Figure 4.6 Single culm bending tests – load versus multiple variables.

Specimen 1B (circled in Figure 4.6) exhibited a unique failure mode which appears to have resulted in an abnormally low capacity. Specimen 1B is the only culm that did not exhibit longitudinal cracking at failure, but rather experienced local crushing on the compression face (see Figures 4.7). The behavior of 1B suggests a softer compressive response than was observed in the other tests - the reason for this anomaly is unknown. In discounting the results of 1B, a relationship between the number of engaged nodes and flexural capacity also becomes clear (Figure 4.6d), although this is not as significant as for pull-out tests. These results appear to indicate slip between the grout plug and bamboo culm is not as significant a factor in flexural response as in pull-out response. In the case of flexure, the applied shear force (lateral load) will help to engage friction between the grout and bamboo - in essence 'clamping' half the diameter of the culm.

Figure 4.7 Specimen 1B suffered local crushing rather than splitting.

A summary of the moment-rigid body rotation behavior of the single culm tests is shown in Figure 4.8, where the specimens with a 24" embedment length are shown having dashed lines. The improvement resulting from the larger embedment length is clear in this figure. In general, the larger embedment also appears to result in a stiffer overall column behavior, which should be expected due simply to the longer extent of the grouted region of the culm.

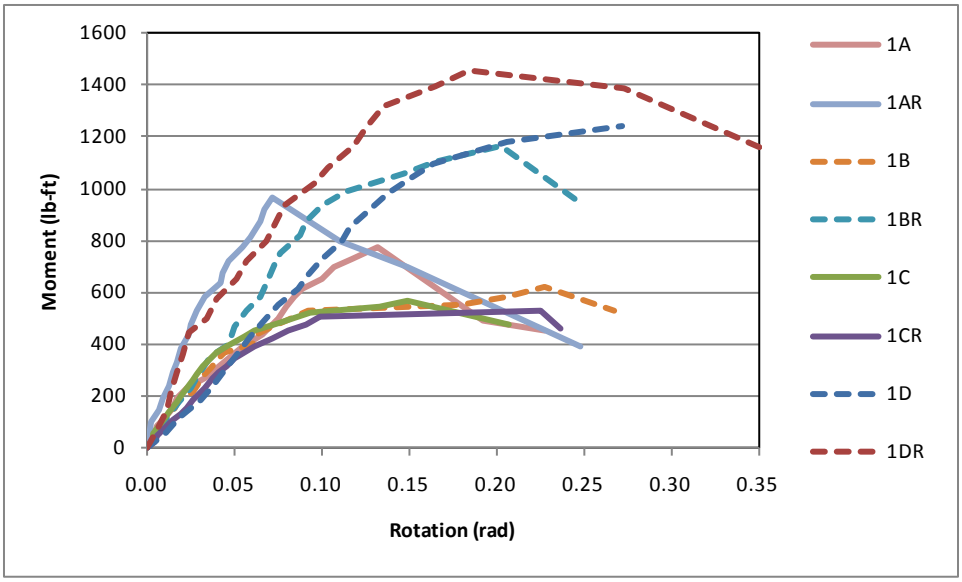

Figure 4.8 Summary of moment-rotation for single culm tests.

4.2.1 Displacement of Single Culm Column Base Tests

Following the procedure described in Section 2.5.1.1, the displacement due to rigid body rotation (δ_θ) and flexure (δ-δ_θ) were separated. The components of the total rotation (δ) are shown in Figure 4.9. Most specimens experienced roughly 6 in. of displacement before failure. The displacement due to rigid body rotation of the culm clearly dominates the mid-height displacement, and is generally one to four times greater than the displacement due to flexure. Figure 4.10 shows the ratio of rigid body to flexural component ($\delta_\theta/(\delta-\delta_\theta)$) of the total displacement for all specimens. There is no obvious behavioral trend, however this ratio does tend to increase as the applied load increases. This indicates that the limited flexural stiffness is degrading with increasing loads. Finally, at failure, the rigid body component increases dramatically (Figure 4.9), indicating the final splitting failure and resulting loss of capacity described in Section 3.3 and shown in Figure 3.4.

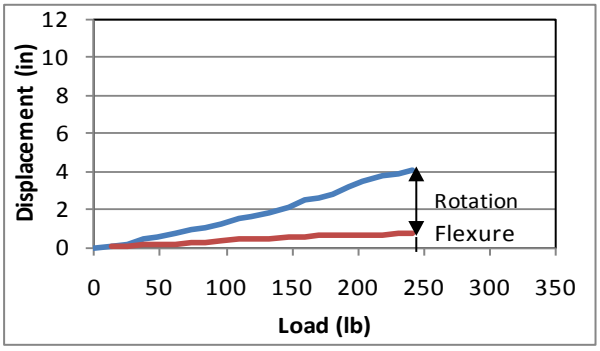

(a) Components of displacement vs. load ($1A_R$)

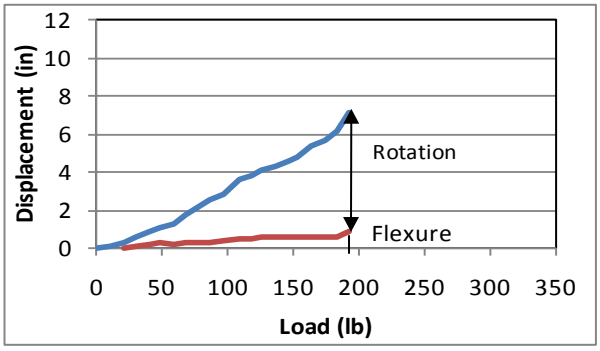

(b) Components of displacement vs. load (1A)

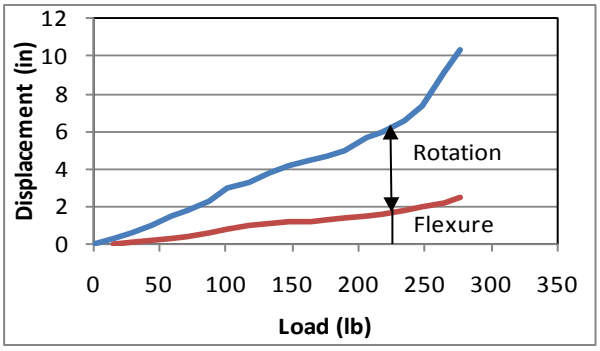

(c) Components of displacement vs. load ($1B_R$)

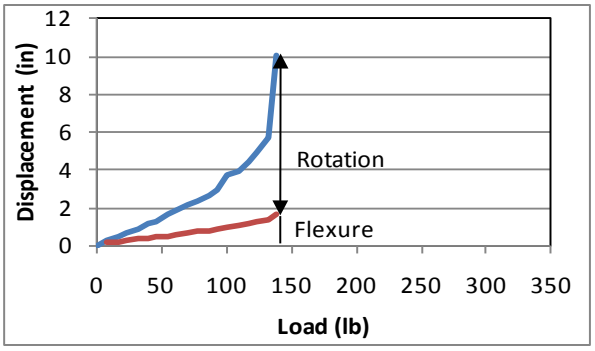

(d) Components of displacement vs. load (1B)

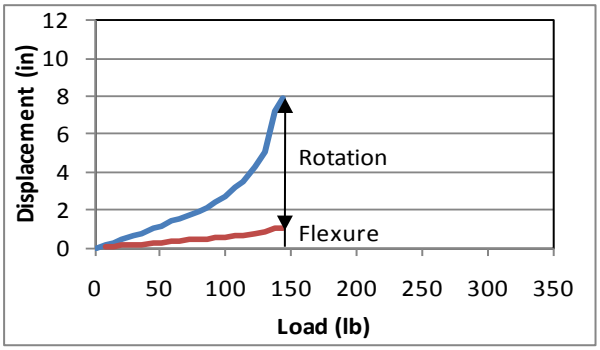

(e) Components of displacement vs. load (1C)

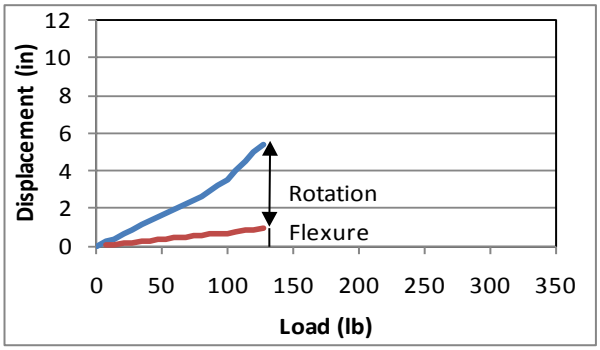

(f) Components of displacement vs. load ($1C_R$)

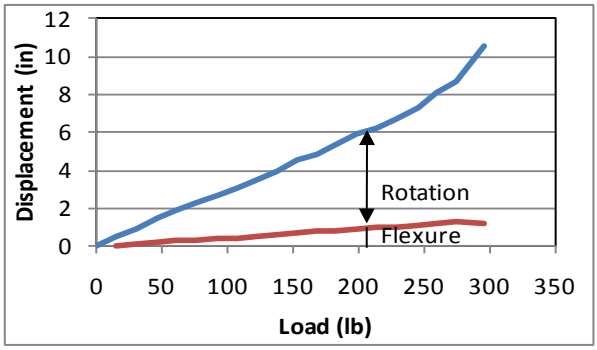

(g) Components of displacement vs. load (1D)

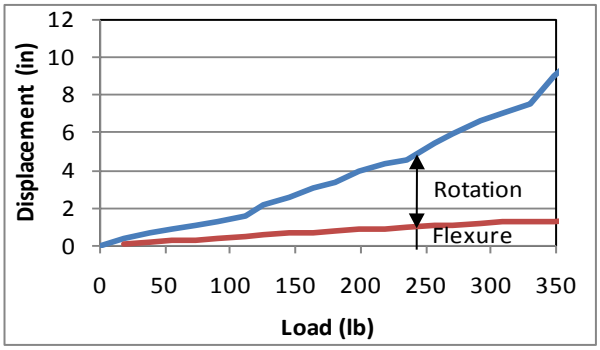

(h) Components of displacement vs. load ($1D_R$)

Figure 4.9 Single culm column bases – load vs. displacement.

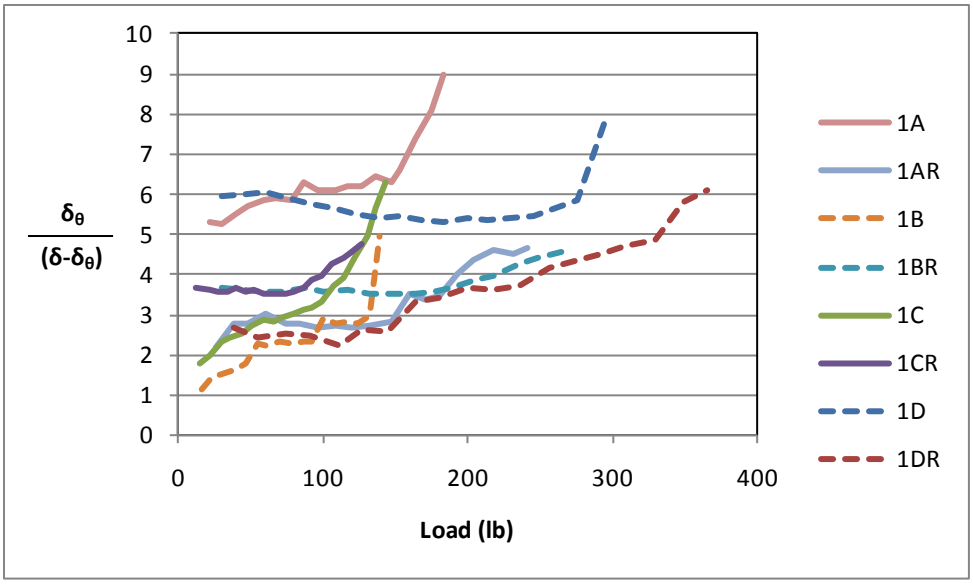

Figure 4.10 Single culm bending – ratio of displacement due to rigid body rotation vs. displacement due to flexure.

4.2.2 Single Culm Grouted-Bar Column Base Behavior

Using Equations 2.5 and 2.6, one can calculate the apparent flexural stiffness, EI_{culm}, as well as the effective flexural stiffness, EI_{eff}, of the single culm column. These values are given in Table 4.1. EI_{culm} was the experimentally observed value for the flexural stiffness of the culm, which is based solely on the displacement due to flexure, and is appropriate for use in modeling the flexural behavior of the culm. EI_{eff} includes the effect of rigid body rotation as well as flexural bending and is useful in developing simple models of column base behavior. Alternatively, the two values may be combined to directly model culm flexure and rigid body rotation as a rotational spring in a frame model.

Since the average geometry of each culm is known, it is possible to normalize EI_{culm} by the moment of inertia (I) to obtain the apparent modulus of elasticity, E_{culm}, of the bamboo (see Table 4.1). The values calculated in this manner have a high degree of variation since average geometric properties and derived displacement values are used. Additionally, the values shown

in Table 4.1 were obtained at a load equal to 50% of the ultimate load achieved. As has been noted, the stiffness does decrease with increased loading, thus the value of E_{culm} will be calculated as being greater or less than that shown in Table 4.1 depending on the load level considered. Nonetheless, a reasonable estimate of E_{culm} is derived which can also be used in an analytical context, particularly where a model attempts to capture the effects of variation in geometry. The E_{culm} value is a 'gross section' modulus and should therefore be compared with comparable full-culm values. The experimentally measured value of E_{culm} in this study was found to be 1700 ksi (see Section 2.1.1).

Table 4.1 Single culm column apparent and effective modulus.

Specimen	Culm	Bar	Embedment Length	EI_{eff} (δ_{total})	EI_{culm} (δ_{total} - δ_{θ})	E_{culm} (δ_{total} - δ_{θ})
			in	kip-in^2	kip-in^2	ksi
1A	O3	#4	12	1233	8780	1342
$1A_R$	O1	#4	12	2734	10120	1519
1B*	N2	#4	24	1197	3914	779
$1B_R$	N1	#4	24	1455	4637	917
1C	L2	#5	12	1504	5879	1380
$1C_R$	L1	#5	12	1109	4995	1112
1D	M2	#5	24	1248	8063	1721
$1D_R$	M3	#5	24	1983	8798	1685

*Denotes gauge failure during testing

Combining the behavior of the single culm column from Table 4.1 with the moment versus rotation plot presented in Figure 4.8, both the flexural behavior of the culm as well as the rigid body rotation at the joint have been explored. This information is adequate to describe the behavior of the single culm connection both in future engineering practice and in research.

4.3 FOUR CULM COLUMN BASE TESTS

An analysis similar to that conducted for single culm columns was conducted for the four-culm columns. In considering capacity, bar embedment length and, to a lesser extent, the number of engaged nodes affected the ultimate capacity of the four-culm specimens. A summary of the individual culm moment-rigid body rotation behavior of the four culm tests is shown in Figure 4.11, where the specimens with a 24” embedment length are shown in dashed lines.

Culm behavior was not terribly different than that observed in the single culm tests. When normalized for the different culm size used in the single and four culm tests, the capacity of the four culm arrangement is approximately five to ten times greater than a single culm (Table 4.2) indicating some degree of composite behavior is engaged and the column is behaving as more than the sum of the culms. In Table 4.2, a value of the ratio of normalized capacities equal to four would indicate that the capacity is simply the sum of the capacities of the individual culms. If on the other hand, the four-culm column behaved as a fully composite section, the same normalized ratio would be on the order of 40; that is, the fully composite four-culm column capacity should be 40 times the individual culm capacity. Thus the four-culm column behavior falls between that of the sum of the behaviors of four individual culms and the fully composite behavior, and is closer to that of the individual culms. This behavior is discussed further in Section 4.3.2, below.

Table 4.2 Summary of normalized column capacities.

	single culm column			four-culm column			ratio of four-culm to single culm normalized values
Test series	average moment capacity	average I_{culm}	moment / I_{culm}	average moment capacity	average I_{culm}	moment / I_{culm}	
	ft-lb	in^4	(ft-lb)/in^4	ft-lb	in^4	(ft-lb)/in^4	
A	868	6.60	132	1802	2.83	637	4.8
B	894	4.99	179	3700	2.53	1465	8.2
C	552	4.38	126	3256	2.54	1283	10.2
D	1352	4.95	273	4244	2.38	1787	6.5

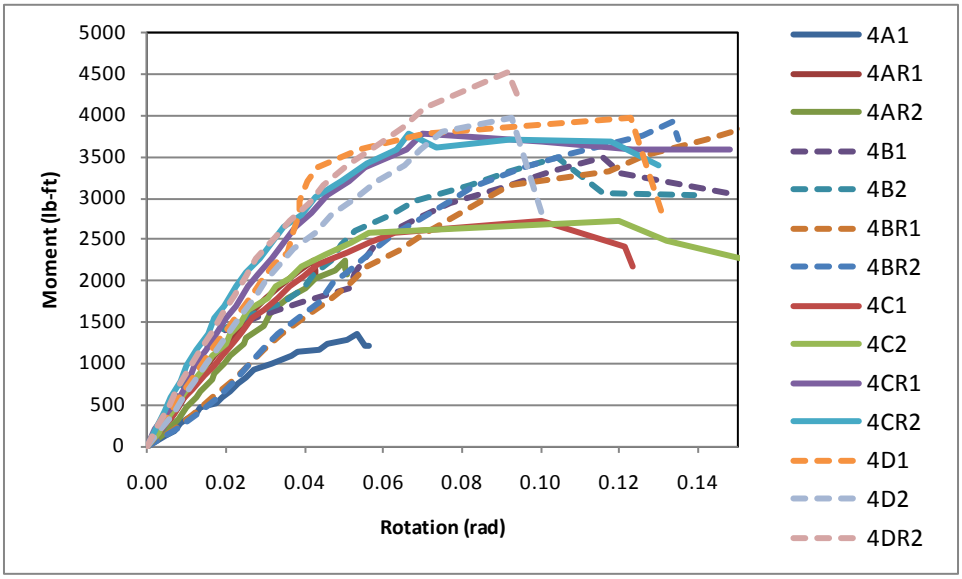

Figure 4.11 Four culm column base tests – summary of moment-rotation behaviors.

4.3.1 Displacement of Four Culm Column Base Tests

Following the procedure described in Section 2.5.1.1, the displacement due to rigid body rotation (δ_θ) and flexure (δ-δ_θ) were separated. The components of the total rotation (δ) are shown in Figure 4.12. The displacement due to rigid body rotation of the culm clearly dominates the mid-height displacement, and is generally one to three times greater than the displacement due to

flexure. Figure 4.13 shows the ratio of rigid body to flexural component ($\delta_\theta/(\delta-\delta_\theta)$) of the total displacement for all specimens. As with the single culm tests, there is no obvious behavioral trend, however this ratio does tend to increase as the applied load increases. This indicates that the limited flexural stiffness is degrading with increasing loads.

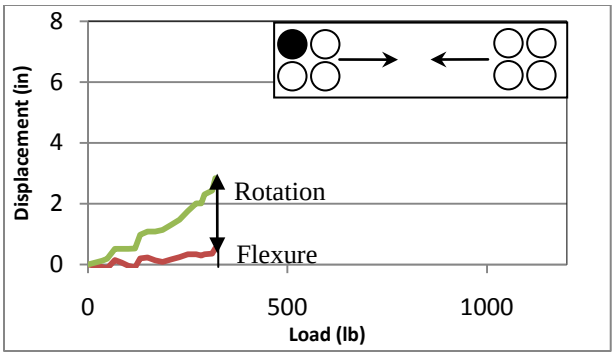

(a) Components of displacement vs. load (4A1)

Gauge Failure

(b) Gauge failure (4A2)

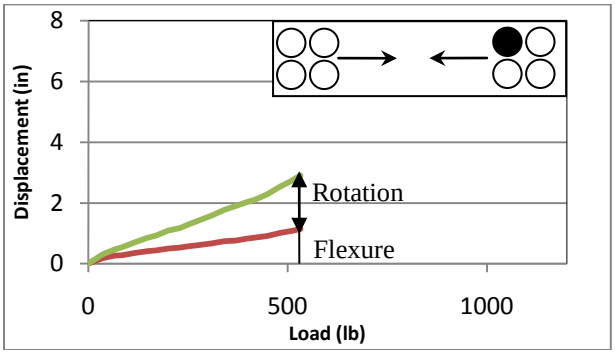

(c) Components of displacement vs. load ($4A_R1$)

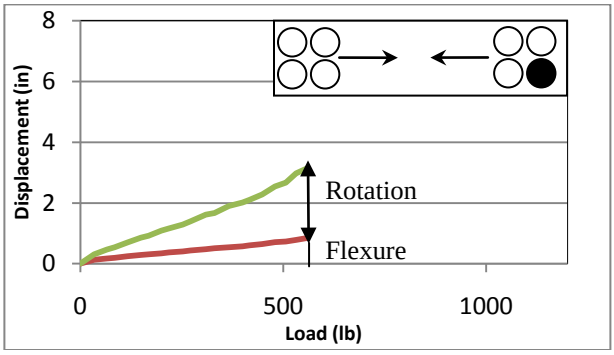

(d) Components of displacement vs. load ($4A_R2$)

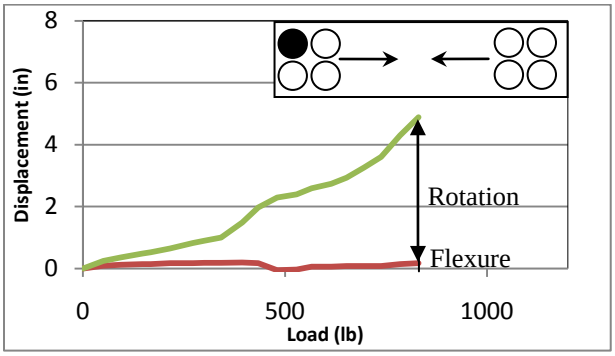

(e) Components of displacement vs. load (4B1)

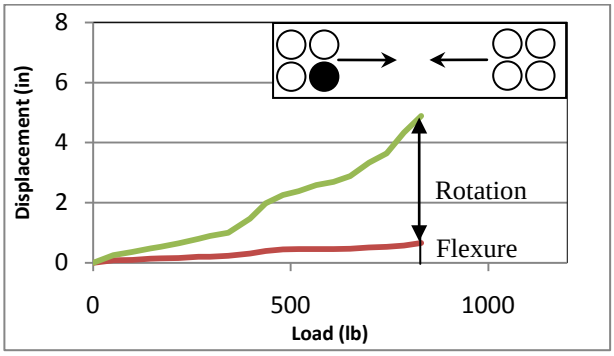

(f) Components of displacement vs. load (4B2)

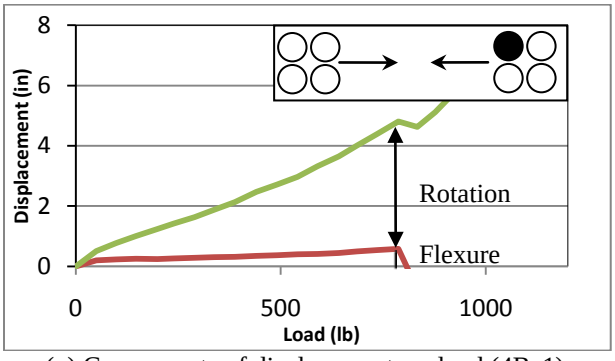

(g) Components of displacement vs. load ($4B_R1$)

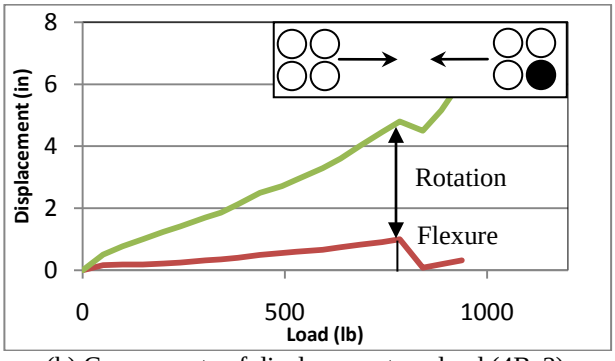

(h) Components of displacement vs. load ($4B_R2$)

Figure 4.12 Four culm column bases – components of displacement vs. load (part 1).

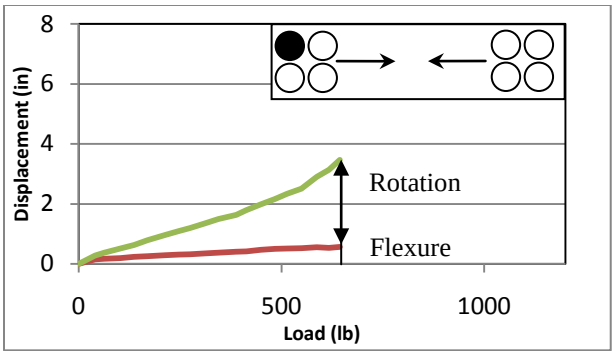

(i) Components of displacement vs. load (4C1)

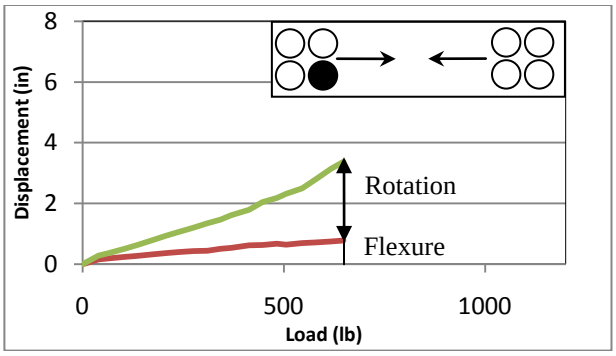

(j) Components of displacement vs. load (4C2)

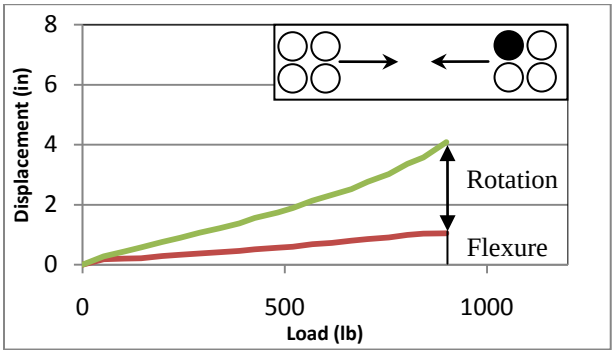

(k) Components of displacement vs. load ($4C_R1$)

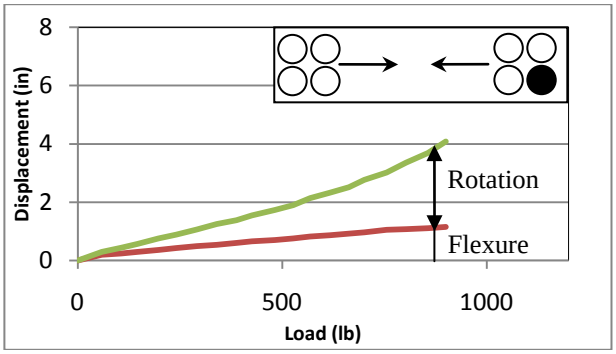

(l) Components of displacement vs. load ($4C_R2$)

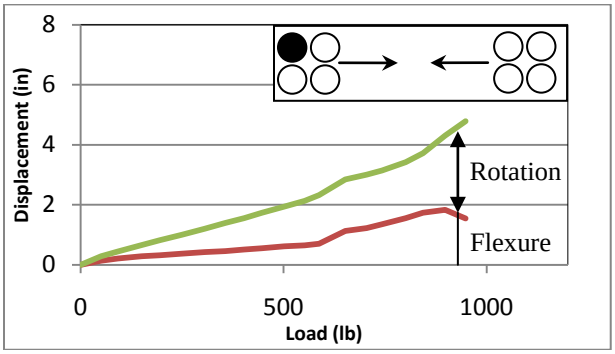

(m) Components of displacement vs. load (4D1)

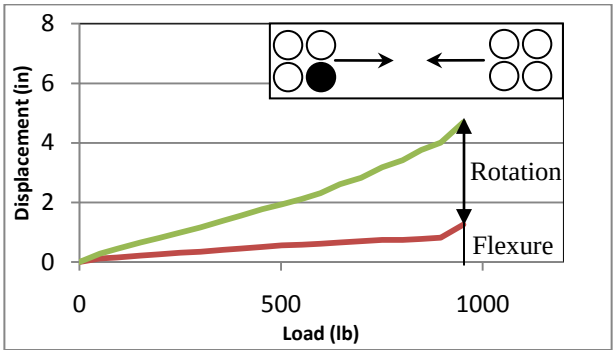

(n) Components of displacement vs. load (4D2)

Gauge Failure

(p) Gauge failure ($4D_R1$)

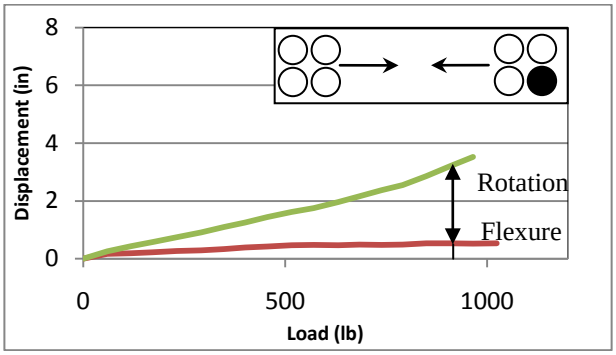

(p) Components of displacement vs. load ($4D_R2$)

Figure 4.12 Four culm column bases – components of displacement vs. load (part 2).

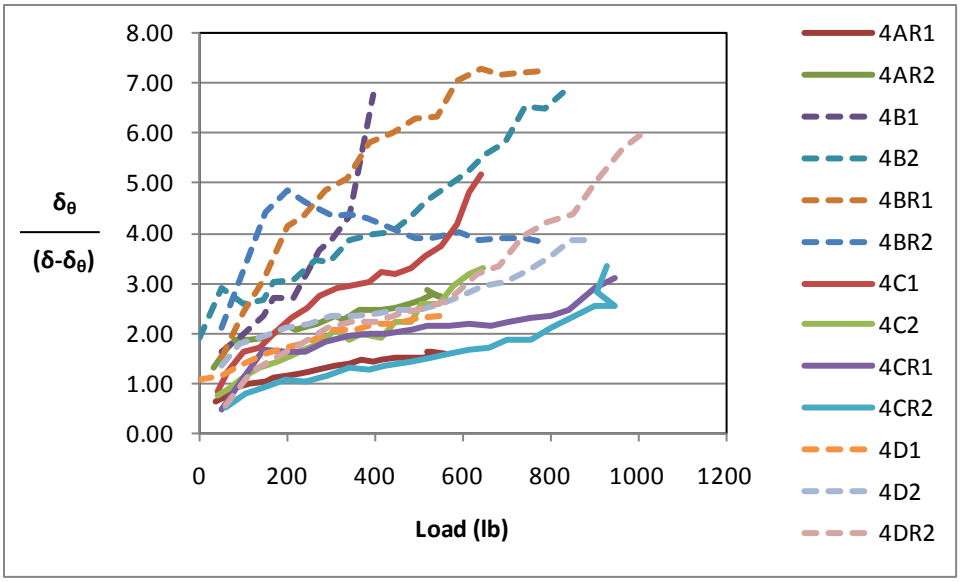

Figure 4.13 Four culm bending – ratio of displacement due to rigid body rotation vs. displacement due to flexure.

4.3.2 Four Culm Grouted-Bar Column Base Behavior

Using equations 2.6 and 2.7, one can calculate the effective flexural stiffness of the four-culm column, EI_{eff}, as well as the apparent flexural stiffness of the column, EI_{column}. The former includes the effects of rigid body rotation while the latter does not. These values are presented in Table 4.3. As described above, the behavior of the four-culm column is more complicated as it appears to fall between the expected behaviors of the sum of four individual culms and the composite behavior of the four-culm column. This behavior can be expressed as falling between that described by the two moments of inertia $4I_{culm}$ and I^*_{column} given in Table 4.3 and described in Figure 4.14:

$$4I_{\text{culm}} = 4\left(\frac{\pi(\frac{D_O}{2})^4}{4} - \frac{\pi(\frac{(D_O-2t)}{2})^4}{4}\right) \qquad \text{(Eq. 4.1)}$$

Where the term in parentheses is the moment of inertia of a single culm, I_{culm}, D_o is the outside culm diameter and t is the culm wall thickness. The fully composite column moment of inertia is therefore:

$$I^*_{column} = 4(I_{culm} + Ad^2) \quad \text{(Eq. 4.2)}$$

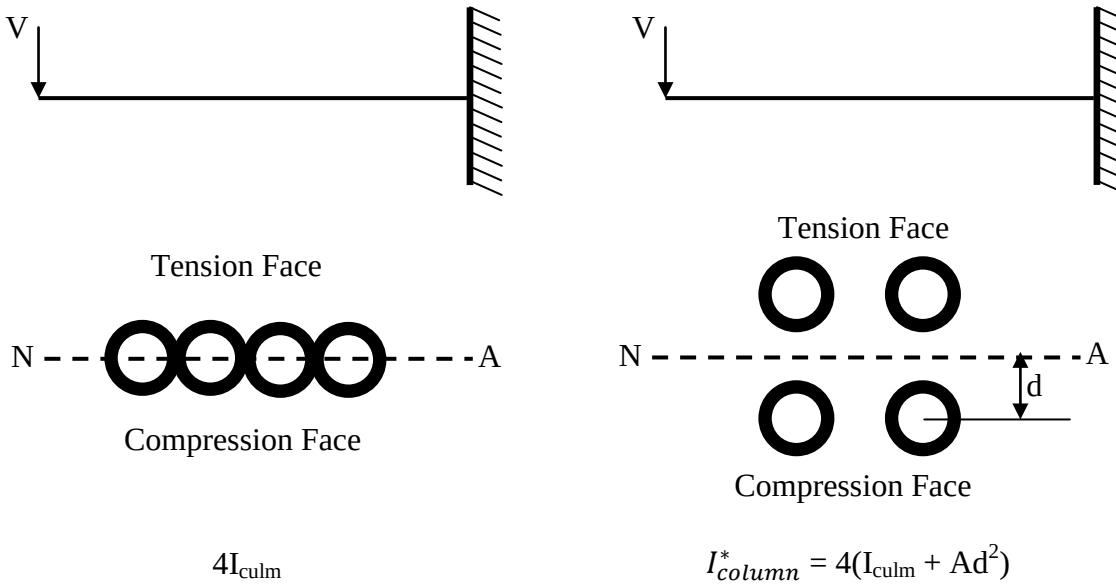

(a) Sum of individual culm behaviors (b) Composite column behavior

Figure 4.14 Moment of inertia calculations.

In this case, using an assumed value of E_{culm} = 1700 ksi (see Section 2.1.1), the apparent value of the column moment of inertia, I_{eff}, can be calculated from Equation 2.6. This was done at a load level of 50% of the ultimate capacity and the results are given in Table 4.3.

Table 4.3 Stiffness and moments of inertia of four-culm column bases.

			Observed experimental values using E = 1700 ksi			Calculated from geometric properties (Equations 4.1 and 4.2)		
Specimen	Bar size	Embedment Length	EI_{eff}	EI_{column}	I_{column}	I_{culm}	$4I_{culm}$	I^*_{column}
		in	kip-in^2	kip-in^2	in^4	in^4	in^4	in^4
4A1	4	12	5797	43447	26	2.72	10.9	113.5
4A2*	4	12	8788	28383	17	2.84	11.4	115.8
$4A_R1$	4	12	7400	16911	10	2.79	11.2	116.1
$4A_R2$	4	12	7370	23500	14	2.96	11.9	112.9
4B1	4	24	8132	93994	55	2.79	11.2	118.5
4B2	4	24	8132	40616	24	2.79	11.2	116.1
$4B_R1$	4	24	6649	48395	28	2.30	9.2	92.5
$4B_R2$	4	24	6649	32491	19	2.22	8.9	99.8
4C1	5	12	8410	33306	20	2.55	10.2	100.0
4C2	5	12	8608	24856	15	2.52	10.1	97.9
$4C_R1$	5	12	10018	30763	18	2.36	9.4	105.2
$4C_R2$	5	12	10051	24641	14	2.72	10.9	113.5
4D1	5	24	9432	29977	18	2.06	8.2	95.2
4D2	5	24	9432	32611	19	2.36	9.4	105.2
$4D_R1$*	5	24	12134	20652	12	2.36	9.4	105.2
$4D_R2$	5	24	11893	43619	26	2.72	10.9	113.5

*Denotes gauge failure during testing

As anticipated, the experimentally observed value of I_{colunn} falls between $4I_{culm}$ and I^*_{column} at a value of approximately $8I_{culm}$ or $0.2I^*_{column}$. This result indicates that the partially restrained base is acting 'more like a hinge than a fixed boundary condition'. A potential method for increasing the amount of composite action is presented in the future research portion of chapter five (section 5.1.2).

Combining the partially composite behavior of the four culm column from Table 4.3 with the moment versus rotation plot presented in Figure 4.11, both the flexural behavior of the column as well as the rigid body rotation at the joint have been explored. This information is adequate to describe the behavior of these joints both in future engineering practice and in research.

5.0 CONCLUSIONS AND FUTURE RESEACH

This study presents results from a series of tests performed on Tre Gai bamboo to determine the mechanical behavior of one of the simplest and most common types of multi- and single-culm foundation connections, the ‘grouted-bar column base’. These connections consist of a reinforcing bar embedded in a concrete foundation and then grouted into the bamboo column. The objective of this work was to develop an understanding of the complex behavior of these column base systems in the context of the behavior of a prototype bamboo framing system. To meet this objective, three series of tests were conducted; pull-out tests, single culm column base lateral load tests, and four column base lateral load culm tests.

When engaged in direct tension, friction between the grout plug and the bamboo wall had previously been reported to be a primary factor in the determination of ultimate pull-out strength, and therefore a limit state behavior of a grouted-bar connection. Tests performed in this study demonstrated only a small frictional component to pull-out resistance. The mechanical shear key behavior of the grout plug bearing at a node was found to dominate the pull-out strength. For the culms tested, this shear resistance was found to be approximately 2200 lb per engaged node. The lack of a significant friction component was likely due to the quality of the grout used in the specimens, and mirrors the conditions encountered in the field. Although not specifically investigated in this study, anecdotal evidence clearly demonstrated that active clamping pressure in the form of hose clamps effectively engaged sufficient friction to arrest slip entirely.

The shear key behavior of the nodes is engaged as the grout plug slips (see Figure 4.4). Due to the rounded shape of the node, radial stresses develop, which, due to the poor transverse tensile strength of the bamboo, result in longitudinal splitting of the culm. The splitting results in the loss of any available friction and likely affects the integrity of the node. As the node fails in shear, residual capacity is developed through friction as the 'captured' nodal regions slip through the culm.

When single culms were engaged to resist lateral load, embedment length of the grouted bar had a greater effect on capacity than the number of nodes engaged. This apparent increased frictional response is believed to result from the 'clamping' action between the bamboo wall and the grout plug as the system is required to resist lateral load. All single culm column base tests also experienced a significant amount of 'pinching', or reduction in unloading/reloading stiffness, in their hysteric behavior. This is an indication of relatively poor energy dissipation of this connection type.

The failures were generally soft, with capacity degrading slowly after the ultimate load had been reached and longitudinal splitting had occurred. The displacement due to rigid body rotation of the culm clearly dominated the lateral displacement, and was generally two to four times greater than the displacement due to culm flexure. After ultimate load had been reached, the displacement due to rigid body rotation increased dramatically as the joint failed. The overall behavior of the joint was found to follow an approximately bilinear relationship, which can be approximated for the purposes of modeling with a bilinear rotational spring. Finally, the flexural behavior of the single culm specimens can be modeled using the moment of inertia of the culm (excluding the grout plug) and the modulus of elasticity obtained from full-culm compression tests.

The behavior of the four culm column bases was similar to the single culm columns, although the four culm specimens demonstrated a degree of composite action between the culms and experienced more abrupt failures. When normalized for the different culm sizes used in the single and four culm tests, the capacity of the four culm arrangement was found to be approximately five to ten times greater than a single culm arrangement (Table 4.2). The experimentally observed value of the effective moment of inertia also demonstrated composite action as it was approximately twice the sum of the individual culms or twenty percent of a fully effective cross-section (Table 4.3).

5.1 FUTURE RESEARCH

5.1.1 Modeling a Parameters

One of the most important results of this series of tests has been the development of a significant amount of knowledge on the degree of fixity of the grouted-bar column base connection. This information will be used to model the behavior of the single and four culm column connections in future research (Sharma 2010). Depending on the modeling objectives, a simple cantilevered model or a cantilevered model with a rotational spring support can be utilized (Figure 4.16). The latter is likely more practical for modeling frame structures.

The values for EI_{eff} and EI_{culm} obtained from this test program and listed in Table 4.1 and 4.3. A rotational spring is defined as:

$$M = K_\theta * \theta \qquad \text{(Eq. 5.1)}$$

Where M = Moment (ft-lb)
K_θ = Spring constant (ft-lb/rad)
θ = Rotation (rad)

The constant used for the rotational spring, K_θ, is the slope of the moment-rigid body rotation relationship presented in Sections 4.2 and 4.3. While the choice of how to define a parameter must be made by the engineer, it is recommended that the spring constant follow a bi-linear relationship, as shown in Figure 5.1. Using the representative moment-rigid body rotation relationship of specimen $4C_R1$ shown in Figure 5.1, the value of K is approximately 55,000 ft-lb/rad until the moment reaches 3500 ft-lb, at which point the constant drops to zero. In this example, the spring continues to behave in a plastic manner through a rotation of 0.12 rad, at which point the joint rotation capacity is exhausted.

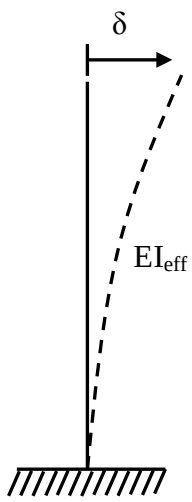

$$\delta = \frac{Vh^3}{3EI_{eff}}$$

(a) Fixed cantilevered column model with effective properties accounting for rigid body base rotation

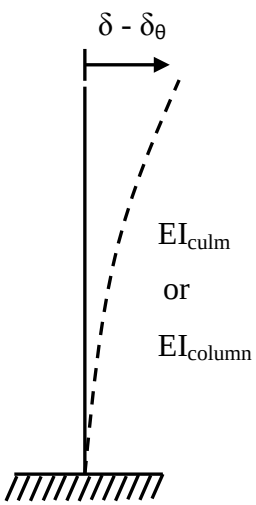

$$\delta - \delta_\theta = \frac{Vh^3}{3EI_{culm}}$$

or

$$\delta - \delta_\theta = \frac{Vh^3}{3EI_{column}}$$

(b) Fixed cantilevered column component of column behavior using actual culm properties

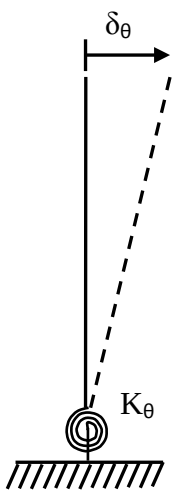

$$\delta_\theta = \frac{M}{K_\theta}$$

(c) Rotational spring component of column behavior

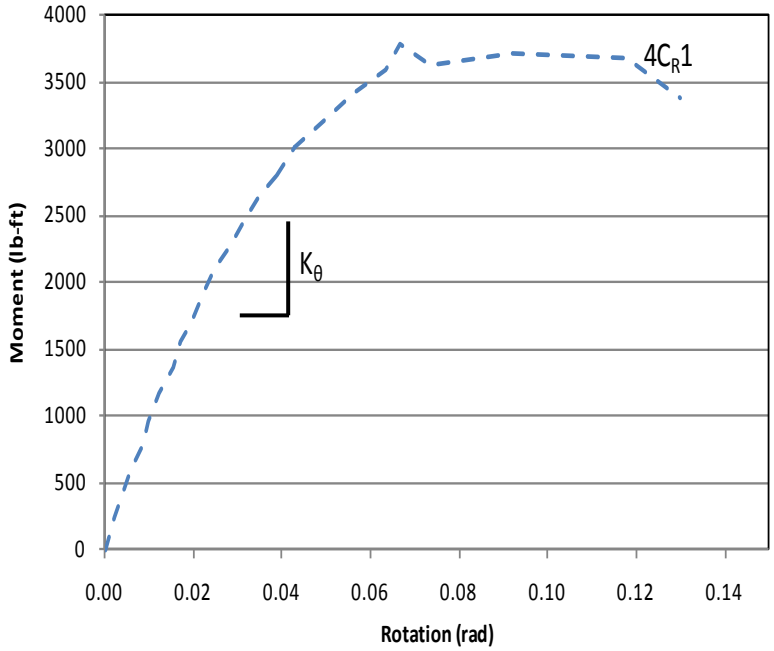

(d) Example of rotational constant determination (specimen $4C_R1$)

Figure 5.1 Partially restrained model parameters.

5.1.2 Column Behavior

It is believed that a greater degree of composite behavior (i.e.: an effectively stiffer column) could be affected by the addition of more locations for shear transfer, or 'stitching', along the column length. These 'stitches' could be similar to commonly used single-bolt bamboo truss connections and would consist of two pieces of bamboo located between column members with a bolt connecting them (see Figure 5.2). The stitches enforce overall column geometry, provide resistance to individual culm buckling and transfer shear between culms. While the amount of stitching required can be calculated, the shear transfer will most likely be limited by longitudinal splitting of the bamboo at the bolt location (Mitch 2009).

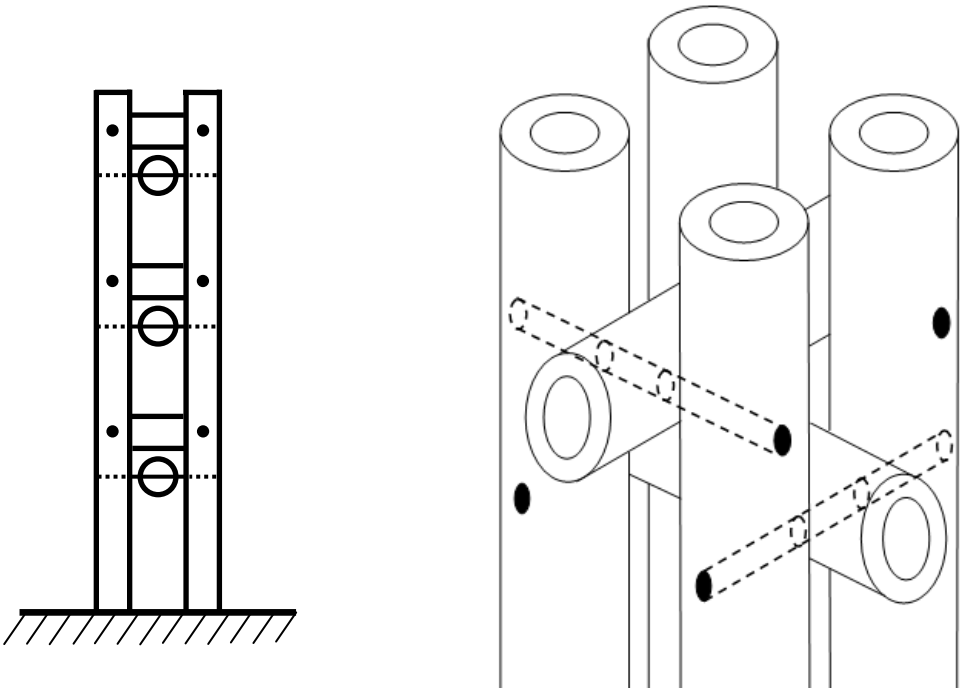

(a) Column with stitching (b) Close-up view of stitching

Figure 5.2 Schematic of 'stitch' connection for shear transfer.

5.1.3 Wall Thickness and Embedded Connections

While not addressed in this document, the effect of wall thickness is a significant concern. While the research presented in this document has all been conducted using a single species of particularly thick-walled bamboo (Tre Gai), this has the disadvantage of preventing a comparison between different wall thicknesses. As the dominant limit state in this test series and most other works has been longitudinal splitting of the bamboo, it can be concluded that the transverse tensile strength is the limiting factor in structural applications of bamboo. As a thin-walled bamboo has a smaller available area to carry this stress, it follows that the thin-walled bamboo may be weaker and behave in amore brittle manner than thick-walled species. The nature of this relationship should be investigated further.

The dominance of the rotation of the joint in the behavior of the single and four culm column bases highlights the need for an alternative to the grouted-bar connection that exhibits less rigid body rotation. One potential alternative, discussed in section 1.2.2, foregoes a mechanical connector and instead embeds the entire culm into the concrete foundation (see Figure 5.3). In some cases a grouted bar may also be provided which may relieve some of the stress on the culm wall when subject to lateral load. This type of connection is believed to provide a much more rigid connection and may reduce the dominance of the rigid body rotation at the column base. A research program similar to that conducted in this document should be performed on this connection before it can be confidently utilized in future designs.

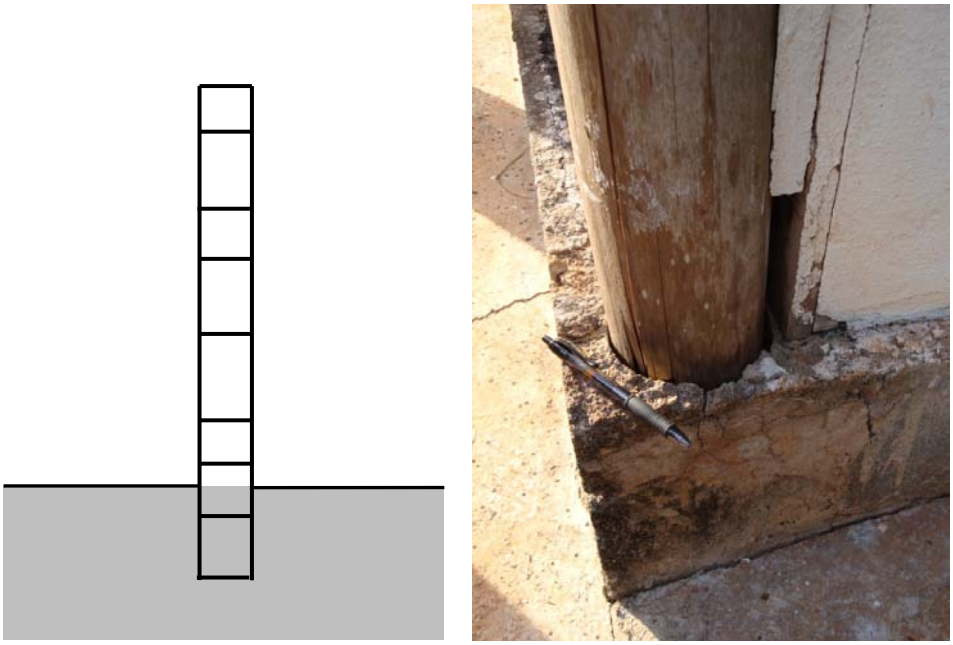

Figure 5.3 Embedded connection.

REFERENCES

Amada, S. and Untao, S. (2001). “Fracture properties of bamboo.” *Composites: Part B: engineering,* Vol. 32, pp 451-459.

American Concrete Institute. (2008). *Building Code Requirements for Structural Concrete (ACI 318-08) and Commentary*.

American Forest & Paper Association. (1997). *National Design Specification for Wood Construction – Supplement*. American Wood Council.

Arce-Villalobos, O. (1993). “Fundamentals of the Design of Bamboo Structures.” *Ph.D. Dissertation*, Eindhoven, The Netherlands: Eindhoven University, 1993, 281.

ASTM International. (2004). *ASTM 942-99 (2004) Standard Test Method for Compressive Strength of Grouts for Preplaced-Aggregate Concrete in the Laboratory*. ASTM, West Conshohocken PA.

ASTM International. (2009). *ASTM E8 (2009) Standard Test Methods for Tension Testing of Metallic Materials.* ASTM, West Conshohocken PA.

Bilham, R., Vinod, K. and Molnar, P. (2001). “Earthquakes: Himalayan Seismic Hazard”. *Science*. August 2001. Vol. 293, no. 5534. 1442-1444.

Civil Engineering (2006). “The Widening Gulf. Civil Engineering Magazine”, American Society of Civil Engineers, 76(8), pp. 56-61.

ICBO Evaluation Service, Inc. (2000). *AC 162: Acceptance Criteria for Structural Bamboo*. Whittier, California.

ICC Evaluation Service, Inc. (2004). “Structural Bamboo Poles” *Testing Report ESR-1636-2004*, Whittier, California.

ICC Evaluation Service, Inc. (2006). "Structural bamboo Poles." *Testing Report ESR-1636-2006*, Whittier, California, 2006.

International Standards Organization (ISO). (2004a). *ISO 22156 Bamboo - Structural Design*.

International Standards Organization (ISO) (2004b). *ISO 22157-1 Bamboo - Determination of physical and mechanical properties - Part 1: Requirements*.

International Standards Organization (ISO). (2004c). *ISO 22157-2 Bamboo - Determination of physical and mechanical properties - Part 2: Laboratory manual*.

Janssen, J.J.A. (1981). "Bamboo in Building Structures." *Ph.D Dissertation*, Eindhoven, The Netherlands: Eindhoven University, 253.

Janssen, J.J.A. (2005). "International Standards for Bamboo as a Structural Material. *Structural Engineering International*. 15(1), 48-49.

Kumar, S., Shukla, K.S., Dev, I. and Dobriyal, P.B. (1994). "Bamboo Preservation Techniques: A Review." *International Network for Bamboo and Rattan (INBAR)*, Beijing, China.

Mitch, D. (2009). "Splitting Capacity Characterization of Bamboo Culms." *Honors College Thesis*, Civil and Environmental Engineering, University of Pittsburgh.

Mitch, D., Harries, K.A., and Sharma, B. (2010). "Characterization of Splitting Behavior of Bamboo Culms", *ASCE Journal of Materials in Civil Engineering* Vol. 22, No. 11.

National Building Code of India. (2005). "Part 6 Structural Design - Section 3 Timber and Bamboo: 3B Bamboo."

Sharma, B.. (2010). "Performance Based Design of Bamboo Structures." *Ph.D. Dissertation*, Department of Civil and Environmental Engineering, University of Pittsburgh.

Sharma, B., Harries, K.A., and Ghavami, K. (2010). "Pushover Test of Bamboo Portal Frame". *Proceedings of the International Conference - Nonconventional materials (IC-NOCMAT)*, September 21-23, 2010, Cairo, Egypt.

Sharma, B., Harries, K.A. and Kharel, G. (2008). "Field Documentation and Survey of Bamboo Structures: Service Learning Opportunities in Sustainability Research", *Proceedings of the Association for the Advancement of Sustainability in Higher Education Conference*, Raleigh NC, November 2008.

Sika Corporation. (2003). "SikaGrout 212 - High performance, cementitious grout." *Product Data Sheet*. Lyndhurst, NJ.

Silberglitt, R., Anton, P., Howell, D. and Wong, A. (2006). *The Global Technology Revolution 2020, In-Depth Analyses Bio/Nano/Materials/Information Trends, Drivers, Barriers, and Social Implications*. Rand Corporation.

Soltani, A. (2010) "Bond and Serviceability Characterization of Concrete Reinforced with High Strength Steel." *Ph.D. Dissertation*, Department of Civil and Environmental Engineering, University of Pittsburgh.

Washington State University. (2002). *WMEL 01-047 - Mechanical Properties of Bamboo*. Wood Materials and Engineering Laboratory Report.